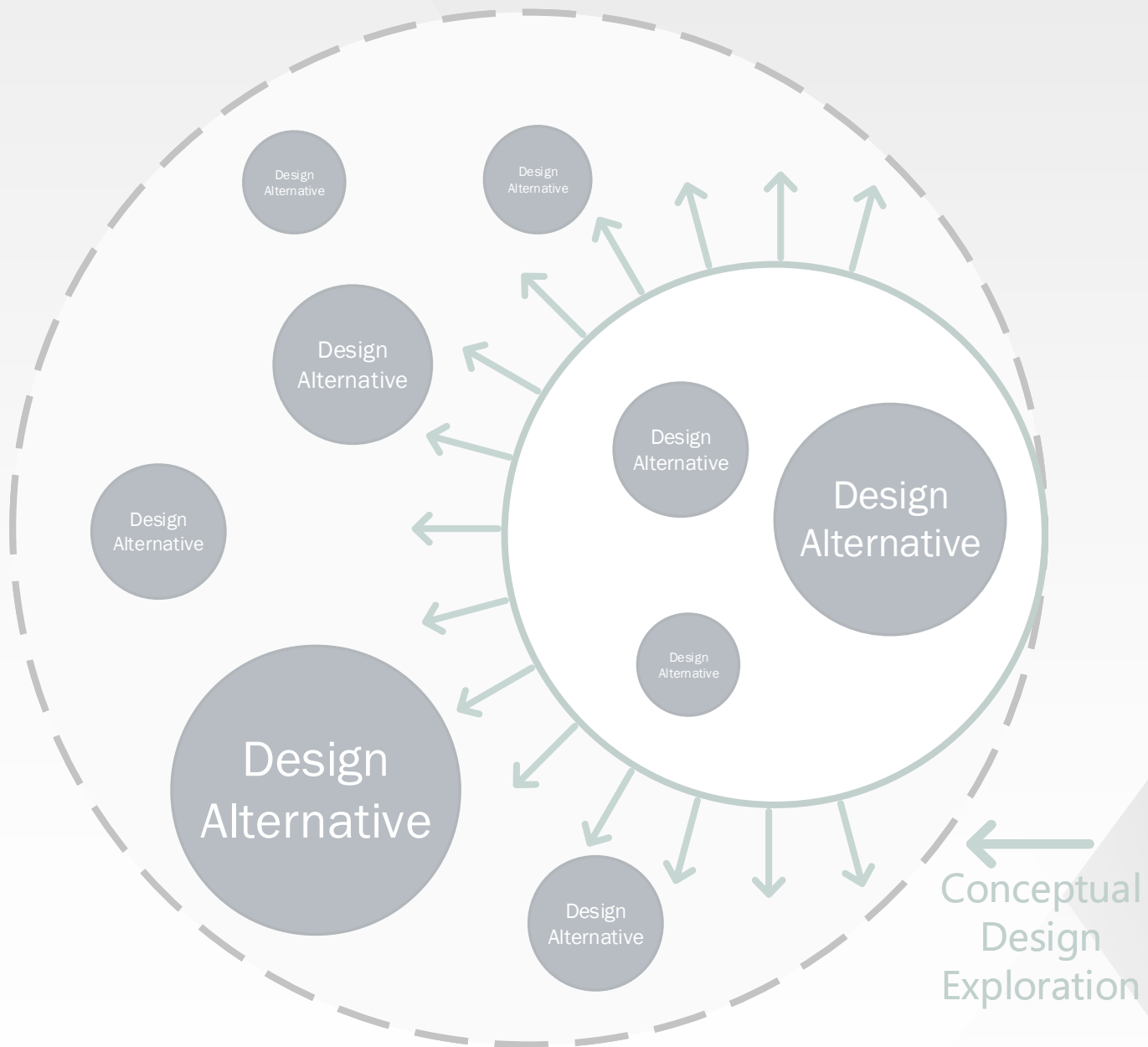


StructuralComponents 9

Early-stage structural analysis and design of Universal Prefab apartment buildings

Master's Thesis
C.J. van Essen

October 25, 2021



This page has been intentionally left blank.

StructuralComponents 9

Early-stage structural analysis and design of Universal
Prefab apartment buildings

by

C.J. van Essen

to obtain the degree of Master of Science
at the Delft University of Technology
in corporation with Royal HaskoningDHV

Student number: 4383168
Chairman: Dr. ir. P. C. J. Hoogenboom, TU Delft
Thesis committee: Ir. S. Pasterkamp, TU Delft
Ir. R. Crielaard, TU Delft
Ir. J. M. Brouns, Royal HaskoningDHV
Dr. ir. J. L. Coenders, White Lioness technologies



This page has been intentionally left blank.

Preface

The completion of this master thesis has been an exciting challenge. For some time now, one of my main interests in the field of civil engineering has been to find efficient solutions for complex problems using parametric programming. In my opinion, the creation (and usage, naturally) of smart applications suitable for analysis of a specific structure or element will become/remain an important aspect in the future practice of civil engineering. For sharing this interest and realising an application of this kind, I could count on numerous Royal Haskoning engineers, all eager to offer support and advice; I thank all of them. I would like to extend special gratitude to Jos Brouns for great advice, encouragement, and enthusiasm.

I would like to thank the full thesis committee for their care; their feedback helped maximize the potential of this research. Thank you, Sander Pasterkamp, for allowing me to rely on your formidable expertise and for your enthusiasm. Pierre Hoogenboom and Roy Crielaard "kept my eyes on the prize" through considerate feedback regarding the overall structure, progress and objectives of this research. I thank Jeroen Coenders for introducing me to the concept of StructuralComponents – which provided exactly what I hoped for for this research – and sharing his enthusiasm. I am glad to have heard his vision on the future of StructuralComponents and to have been a part of this exciting endeavor.

Last but not least, I would like to express many thanks to my friends and family for their motivation and support throughout this project.

This page has been intentionally left blank.

Summary

This research introduces the concept of Universal Prefab (UP), a highly modular building system which uses only prefabricated elements to realise building designs. The discrete structural elements are connected with a standardized connection throughout the entire structure that allows for quick assembly, increasing the efficiency of construction. The patented CD20 building system – a fitting example of the Universal Prefab approach – is of special importance for this research because of its relevance to Royal HaskoningDHV (RHDHV). Characteristic for this system is the column-floor slab connection shown in Figure 1, comprising a corner shoe on the slab which fits the pins on the ends of the columns below and above the plate. Stability is provided by wall-elements assembled into a "singular" vertical shear wall.

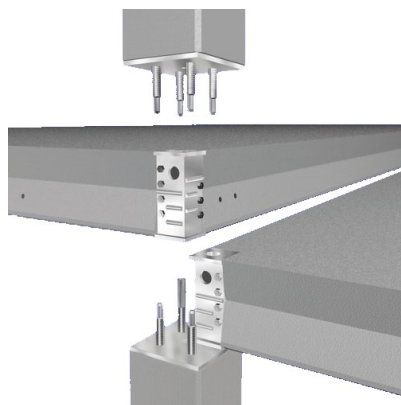


Figure 1: Characteristic CD20 column-plate connection (CD20 Bouwsystemen n.d.)

Royal HaskoningDHV has expressed a need for more efficient design composure and conceptual design validation of Universal Prefab structures, in particular for mid-rise apartment buildings. In this way, they hope to offer affordable and rapidly realisable building solutions for the existing residential shortage. Modelling and analysis in the conceptual design phase requires a high flexibility in design composure as well as a simplified but sufficiently accurate representation of the structural system. For this a parametric design tool is proposed following the StructuralComponents concept. This concept aims to provide engineers with computational tools suitable for conceptual design. In general, this is achieved by supplying the engineer with building blocks with which conceptual structural designs can be composed efficiently. Subsequently, visualisation of the relevant analysis results on a clear dashboard provides the desired insight in the resultant structural behaviour.

Based on the defined challenge, the main objective of this research is as follows:

The design and development of a conceptual design tool prototype, that provides clear and quick insight into the force distribution in Universal Prefab apartment building structures, to improve design efficiency and expand the StructuralComponents toolbox.

Additionally, four sub-objectives were defined:

1. Determine the capabilities a parametric tool requires to enable (more efficient) conceptual design of Universal Prefab apartment buildings.

2. Define a suitable analysis model for providing quick structural validation of the considered assortment of conceptual designs.
3. Develop a prototype of the proposed tool.
4. Assess the accuracy of the implemented structural analysis model and examine the observed Universal Prefab structural behaviour.

Assessments of the previous reports on Structural Components and the characteristics of Universal Prefab apartment buildings identified two key functionalities that a conceptual UP design application would require to be of scientific and practical value: analysis of *non-proportionate*¹ shear-wall stability systems and design composure through *user-customisable* floor-plans. Furthermore, accurate modelling of the force distribution due to lateral (façade) loads was considered the main aspect of providing insight into the structural behaviour; integral design justification based on codes or regulations is not provided. It was also concluded that the realisation of a tool prototype with significant practical value would be scientifically valuable for the expansion of the StructuralComponents concept.

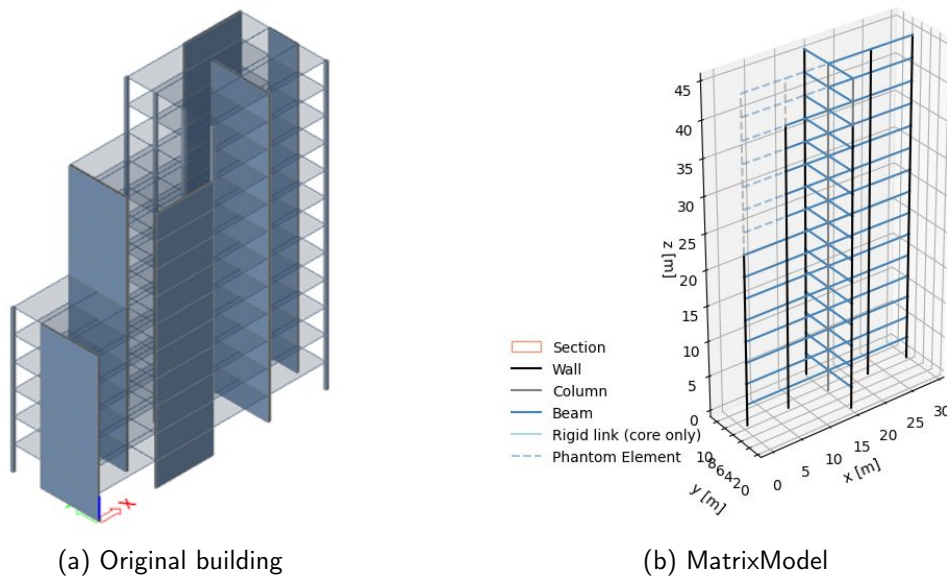


Figure 2: Translation from original design to stick model

A preparatory study of various lateral stability models considered their suitability and accuracy for analysis of conceptual Universal Prefab structural designs. Ultimately, the 2D Flat Stick model (or 'MatrixModel') was devised and selected for further development; an example of an original floor-plan and its 2D Flat Stick representation are shown in Figure 2. This representation, modelling all two-dimensional elements as one-dimensional (stick-)elements, greatly reduces the number of degrees of freedom with respect to Finite Element Analysis while still offering the possibility of a non-rigid floor-system, which was found to be crucial for the modelling of Universal Prefab structures. In the MatrixModel, the original floor-system of slabs and hinges is represented by beams spanning from (stick-)wall to (stick-)wall. The beams are assigned the width of the building in their corresponding direction and are assigned a finite stiffness in the order of magnitude of the wall-stiffness. This representation was proven to be sufficiently accurate for analysis in the conceptual design phase. The implementation of the 2D

¹Non-proportionate (or non-prismatic) structure: a structure in which a non-proportionate change in the stability system occurs over the height (see Section 3.1); e.g. certain stability walls are terminated at a certain level.

Flat Stick representation in a parametric environment enables the composure of a wide envelope of stability wall configurations. A 3D frame analysis implemented in Python scripts proved to be sufficiently quick and well-suited for the analysis of the devised MatrixModel representation of a conceptual UP building design.

Thorough consideration of various alternatives for obtaining the required user-input and generating the MatrixModel led to the tool presented in Chapter 4 and Appendix G. The application possesses a graphical User Interface with which a designing engineer can efficiently compose building designs using customizable building blocks. The visualisation of the composed building design and the generated MatrixModel supports corroboration of the obtained results. Additionally, projects can be saved and opened, realising even more practical value. The calculated shear force and bending moment distributions of each wall are plotted and the values are provided, offering clear insight into the lateral structural behaviour.

From the assessment of various test-case designs it could be concluded that for conceptual designs of proportionate, non-proportionate and core stability systems – ranging from three to thirty storeys – the primary force distribution can be predicted with sufficient accuracy by the developed Matrix Model. Sufficient accuracy cannot be guaranteed for the force distributions of hybrid core-shear wall systems and the walls perpendicular to the axis of loading and the deformation distribution in general.

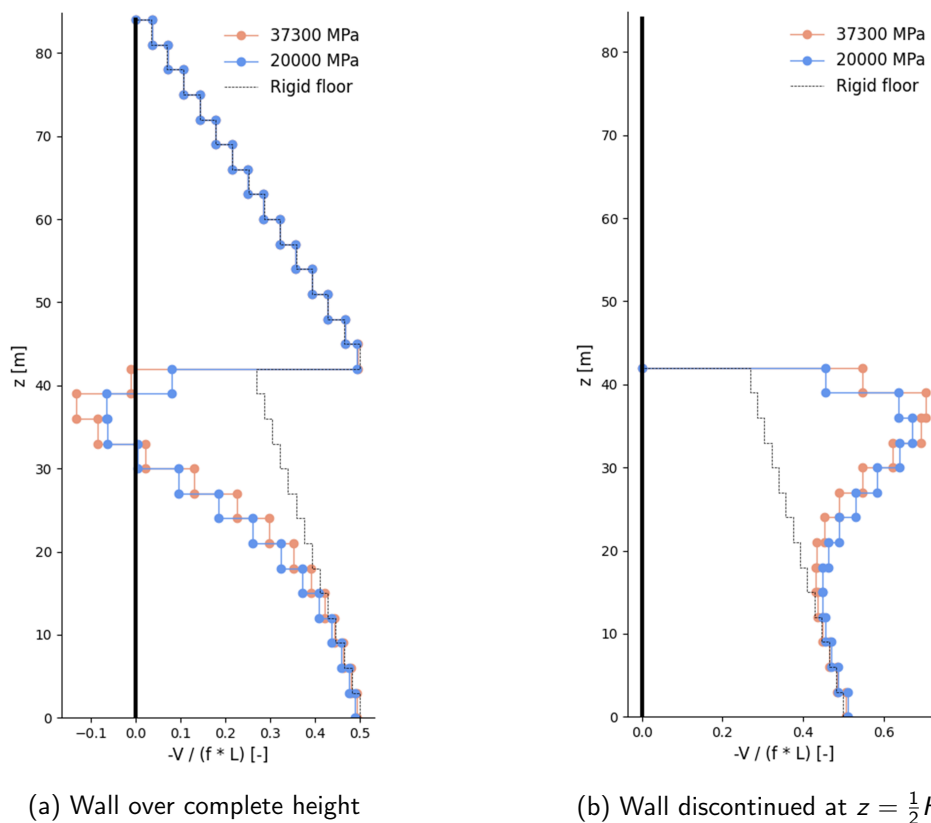


Figure 3: Relative shear-force distribution in walls of non-proportionate building.

The CUPD structural analysis results showed a disturbance in the shear force and bending moment distributions caused by a non-proportionate change in the stability system (see Figure 3), in accordance with the Differential Super Element Method developed by Raphaël Steenberg (2007). It was established that the magnitude of this disturbance is influenced by the floor-beam stiffness: a higher, finite stiffness allows for more redistribution, thus causing a larger disturbance in the force distributions at the transition with respect to the case of a

rigid floor-system. Applying an increased thickness for the floor-system at transition-level has a comparable effect. For excessively large stiffnesses (with respect to the wall stiffness) the disturbance reduces; for a rigid floor-system the lateral load is proportionately distributed over all walls at each storey. Based on the assessment of the aforementioned aspects it can be concluded that the force distribution in non-proportionate Universal Prefab building designs requires scrutiny. The developed tool prototype offers this functionality.

To conclude, the expansion of StructuralComponents was accomplished through the realisation of a tool prototype with significant practical value along with the addition of Universal Prefab structural analysis to the existing toolbox and the combination of user-customisable floor-plans for non-proportionate buildings. The Conceptual Universal Prefab Design Application enhances the conceptual design efficiency of Universal Prefab buildings and provides rapid and clear insight into their lateral structural behaviour. In doing so, more extensive exploration of the conceptual design space and collaboration between designing engineers and other parties are encouraged. The heightened early-stage design efficiency provides incentive for increased construction of Universal Prefab apartment buildings and can consequently lead to a reduction in residential shortage.

Abbreviations

CoT Center of Twist.

CUPD Conceptual Universal Prefab Design.

DoF Degree of Freedom.

DSEM Differential Super Element Method.

FEA Finite Element Analysis.

FEM Finite Element Method.

LCS Local Coordinate System.

OOP out-of-plane.

RHDHV Royal HaskoningDHV.

RMSE root-mean-squared-error.

SC StructuralComponents.

SEM Super Element Method.

UI User Interface.

UP Universal Prefab.

This page has been intentionally left blank.

Contents

Preface	iii
Summary	v
Abbreviations	ix
1 Introduction	1
1.1 Current state of the housing market	1
1.2 Prefabricated concrete structures	2
1.3 Building design practice	4
1.4 Conceptual and parametric design	4
1.5 Problem definition	6
1.6 Objectives	8
1.7 Methodology	10
2 Conceptual Design of UP Apartment Buildings	13
2.1 Background of StructuralComponents	13
2.2 Characteristics of Universal Prefab	16
2.3 Limited scope	19
2.4 Conclusion of chapter	20
3 Structural Analysis Model	21
3.1 Lateral stability analysis	21
3.2 Structural behaviour of Universal Prefab	24
3.3 CUPD Matrix Model	31
3.4 Conclusion of chapter	38
4 CUPD Tool Prototype	39

4.1	System architecture	39
4.2	User-Input & -Interface	40
4.3	System process	42
4.4	Capacities & Limitations	44
4.5	Conclusion of chapter	45
5	Result Analysis	47
5.1	CUPD analysis model accuracy	47
5.2	Influence of the floor stiffness	54
5.3	Influence of the transition-floor thickness	56
5.4	Non-proportionality and comparison with DSEM	57
5.5	Conclusion of chapter	60
6	Discussion	63
7	Conclusion	67
8	Recommendations	69
	References	71
	List of Figures	76
	List of Tables	77
A	Semantics	79
B	Stability Systems	80
C	Reference Modelling - Dummy Elements	82
D	Preliminary Research on UP Behaviour - Results	84
E	Reference Modelling - Core	88
F	Element stiffness matrix - Maple	90
	C.J. van Essen	xii

G User Interface - Figures	93
H CUPD Analysis Accuracy	100
J Floor Stiffness - Figures	112
K Floor Thickness - Figures	115

This page has been intentionally left blank.

1 | Introduction

To present a comprehensive report, this chapter provides an outline of the research context. The first sections serve as the basis for the problem analysis and intend to define the niche in which the objective of this paper means to operate. Subsequently, an explicit main research objective is defined, aimed to alleviate the hindrance experienced in the conceptual design phase, specifically for Universal Prefab building designs. Ultimately, a methodology for achievement of the main objective is outlined.

1.1 | Current state of the housing market

The residential sector faces turbulent times. The years leading up to 2020 saw a strong rise in residential development. Even so, the unceasing growth in number of households increased the already existing shortage of residences to around 331 thousand (Ministry of the Interior and Kingdom Relations 2020). Due to the Covid-19 crisis and the regulations regarding nitrogen and PFAS, quick closure of this gap is not to be expected. The Primos 2020 report predicts a shortage of 419 thousand residences by 2025 (ABF Research 2020). As Figure 1.1 illustrates, the demand for houses and apartments mainly presents itself in urban, more densely populated areas in which, unfortunately, space is often limited.

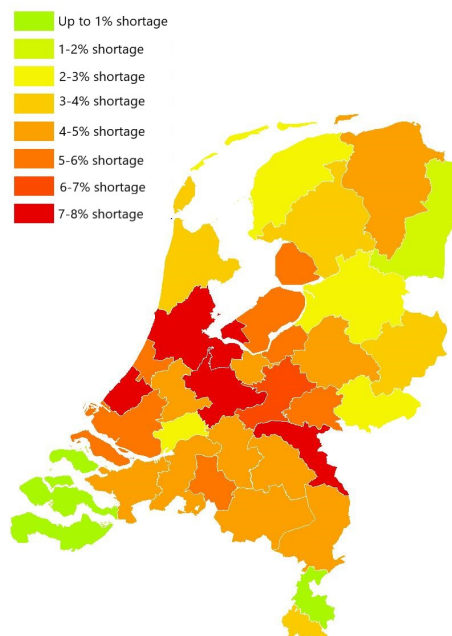


Figure 1.1: Expected residential shortage by 2025 (ABF Research 2020)

Two basic strategies for alleviating the residential shortage will be to either *increase the construction* of residences or to *decrease the demand* for residences. Since this research will be performed from a civil engineering standpoint rather than a sociological one, the latter option will not be part of the scope.

1.2 | Prefabricated concrete structures

Construction of apartment buildings using standardised prefabricated structural elements could be a partial solution to the challenges faced in the residential sector, especially in urban areas. The report of Remkes et al. (2020) on the nitrogen problem proposes more prefab construction as one of the potential paths towards less emissions of nitrogen. Furthermore, research into carbon emissions of both prefab and in-situ concrete has shown that prefabrication can result in an emission reduction of 10% and therefore highly recommends the application of more prefab construction (Dong et al. 2015). This section touches upon the differences between prefab and in-situ construction and introduces a specific approach to prefab construction that has special relevance to this research.

In general, prefabricated structural elements are able to meet higher quality standards than elements casted in-situ, in terms of strength and sustainability. The higher concrete strength applied in prefab structures allows for the use of relatively slender elements, in contrast to elements casted on site. The controlled environment in which prefab elements are fabricated, increases the resistance to outside influences (*Concrete Building Structures* 2016). More slender construction does not only provide more architectural freedom, but also saves resources. Higher resistance to environmental influences is advantageous for the conservation of structural elements and subsequently results in longer lifetimes and/or higher potential for reuse.

As often stated, construction times for prefab buildings are much shorter than for in-situ construction. To put this in perspective however, the preparation of prefab construction often takes considerably more time since all elements have to be defined in detail before they can be manufactured. Consequently, both methods often have similar total project duration (*Concrete Building Structures* 2016). In cases where the size of the construction site is limited, prefab construction combined with efficient planning can be a, literally, fitting solution.

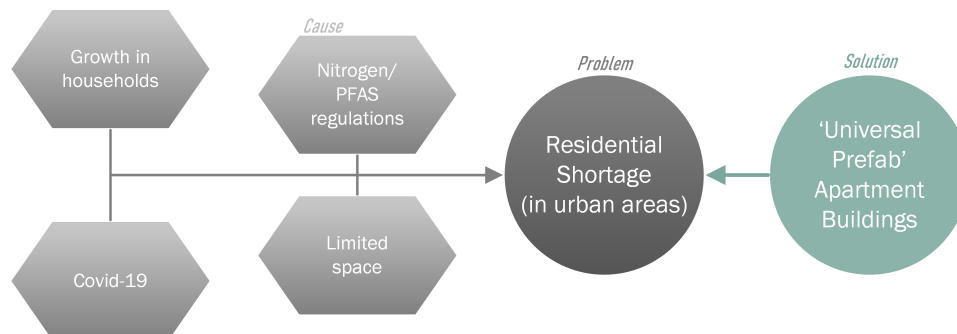


Figure 1.2: Potential solution - 'Universal Prefab' apartment buildings

The choice for prefab or in-situ cast concrete ultimately depends on the costs. The cost of either option depends on the type and size of elements and the repetitiveness within the structure. While the higher strength of prefab concrete offers advantages, the freedom of shape and less complicated transport (especially for large prefab elements) of in-situ casting could better suit a specific project. Furthermore, strength is not always the governing factor and (relatively) high-strength prefabricated elements therefore not always required. In general, the application of prefabricated elements becomes more efficient (and less costly) with increasing use of large and/or equal elements (*Concrete Building Structures* 2016). Otherwise, cast in-situ concrete may be the most efficient option and therefore chosen.

1.2.1 | The Universal Prefab approach

In the general practice of mid- and high-rise construction the structural elements providing lateral stability are cast in-situ; prefabricated elements are used for erection of the surrounding structure (Steenbergen 2007). A distinguishable approach to prefab construction is the application of a highly modular system, in which *only* prefabricated elements are used. The structural elements are available in discrete dimensions and connected using a specific type of connection – universally applied throughout the building. This concept allows for an even higher degree of standardisation – reducing the aforementioned preparation time, high design flexibility and is exceptionally suitable for disassembly and reuse at the end-of-life, making it a potential solution for the current residential shortage (see Figure 1.2).

The specific approach outlined above will be hereinafter referred to as Universal Prefab (UP). The regarded semantics behind this decision can be found in Appendix A. Section 2.2 presents a thorough outline of the characteristics of the UP building system.

Customarily, the lateral stability of UP structures is provided by prefabricated wall elements which can be vertically combined to form "continuous" shear walls. Possibly, such shear walls can be assembled to form a core. Figure 1.4 shows an example of a Universal Prefab stability system. Lateral stability of UP structures is further elaborated upon in Chapter 3.

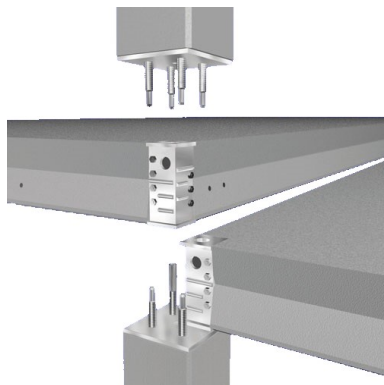


Figure 1.3: CD20 column-floor connection (CD20 Bouwsystemen n.d.)

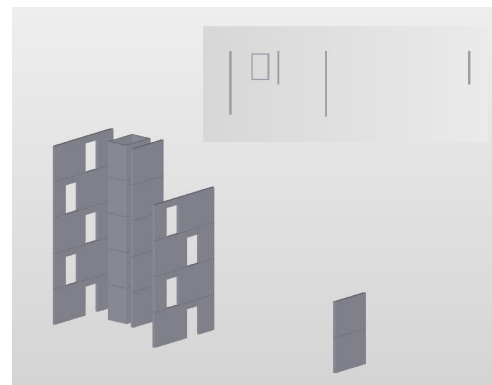


Figure 1.4: Stability system of Fridtjof Nansenhof - Amsterdam

1.2.2 | The CD20 building system

The patented building system of CD20 Building Systems applies the Universal Prefab approach outlined in the previous paragraph, providing a structural system suitable for rapid construction of low- and mid-rise prefabricated concrete structures. The core principle of the CD20 system is the column-floor slab connection, illustrated in Figure 1.3. Based on a pin on the column-end and a corner shoe on the slab, this connection allows for quick (de)construction (CD20 Bouwsystemen n.d.). The four corner shoes of a slab are placed over the pins on the ends of four columns, i.e. a slab is carried by four columns and one column carries a quarter of four slabs. For each storey, the principle works the same, resulting in a highly modular structural system. The prefabricated columns, floor-slabs and shear walls are available in various types and dimensions.

Royal HaskoningDHV (RHDHV) sees potential in erection of apartment buildings using the CD20 system and has gained a substantial amount of experience through the execution of numerous projects with this system (ir. J. Brouns, personal communication, December 10, 2020). Past experience often significantly contributes to efficient collaboration in future projects. Therefore, this research puts an emphasis on the CD20 building system.

1.3 | Building design practice

In the conventional building construction practice, a preliminary building design is formed by an architect and a designing engineering firm^I based on the demands of a project developer (or: client). The level of detail present in this design can vary; generally, at least certain basic design checks have been executed and the design can be assumed to be structurally feasible. Different contractors can tender their proposition for realisation of the desired building, which may differ from the original design within certain limits. Subcontractors like CD20, applying a UP structural system, often have to make certain adjustments to the original design in order for such a system to be applicable and to maximize its advantages. The significantly reduced construction time, lower costs, and reduced environmental impact a Universal Prefab system can offer, occasionally persuade the developer to allow the necessary changes (ir. J. Brouns, personal communication, February 11, 2021).

To present a feasible tender design, the required changes to allow for application of a UP system have to be verified. Royal HaskoningDHV provides this validation for, amongst others, CD20 Building Systems. This conceptual design validation mainly focuses on lateral stability and gravitational loads, with emphasis on the changes made to the "original" tender design. For relatively straightforward building designs, this is done with (Excel-)automated, relatively basic calculations (ir. J. Brouns, personal communication, February 11, 2021). Correspondingly, more elaborate building designs (e.g. non-prismatic^{II}, non-rectangular) require more elaborate calculation and consequently more time.

Besides the design and tender procedure described above, the (relatively) new Design/Engineering & Build concepts are an often applied approach in current residential construction. These concepts, also known as UAV-GC contracts, transfer more design and/or engineering responsibilities to the primary contractor, whom is included earlier^{III} in the design process (Jorritsma Bouw n.d. Projectburo B.V. 2015). The early-stage inclusion of a contractor allows its expertise to be optimally applied. Combined with UP building systems, the Design/Engineering & Build concepts can provide quick building solutions. The highly modular and repetitive UP approach to construction results in relatively simple designs: standardised elements with universal connections on a fixed grid. Consequently, the contractor is free to design an optimal support structure, within certain elemental limits set by the client.

RHDHV cooperates with project developers and (sub-)contractors to provide quick mid-price apartment building solutions, by application of the Design/Engineering & Build concepts for UP building systems (ir. J. Brouns, personal communication, February 11, 2021). By including subcontractors like CD20 in an early design phase, RHDHV aims to assist project developers in composing more efficient and less costly building designs.

1.4 | Conceptual and parametric design

The goal of the conceptual design phase is to formulate a number of design concepts that are able to satisfy the demands of the client. The characteristics of the object to be realised are defined and used to develop several fitting solutions. However, generally only a very limited number of alternatives is generated due to a limited supply of suitable computational design applications (Flager et al. 2009). Most existing computational tools focus on later stages in the

^IDesigning engineer: Engineer who produces the structural design (Kennispotaal Constructieve Veiligheid n.d.)

^{II}Non-prismatic building: building with a stability system that changes in plan over the height (Steenbergen 2007)

^{III}In contrast to "conventional" construction practice

design cycle and require a lot of details to be known in order to create highly accurate models (Rolvink 2010). The conceptual design stage is in need of applications which can facilitate more extensive design alternative exploration (see Figure 1.5). For such tools, Flager et al. (2009) propose parametric representation of a structure to provide a user with the ability to easily change variables according to the application-specific logic, thus allowing rapid, basic structural validation of a design alternative. The important task bestowed upon the developer of said application is to find the optimum between design freedom and number of required input parameters.

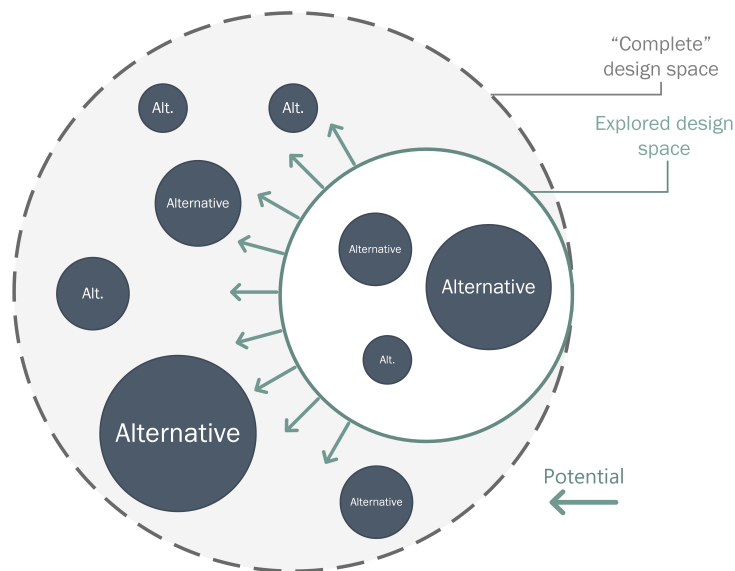


Figure 1.5: Visualisation of the conceptual design space

1.4.1 | StructuralComponents

The concept of StructuralComponents (SC) has been researched and developed for more than a decade and aims to provide structural engineers with computational design tools suitable for use in the conceptual design phase. These tools allow engineers to 'compose, define, explore, communicate and visualise structural design concepts during the early design stages' (Rolvink 2010, p.viii), in order to arrive at an optimized structure. The ideology behind SC is to provide a tool with which an engineer can compose (or replicate) a building design and quickly assess its feasibility by visualisation of relevant analysis results. For efficient design composition, so called structural components are developed. These building blocks represent parts of the structure^{IV} which can be combined to form a complete conceptual building design. The results of the structural assessment of said design are presented on a clear dashboard. The building block-dashboard approach of StructuralComponents provides engineers with tools for efficient early-stage structural design.

Of special relevance to this research, due to their similar objectives and relatively recent publications, are StructuralComponents5 (SC5) and StructuralComponents6 (SC6) by Babette Hohrath and Leah Dierker Viik respectively. An elaboration on the concise outline below is provided in Section 2.1. In her master's thesis, Hohrath (2018) developed an application for validation of the feasibility of mid-rise concrete building designs. For this, three "super elements" (Section 2.1.2), previously derived by Steenbergen (2007), were implemented in a Grasshopper tool. The feasibility checks in SC5 focused on both structural and architectural

^{IV}Not necessarily only structural parts, but also operational functionalities (e.g. assembly of elements and structural analysis calculations) can be represented by structural components

aspects. Continuing this research, Dierker Viik (2019) developed a similar tool that allowed the user more freedom in design. The engineer can design his/her own configuration of stability elements, forming a custom-made building block. This tool is suitable for prismatic building designs and assumes the floors to be infinitely rigid.

1.5 | Problem definition

The current nitrogen-plight is a substantial obstacle to the alleviation of the residential shortage in the Netherlands, especially in urban areas. Furthermore, the general challenge of a changing climate has to be faced and the construction sector is obliged to reduce its own impact on the environment, as are all branches of society. TU Delft professor of Climate Design & Sustainability Andy van den Dobbelsteen sees potential for more timber and prefab construction (Belzen 2019). As stated in Section 1.2, the construction of apartment buildings using prefabricated concrete elements could contribute to alleviation of the current residential shortage, especially with respect to the challenges posed by finite space and environmental restrictions.

The conceptual design phase would benefit from computational tools specifically suitable for exploring the large amounts of alternatives characteristic for this stage of the design process. By facilitating a simple change of variables and subsequently visualising the structural consequences, these parametric design applications should allow for broad exploration of the design space. The StructuralComponents "building-block and dashboard" concept aims to supply the wants for these computational tools capable of quick (structural) validation of conceptual designs. To arrive at such applications, an analysis model able to provide quick insight into the force flow of the structure is required.

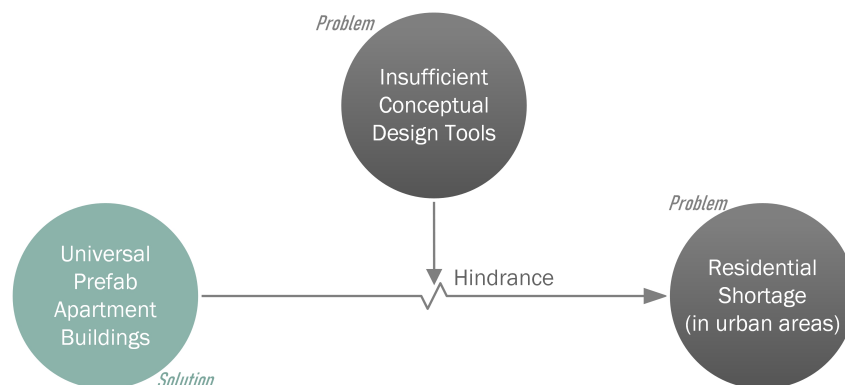


Figure 1.6: The problem definition

In addition to the potential of prefabricated structural elements, the Universal Prefab construction method (Section 1.2.1) provides the advantages of a high modularity and systematic approach to building construction. This modularity and repetition makes it exceptionally suitable for implementation in the conceptual design tools following the StructuralComponents concept: the elements and connections in every part of the building are compatible and the prefab elements themselves are already small building blocks. This would provide the tool's user with the ability to quickly construct a configuration of the standardised stability elements and visualise the results of a pre-programmed analysis procedure. The enabled broad and agile exploration of alternatives for an apartment building design brings the advantage of a more optimal design, resulting in lower costs, less environmental impact, and possibly a significantly shorter design duration.

Royal HaskoningDHV has expressed interest in such a parametric application, suitable for con-

ceptual design and preliminary analysis of Universal Prefab apartment buildings. They already provide basic validation of *existing* conceptual designs and want to develop this process, as stated in Section 1.3. Additionally, RHDHV aims to provide the construction sector with computational tools suiting the Design/Engineering & Build concepts, in which a contractor is given more influence on the design. To realise the functionalities required for such a design tool, two key challenges require attention (visualised in Figure 1.7):

1. Parametric Design: The final design tool will be applied in the *conceptual* design phase. It is necessary to develop a logic (or workflow) that constructs an analysable structural model from limited user input. The StructuralComponents "building-block and dashboard" approach can be used to supply the user with adaptable (structural) components. The combination of user input and certain predefined logic/assumptions inside the components should be sufficient to realise an analysable model from these components.
2. Structural Analysis: To acquire accurate results on the structural behaviour, the lateral behaviour of the structures under consideration has to be investigated. The accuracies of different lateral stability analysis models have to be examined. For a conceptual design, the required level of accuracy is lower than in a later design phase, the analysis model selected may reflect this.

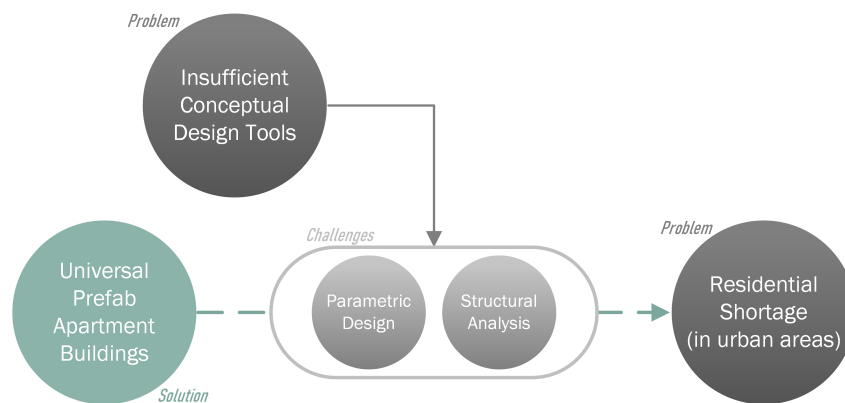


Figure 1.7: Visualisation of key challenges within the problem context

To conclude, there has been established a need for a computational tool that is able to provide insight into the structural behaviour of UP apartment building designs in the conceptual design phase. The StructuralComponents building block-dashboard approach could help satisfy this need, provided that the structural analysis model for UP apartment buildings is adequately implemented in parametrically adaptable structural components.

1.6 | Objectives

Based on the defined problem, this section formulates the main goal of this project (visualised in Figure 1.8). Subsequently, several sub-objectives are presented.

Objective | *The design and development of a conceptual design tool prototype, that provides clear and quick insight into the force distribution in Universal Prefab apartment building structures, to improve design efficiency and expand the StructuralComponents toolbox.*

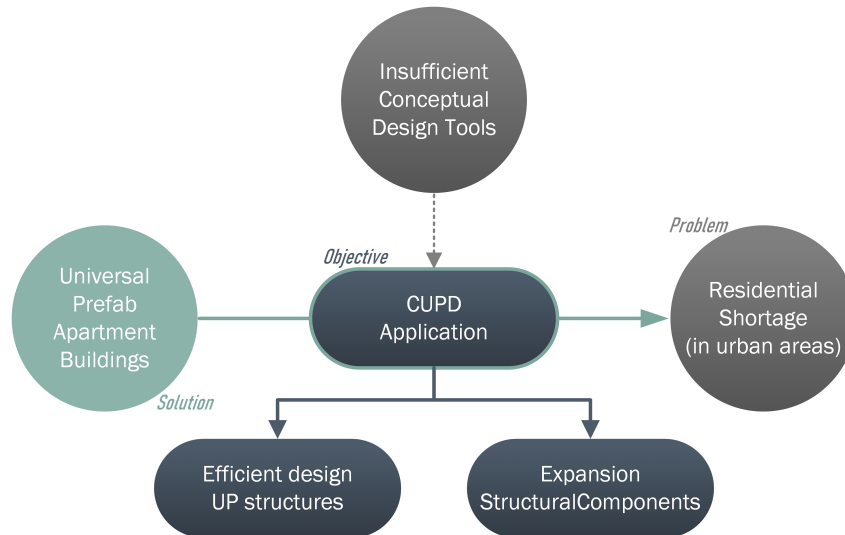


Figure 1.8: The research objective

Inspired by the goal of StructuralComponents to provide engineers with conceptual design tools, the author proposes an application – hereinafter also referred to as the CUPD Application^V. The function of this application is to enhance the efficiency of conceptual Universal Prefab apartment building design. This enables designing structural engineers to thoroughly explore the conceptual design space and potentially collaborate more efficiently with other parties present in this stage, such as an architect or client. To arrive at a sufficiently accurate analysis model suitable for conceptual designs, the structural behaviour of UP apartment buildings requires investigation. The free design composure (within certain limits, naturally) follows from a parametric implementation of the analysis model. The expansion of StructuralComponents is brought by research on its applicability for buildings with a UP structural system, as well as emphasis on the practicality of the tool and an expansion of the envelope of building designs incorporated in the SC-toolbox.

The intended users of the CUPD-application are structural engineers who are required to analyse structural behaviour in the conceptual design stage. As stated before, the proposed tool provides an estimation of the lateral load distribution over the stability walls in a composed conceptual design, using computational analysis for doing so. In accordance with the intended demographic, clear understanding of structural mechanics and UP building design is assumed present. In combination with data provided by the application, this present knowledge allows the engineer to verify the structural analysis results.

Four sub-objectives were defined based on the key challenges identified in Section 1.5. Below, these have been stated and elaborated upon; a visualisation is shown in Figure 1.9. These sub-objectives form the basis of this research: each chapter focuses on the achievement of its corresponding objective. The complete project phasing and proposed methodology are treated

^VConceptual Universal Prefab Design (CUPD)

in Section 1.7.

Sub-objective 1 | Conceptual Design of UP Apartment Buildings

Determine the capabilities a parametric tool requires to enable (more efficient) conceptual design of Universal Prefab apartment buildings.

It is of importance to investigate the functionalities and freedoms required for a conceptual design application, which is reflected by this objective. The user should be provided the proper means for efficient composure of conceptual UP building designs. Examination of the previous research projects on StructuralComponents can identify opportunities for advancement and help to avoid obstacles. Additionally, detailed elaboration of the characteristics of the Universal Prefab system can provide an understanding of the required functionalities for this structural system specifically.

Sub-objective 2 | Structural Analysis Model

Define a suitable analysis model for providing quick structural validation of the considered assortment of conceptual designs.

To achieve this objective, the author should first investigated the principles behind the structural behaviour of UP structures. The structural analysis model implemented in the proposed application should be able to provide a sufficiently accurate estimate of the structural behaviour for the envelope of incorporated designs. The required range of applicability and the analysis of *conceptual* designs pose certain requirements on the model. Therefore, the assessment of potential analysis models should be based on multiple criteria: accuracy, envelope of incorporated designs, rapidity and required user input.

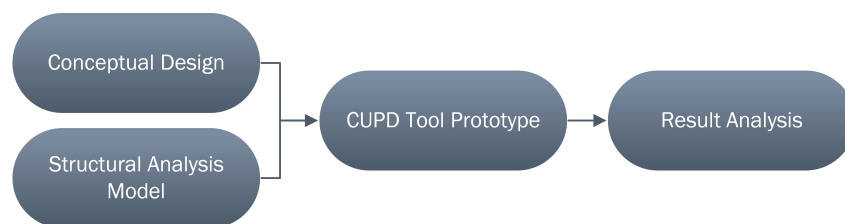


Figure 1.9: The defined sub-objectives

Sub-objective 3 | CUPD Tool Prototype

Develop a prototype of the proposed tool.

The development of a prototype allows the author to explore the possibilities and boundaries of the proposed tool. Undoubtedly, this prototype will deviate from the original design due to known and unknown unknowns. A logic has to be defined that is able to construct an analysable model from limited user input while offering the user as much design freedom as possible; a user interface has to be developed to enable a user to provide said input. Furthermore, the selected structural analysis should be programmed and the results clearly visualised. This cannot only be a theoretical exercise: the author is required to actually realise (a prototype of) the proposed application, the handling of encountered challenges and possibilities forms a crucial part of the research done for this project.

Sub-objective 4 | Result Analysis

Assess the accuracy of the implemented structural analysis model and examine the observed Universal Prefab structural behaviour.

The results of the performed structural analyses can be used to identify the characteristics of Universal Prefab structural behaviour. Knowledge of the consequences of selecting a UP

building system can support engineers in later design stages or even the development of more conceptual design tools (or the improvement of CUPD). Furthermore, assessment of the practical capabilities of the developed tool prototype outlines the boundaries of the current version and may identify opportunities for improvement. Naturally also a quantitative evaluation of the prototype's analytical capabilities is required.

1.7 | Methodology

This section outlines the main stages of the research process. Based on the research context and sub-objectives provided by the previous sections, a methodology stating the steps required to achieve the defined objective is presented.

To provide guidance, the research process has been subdivided into three phases: (1) *System Design*, (2) *Development* and (3) *Result Analysis* (Figure 1.10). Before the application is ready for development, it is important to have a thorough perception of the software architecture (or 'logic'), structural analysis model and design capabilities to be implemented. Therefore, the System Design phase concerns the achievement of Sub-objectives 1 and 2. The design of the intended application formulated in this initial phase provides a sound basis for its development (Phase 2, Sub-objective 3). The last phase, Result Analysis, aims to achieve Sub-objective 4: assessment of the tool prototype and UP structural behaviour. For each phase, a number of research questions have been defined which are answered through the completion of that phase.

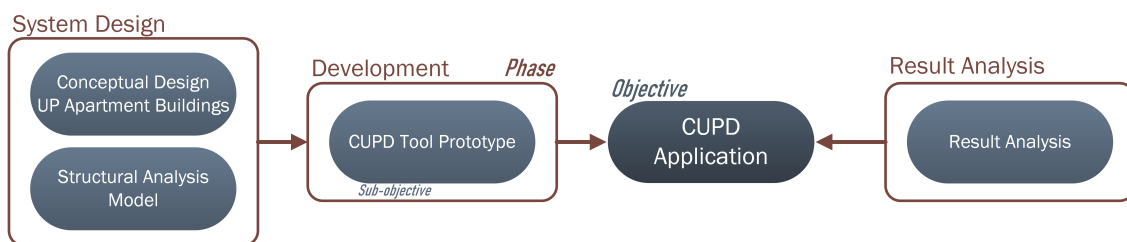


Figure 1.10: The research process

Phase 1 | System Design

The first phase has been broken down into the completion of two sub-objectives. The achievement of said objectives provides a thorough understanding of the functionalities – regarding both structural analysis and parametric design – the intended application requires.

Sub-objective 1 | A background review of the previous work on StructuralComponents is carried out, determining the strengths and weaknesses of the developed models and tools. This identifies opportunities for expansion of the toolbox, the areas in which this project can contribute. Additionally, with emphasis on the CD20 system for apartment buildings, the characteristics of the Universal Prefab structural system are outlined. Subsequently, the influence of this specific structural system on the composure of conceptual designs is assessed. Ultimately, these investigations lead to the scope definition of the intended application regarding the envelope of incorporated stability systems, the extent of the offered design freedom and incorporated/excluded features (e.g. foundational stiffness).

Sub-objective 2 | The determination of the ultimately implemented structural analysis model starts with a short elaboration of various lateral stability analysis alternatives. This elaboration of alternatives concerns their range of applicability and an estimation of their accuracy for the intended building design types. Subsequently, the structural behaviour of Universal Prefab

structures is investigated: a reference model, accurately representing the CD20 building system, is compared to a simplified model with a variable floor stiffness. Distinctive building designs are modelled to examine the influence of features such as building height and non-prismatic stability systems on the structural behaviour. In a similar manner, the accuracy of the various stability analyses is inspected for each building design. Ultimately, the approach judged to be most suitable for implementation is described in detail.

This phase will provide answers to the following research questions:

- I. What are the opportunities for expansion of the StructuralComponents-toolbox this research will focus on?
- II. What characteristics of Universal Prefab are important to consider in early-stage design?
- III. Into what kind of structural behaviour should the intended application provide insight?
- IV. What is the required accuracy for justification of conceptual designs?
- V. What is a simplified method of modelling a UP structure that is suitable for conceptual design and early-stage structural analysis?
- VI. What is a sufficiently accurate method of modelling the floor-system in Universal Prefab structures in the conceptual design phase?
- VII. What structural analysis method is suitable for analysis of the selected simplified representation and how should it be implemented to guarantee sufficient speed?

Phase 2 | Development

The second project phase concerns the development of both the lateral stability model and subsequently the realisation of the tool prototype. Based on the selected structural analysis method and the selected design functionalities, a conceptual design of the tool prototype is realised to serve as a guideline in the Development phase. The development process will undoubtedly require changes in this design, which have to be incorporated. Furthermore, an assessment is made of which analysis results are relevant for visualisation on the dashboard.

Prior to any programming, a format of the user input is defined. Based on this format and through object-oriented-programming^{VI} the building blocks of the application are programmed, containing the attributes that depend both on user input and predefined principles. The parametrically instructable structural analysis model is tested and refined till satisfactory. Subsequently, the user interface is developed in correspondence with the defined input-format and connected to the structural analysis model.

This phase will provide answers to the following research questions:

- VIII. What input-parameters are minimally required for modelling of the considered buildings in the conceptual design phase?
- IX. Based on the minimally required input, what is a sufficiently efficient procedure for the composure of conceptual Universal Prefab building designs?
- X. What procedure should be followed to generate a specific instance of the elected analysis model from the provided (limited) user input?

^{VI}'Object Oriented Programming is a programming paradigm that ... is used to structure a software program into simple, reusable pieces of code blueprints (usually called classes), which are used to create individual instances of objects.' (Doherty 2020)

Phase 3 | Result Analysis

Result assessment is an important part of the research process. The investigation into the structural behaviour of Universal Prefab will be used to outline the consequences of choosing such a structural system for a building. As stated for Sub-objective 4, this can lead to more efficient design of such buildings. To validate the implemented analysis model, its results are compared to Finite Element Analysis results. Additionally, a comparison is made to the results of other lateral stability analysis methods.

This phase will provide answers to the following research questions:

- XI. What is the accuracy of the implemented analysis model for various test-cases?
- XII. How is the force distribution effected by various characteristics of the floor- and stability-system?
- XIII. How do the results of the developed analysis model compare to existing analyses?

2 | Conceptual Design of UP Apartment Buildings

In order to determine the capabilities required for composing conceptual designs of UP apartment buildings, the practice of conceptual design is explored in this chapter. Initially, a background review of the StructuralComponents toolbox is presented, elaborating on the methods implemented in past research. Within the Engineering & Build methodology (introduced in Section 1.3), the CUPD-tool has to provide sufficient value. The increased influence of the contractor in the early design stages presents a niche for parametric design applications suitable for composition and analysis of conceptual designs. To provide insight into the structural behaviour of such designs, for UP apartment buildings specifically, an investigation is made into the characteristics of this building system.

Ultimately, this chapter provides an answer to research questions I to IV:

- I. What are the opportunities for expansion of the StructuralComponents-toolbox this research will focus on?
- II. What characteristics of Universal Prefab are important to consider in early-stage design?
- III. Into what kind of structural behaviour should the intended application provide insight?
- IV. What is the required accuracy for justification of conceptual designs?

2.1 | Background of StructuralComponents

The implementation of the structural analysis and elements in the building block-dashboard approach of SC was identified as a key challenge on the path towards a suitable tool (see the Problem definition). The review of SC5, SC6 and SC7 below, serves as a basis for the incorporation of StructuralComponents in the CUPD-application presented in Chapter 4. To give a summary of all previous work would not be relevant for this research¹.

2.1.1 | StructuralComponents 5

The objective of SC5 was to develop a tool prototype for validation of the feasibility of conceptual mid-rise concrete building designs, focusing both on structural and architectural feasibility aspects. Hohrath (2018) implemented three structural components (see Figure 2.1) which the user may combine vertically to form a building design. The analytical representations of these building blocks, originally derived as super elements by Steenbergen (2007), were re-derived with Maple and implemented manually in a Python (*Python* n.d.) library. An interface in Grasshopper (Robert McNeel & Associates n.d.) provided the dashboard for design composure and result visualisation. The Differential Super Element Method implemented in SC5 (see Section 2.1.2) allowed for the incorporation of a finite floor stiffness and therefore also composure of non-prismatic floor plan designs.

Hohrath concluded that the developed SEM-based tool was quick and flexible for conceptual

¹A summary of all published papers on StructuralComponents can be found in the master's thesis of Romero (2019) – "StructuralComponents 7".

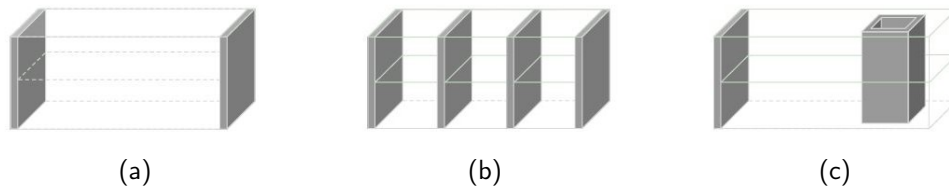


Figure 2.1: Structural components of SC5 (Hohrath 2018)

design validation and could improve the collaboration between engineers and architects if further developed for practical application.

2.1.2 | (Differential) Super Element Method

Traditionally, the Super Element Method is used to condense the degrees of freedom of super elements, which represent substructures of the complete structure (Rolvink 2010, see Figure 2.2). Their existence speeds-up the computational process and simplifies the interpretation of the modelling results (Egeland and Araldsen 1974). In his dissertation, Raphaël Steenbergen (2007) developed another method of forming super elements. The differential equations describing the super element's behaviour are derived, from which the element definition – in the form of the element stiffness matrix – follows. The model found by this analytical approach efficiently provides insight into the force flow. As stated by Steenbergen and Blaauwendraad (2007), the Differential Super Element Method (DSEM) adequately highlights which parameters characterise the structural behaviour of a building, for which Finite Element Analysis (FEA) is much less convenient.

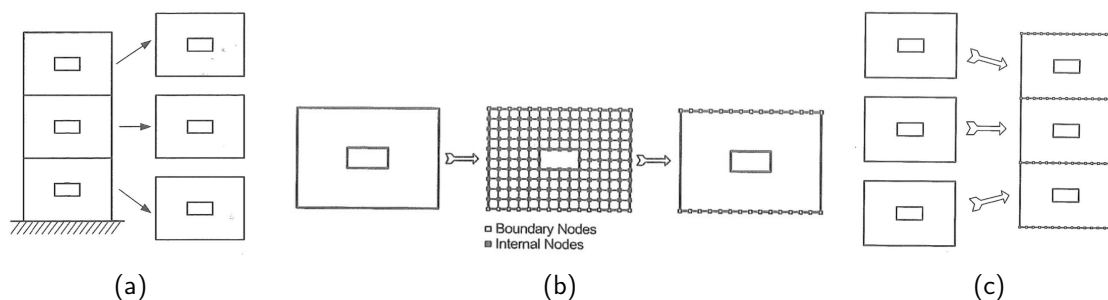


Figure 2.2: Procedure for traditional SEM (Hohrath 2018)

2.1.3 | StructuralComponents 6

Inspired by the work of Hohrath (2018), the goal of SC6 was to develop a tool that can provide 'early-stage structural validation for flexible topologies of concrete mid-rise buildings made of shear walls, cores and floors' (Dierker Viik 2019, p.10). Rather than implementation of the DSEM, Dierker Viik opted for the assumption of infinitely rigid floors. The application is able to model prismatic buildings with a rectangular floor plan, on which wind load can be applied in two directions (see Figure 2.3). The analysis model selected, further elaborated upon in Section 3.1.1, was judged to provide sufficiently accurate estimates for the *governing* deflection, shear force and bending moment if out-of-plane (OOP) floor effects are minimal.

2.1.4 | StructuralComponents 7

In his master thesis, Romero (2019) focused on the research and development of a computational tool that determines the feasibility of concrete structures in which the stabilising action is provided by a rigid frame. A study on the structural behaviour of rigid frames showed that a applicability of the conventional model – a shear beam representation – in a parametric en-

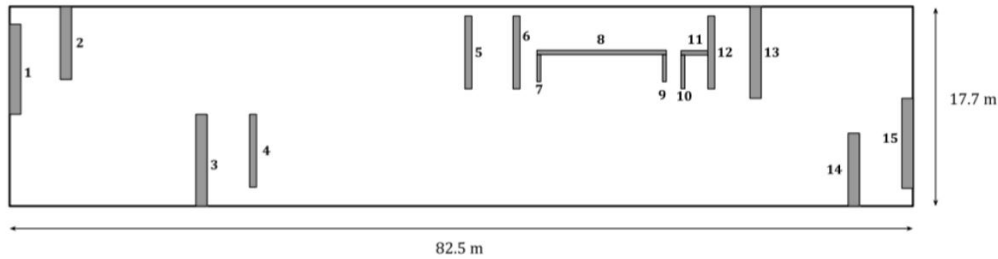


Figure 2.3: Rectangular, prismatic floor plan of SC6 case study

vironment is limited. Two new methods, a correction of the conventional model and a method based on Timoshenko beam theory, were developed and judged to be sufficiently accurate (error of less than 15%) for the conceptual design phase.

The prototype of the design application allows the user to stack two different geometries of rigid frames on top of each other. The tool estimates the shear and bending stiffness of the building blocks and the structure is calculated – following Timoshenko beam theory – as a vertical cantilever with two fields (see Figure 2.4).

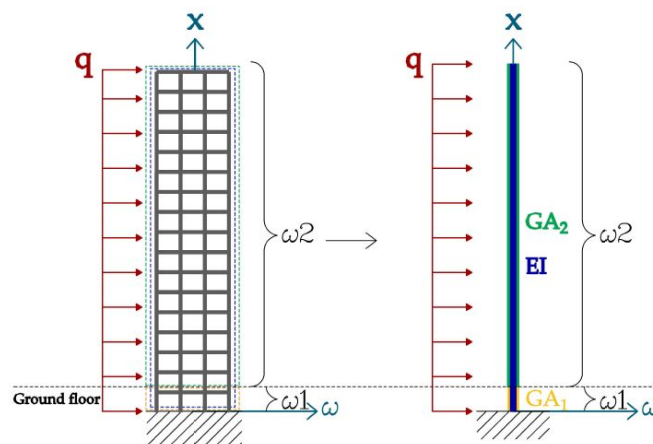


Figure 2.4: Timoshenko representation of rigid frame mid-rise building (Romero 2019)

2.1.5 | Reflection

The author definitely does not wish to depreciate previous works or authors; merely a reflection is given to identify opportunities for this thesis. The previous reports were of crucial importance to the formation of this research and a fundamental source of knowledge for the author.

In a perfect situation, one would combine the advantage of the structural analysis model of SC5 – accurate for non-rectangular, non-prismatic designs – with that of the SC6 model – free composure of floor plans, but unfortunately this was deemed unattainable (Dierker Viik 2019). This required the author to search for a different approach to the analysis of UP structural behaviour, which was documented in Chapter 3 – Structural Analysis Model. Specifically, the focus is on the combination of accurate modelling of non-prismatic designs and free composure of floor plans.

As stated clearly, one of the primary objectives of this research is the expansion of the StructuralComponents concept. Similar to SC7, this expansion is partially achieved by investigation of the behaviour of a specific structural system and the development of a corresponding analysis model suitable for implementation in structural components. Romero (2019) comprehensively

analysed rigid frame behaviour and the accuracy of the models he developed. While he thus arrived at a thoroughly substantiated structural model, the practical application of the tool (i.e. design freedom) was somewhat limited. Such practical limitations also presented itself in SC5 and SC6: the interface in Grasshopper has its limits regarding usability¹¹. Therefore, this research will not only focus on the development of an analysis model for Universal Prefab structures, but also on determination of the functionalities required to provide a StructuralComponents implementation with practical value. A balance was sought between providing the user with accurate results and sufficient design freedom and capabilities. The latter also requires a practical UI with clear visualisation and a step-by-step design process.

2.2 | Characteristics of Universal Prefab

Section 1.2.1 introduced the concept of Universal Prefab. The general characteristics of UP structural systems are presented below, to be used as a basis for the lateral stability analysis treated in Chapter 3. Special emphasis is placed on the CD20 structural system – its connections and elements – due to its relevance to this research, as stated in Section 1.2.2.

Universal connection | Characteristic for structures implementing the Universal Prefab concept is the universal connection – consistent throughout the building, enabling a kind of 'Lego'-approach to construction. While in 'regular' buildings the prefabricated elements sometimes do have rigid connections, this virtually never occurs in UP structures. The column-floor slab connection in the CD20 building system consists of pins on the end of the columns that fit into steel corner shoes on the slabs (see Figure 1.3). The corner shoe fits two pins (one from both sides of the slab), aligning the column above with the one below. The connection does not transfer bending moments and therefore out-of-plane floor effects (to a certain degree) do not influence the global structural behaviour, as illustrated in Figure 2.5. The universal connection ensures the consistency characteristic for UP building systems and enables CD20 buildings to be constructed rapidly; the elements can be lifted and placed directly from the lorry (CD20 Bouwsystemen n.d.).

Lateral load distribution | Making use of relatively thin, separate floor elements rather than a monolithic, cast in-situ floor slab requires more consideration of the horizontal load distribution. The hinged column-floor slab joint couples the floor elements together at their corners and the seam (NL: voeg) between the sides of two plates is filled with concrete. These connections enable distribution of the lateral forces through the floor slabs. The 'seam-joint' between two plates can transfer shear forces from slab to slab, but lacks the reinforcement to offer resistance in tension. At its corners, the horizontal loads on the plate are distributed over the whole lateral system by the column-floor slab connection. The horizontal stiffness of this joint is very large compared to the stiffness of the floor slabs themselves, but the complete system of thin

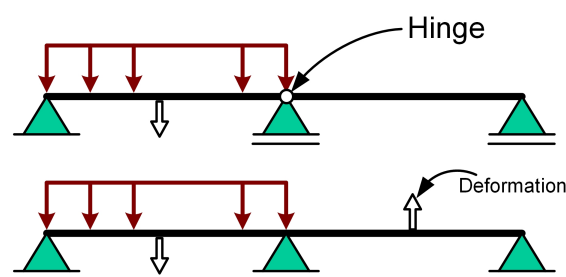


Figure 2.5: Hinged versus rigid connection of floor-slabs

¹¹A common problem with Grasshopper is the spaghetti-monster a script can become.

plates and connections has a lower stiffness than a monolithic, cast in-situ slab. Whether or not the floor system can be assumed to act as a rigid link between the stability walls depends on multiple factors (ir. S. Pasterkamp, personal communication, January 7, 2021):

- non-proportionate changes in the stability system,
- the ratio (in volume) between the floor and stability elements,
- the stiffnesses of the horizontal connections

The consequences of choosing either modelling approach are of significant influence on the analysis model ultimately selected for the CUPD-tool. Chapter 3 presents an investigation into the influence of floor stiffnesses on the global structural behaviour and whether or not the rigid-floor assumption is valid for UP building designs.

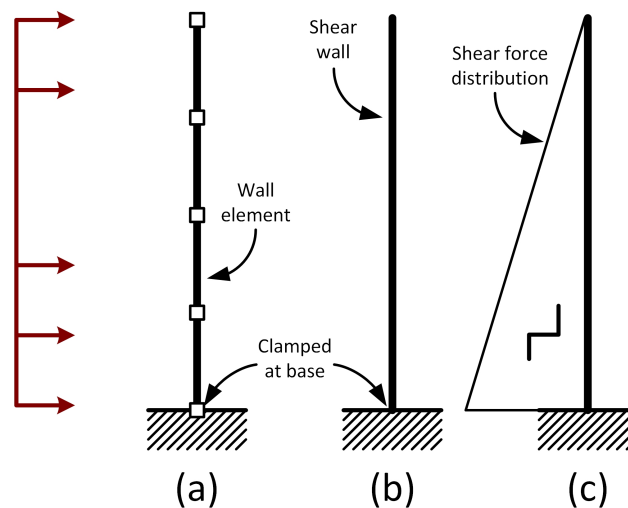


Figure 2.6: Wall elements forming a continuous shear wall, with corresponding shear force distribution

Lateral stability | As stated in the introduction of the Universal Prefab system, the lateral stability of UP apartment buildings is generally provided by a core or shear wall system or their combination; Appendix B gives a concise summary of said stability systems. In contrast to general practice, the stability elements in are not cast in-situ. To realise the required stabilising action, prefabricated wall elements are combined to a single, vertically continuous shear wall (see Figure 2.6a & b, CD20 Bouwsystemen n.d.). In this way, the modular Universal Prefab approach to construction can be maintained. Optionally, a core can be formed out of a non-planar assembly of wall elements. Shear walls forming a non-planar assembly (e.g. a T- or U-section or a core) generally behave more stiff, due to the additional support in the OOP direction. However, this collaboration is often (partially) neglected in the conceptual design phase since activation of this additional support cannot always be guaranteed (ir. J. Brouns, personal communication, April 30, 2021). The elements perpendicular to the in-plane direction of a certain wall act as a kind of flanges, providing additional stiffness. It may occur that in the upper storey(s) of the building some shear walls are terminated (i.e. the wall elements are not present on these floors), due to the lower internal shear force at this level (see Figure 2.6c). A building with a staircase design, in which a wing of the building terminates on a certain level, presents another form of non-prismatic design that regularly occurs.

Structural elements | The CD20 structural elements are produced in certain discrete dimensions, presented in the *Bouwperspectief* (CD20 Bouwsystemen n.d.). The columns – clamped at the foundation – are generally available with variable length in two different cross-sections; the choice for either depends on the height of the building. The thickness of a floor slab generally depends on its span, with an average of 200mm. In apartment buildings, a layer

of aerated concrete (NL: gasbeton) can be placed on top of the floor slab, for installations and wiring (ir. J. Brouns, personal communication, February 17, 2021). This layer has no structural contribution, but incorporation of the installations in the prefabricated floor slabs would result in a higher thickness than structurally required. The shear wall elements have an average thickness of 250mm and are rigidly connected in their vertical plane, forming a single 'continuous' cantilever. When assembled to form a core, the perpendicular wall elements are non-rigidly connected in the out-of-plane direction; Section E.1 provides an elaboration on the configuration and connection of stability walls within a UP core. Figure 2.7 summarises the general element specifications. Deviation from the standard elements is possible, but naturally translates into longer preparation and production time and higher costs.

Column	Floor slab	Stability wall
Variable length	Length: 5.4m or 7.2m	Variable length
Up to 5 stories: 200x200mm More than 5 stories: 300x300mm	Width: 3.6m	Storey height
C50/60	Thickness: 200mm (on average)	Thickness: 250mm
	C50/60	C50/60

Figure 2.7: General characteristics of prefab CD20 elements

2.2.1 | Influence on design and analysis

Applying a UP structural system poses guidelines on the composition of building designs. The CD20 building system is most efficient when equal elements (and therefore distances) are applied throughout the building. This repetitive nature requires consistent grid dimensions in which it is unfavorable to apply singular variations. The 'guided' composure of design may seem disadvantageous, but for a parametric design application it imposes some of the necessary restrictions upon the design freedom. When implementing certain logic in a parametric environment, complete freedom can never be guaranteed: the underlying processes have to function correctly for all input possibilities, which therefore have to be limited.

Regarding early-stage structural analysis, the application of a UP building system requires a somewhat different approach than for a traditional building. The lateral stability in a CD20 building is provided by a collaboration between the vertical stability walls and the floor slabs, enabled by the column-floor slab connection as elaborated upon in Section 2.2. The investigation into the modelling of such a lateral system (Section 3.2) showed that this system of hinged, discrete floor slabs behaves less stiff than a monolithic floor and cannot be assumed to act as a system of virtually rigid links between the stability walls^{III}. In a building with a non-rigid floor system, the redistribution of lateral load over the stability walls is more complex than with a rigid floor-system, especially for non-prismatic buildings (Steenbergen 2007). For the composure of conceptual UP building designs, clear insight into this lateral load distribution is crucial for the feasibility assessment of said designs. A conceptual design application would benefit from the ability to accurately predict this redistribution of lateral loads in a wide range of building designs.

^{III}The invalidity of the rigid-floor assumption for UP structures had been expected since the start of this research.

2.3 | Limited scope

Additional to its objectives, 'every project has its limitations' (Breach 2009, p.21). This section outlines the scope of the intended design application, regarding the incorporated stability systems, the extent of offered design freedom, and additional features.

2.3.1 | Structural Analysis

Mid-and high-rise buildings are subject to substantial wind loading. Therefore, lateral stability analysis plays a key role in determining the feasibility of conceptual designs. Correspondingly, the interest of RHDHV mainly lie at determination of the force distribution due to lateral loads. Furthermore, the relatively low stiffness of the floor-system complicates the redistribution of lateral loading. Consequently, this application focuses on accurate prediction of the shear force and bending moment distributions in Universal Prefab structures, due to lateral (façade) loading. The application is not intended to provide "full" design justification based on codes and/or regulations.

In the conceptual design phase, generally an error below 20% is considered sufficiently accurate (ir. S. Pasterkamp, personal communication, May 12, 2021), which will be the aim for the structural analysis accuracy.

2.3.2 | Stability systems

Modern day mid-rise (apartment) building designs are characterised by an innumerable amount of different stability systems. Needless to say, this research does not incorporate each one into the proposed prototype. This would, if at all possible, only reduce the advantage of a parametric design approach^{IV}. Therefore, the CUPD-tool aims to provide lateral load distribution calculation for the stability systems listed below:

- Shear wall system
- Core system
- The combination of both, a hybrid core-shear wall system

The systems listed above make up a large portion of UP apartment building designs (ir. J. Brouns, personal communication, January 6, 2021), making this a logical choice. Furthermore, the principle on which stability is provided is very similar for these systems, making this a logical boundary.

2.3.3 | Building designs

The focus of the design and analysis capabilities of the prototype tool are on UP apartment building designs; the general logic may be applicable on other types of buildings as well. Special emphasis has been placed on the CD20 building system, due to its relevance for RHDHV.

The performed structural analysis will include static analysis only. Dynamic analysis is regarded to be too extensive a subject to include as well. This limitation excludes buildings with a height exceeding 100 meters or a slenderness ratio larger than 1:4 (*NEN-EN 1991-1-4* 2005), often categorized as high-rise buildings.

The applicability of the proposed tool would suffer greatly if lacking the functionality to model non-prismatic type of designs. Especially staircase-type designs frequently occur for UP apartment buildings and for these designs the most hindrance is experienced in the current design practice. Their non-proportionality^V causes a more complex internal force distribution for which the relatively basic (Excel-)automated calculations are less accurate. Additionally, a somewhat

^{IV}Too wide a scope of incorporated possibilities decreases the efficiency of a parametric approach, by requiring more user input and time.

more practical implementation of non-prismatic designs with StructuralComponents would expand the current toolbox. While the accuracy of the SC5 super elements was excellent, a conceptual design tool for UP structures requires more flexibility in design. Dierker Viik (2019) took the first step towards more design freedom, with her tool for prismatic building plans. This research will aim to incorporate non-prismatic structures as well, while providing sufficient design flexibility.

Additional to non-prismatic designs, the intended application incorporates plan asymmetric structures, in which twisting occurs (see Section 3.1). The user is only able to compose rectangular floor-plans.

2.3.4 | Foundation stiffness

The influence of foundational stiffnesses will be excluded. Identical stability walls with different foundational stiffnesses will not attract the same amount of lateral load. To avoid this effect, the application will assume each wall is rigidly connected to the foundation.

2.4 | Conclusion of chapter

This chapter provides the following answers to research questions I to IV:

- I. Analysis of *non-proportionate* shear wall stability systems combined with design composition through *user-customizable* building blocks has been identified as the appropriate foundation for the application proposed by this research. Furthermore, the realisation of a tool prototype with *significant practical value* was determined to be scientifically valuable for the expansion of the StructuralComponents concept.
- II. The floor-system of discrete slabs and hinged connections is expected to be of significant influence on the lateral behaviour of UP buildings due to its relatively low stiffness.
- III. It was determined that especially relevant in an early design stage is the accurate modelling of the lateral structural behaviour and force distribution. Consequently, this research focused on the modelling of said behaviour for a wide range of building designs instead of providing integral design justification based on fixed regulations.
- IV. A model with an error below 20% would be considered sufficient for implementation in the CUPD application.

^vNon-proportionate structure: a structure in which a non-proportionate change in the stability system occurs over the height (see Section 3.1)

3 | Structural Analysis Model

To provide validation of Universal Prefab apartment building designs, their structural behaviour has to be modelled and the implemented analysis model has to be sufficiently accurate. This chapter outlines different stability analyses and presents the investigation into the structural behaviour of UP buildings. Subsequently a suitability assessment of the analyses for modelling said behaviour is performed. The analysis model chosen for implementation is elaborated in depth.

Ultimately, this chapter provides an answer to research questions V to VII:

- V. What is a simplified method of modelling a UP structure that is suitable for conceptual design and early-stage structural analysis?
- VI. What is a sufficiently accurate representation of a UP floor-system in the conceptual design phase?
- VII. What structural analysis method is suitable for analysis of the selected simplified representation of Universal Prefab structures and how should it be implemented to guarantee sufficient speed?

3.1 | Lateral stability analysis

Mid- and high-rise buildings are subject to substantial wind loading. Therefore, lateral stability analysis plays a key role in determining the feasibility of mid- and high-rise structural designs. Appendix B gives an introduction to the basics of the core and shear wall systems. Each of these systems essentially uses shear walls to provide lateral stability: their behaviour follows the same basic principles. This section elaborates upon analysis of this behaviour. First, certain characteristics of systems with shear walls are introduced. Thereafter, different analysis approaches are shortly described and a reflection is given upon a possible implementation in the proposed tool.

The book of Smith and Coull (1991) – *Tall Building Structures: Analysis and Design* – is the source of the definitions below.

Proportionality | In a proportionate structure (see Figure 3.1a), the ratio of flexural rigidity between stability walls does not change over the height of the building. Consequently, while the stiffness of a wall may change over different storeys, it will always attract the same portion of the horizontal load. When a non-proportionate change of stability elements occurs (see Figure 3.1b), a redistribution of horizontal forces takes place. This redistribution can only flow through the horizontal links between stability elements.

Twisting | If the stability walls in a structure are asymmetrically distributed about the axis of loading, this structure will be subject to rotation as well as translation. The eccentricity of the resultant load with respect to the Center of Twist (CoT) generates an additional horizontal moment¹, which is distributed proportionally over the stability walls. If a structure is *symmetric* on plan about the axis of loading, generally no twisting occurs.

¹The center of twist 'is located at the "centroid" of the flexural rigidities of the walls' (Smith and Coull 1991, p.187)

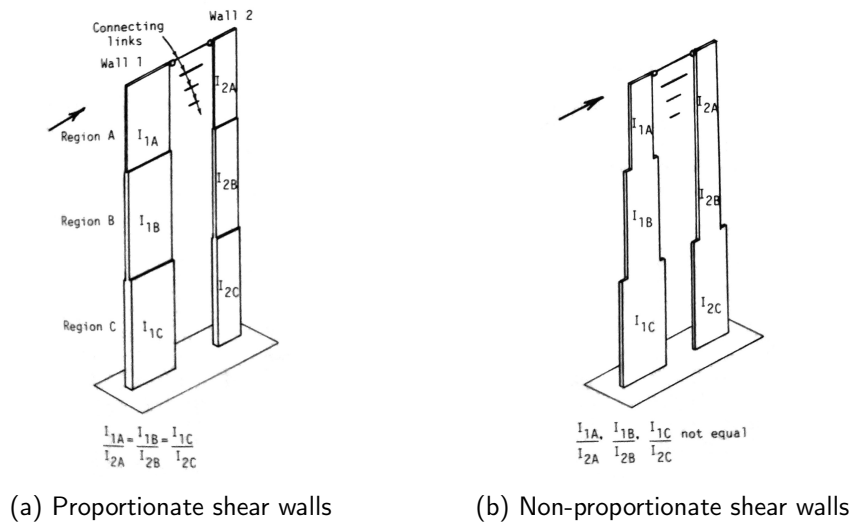


Figure 3.1: Proportionality of shear walls (Smith and Coull 1991)

Perpendicular walls | The stability walls are generally assumed to have negligible stiffness in their OOP direction. Walls orientated perpendicular to the axis of loading do therefore not contribute to the stability of the structure (in the considered direction). However, if a structure twists as well as translates, the perpendicular walls contribute to the torsional stiffness of the structure. The forces introduced by the external horizontal moment (due to the eccentricity of the loading) is distributed over all walls. In the remainder of this report, "primary walls" will indicate walls parallel to the axis of loading, while "secondary walls" indicate the perpendicular walls of the building.

The Universal Prefab structures under consideration are often proportionate, or can at least be presumed as such. However, staircase designs like the one shown in Figure 1.4, in which a whole wing is terminated at a certain level, are quite common and would certainly qualify as being non-proportionate. Section 2.3.3 already stated the importance of incorporating such non-proportionate designs in the proposed application. Hence, the ultimately selected analysis model must be able to model these types of structures accurately. In UP buildings, walls are generally placed in both directions.

3.1.1 | Analysis of proportionate structures

Proportionate structures are relatively simple to model, due to their statical determinacy. The horizontal force is divided over the stability walls proportionately to their flexural rigidity. If twisting occurs (see Figure 3.2a), the additional horizontal torque acting on the stability system has to be distributed over both the primary^{II} and secondary walls by ratio of their distance to the center of rotation.

StructuralComponents 6 | The analysis model adopted by Dierker Viik (2019) describes the behaviour of proportionate buildings assuming a rigid floor system. The model is based on the same principle^{III} as the approach outlined previously (and yields equal results), but instead estimates deflections and force distributions with a system of differential equations derived from force and moment equilibrium and displacement continuity. The results of this analytical model were compared to that of a Finite Element model. The governing deflections, shear forces and bending moments in a building with minimal OOP effects could be estimated within a difference of 10%. To guarantee this accuracy, a range of maximum allowable floor thickness

^{II}See paragraph "Perpendicular walls" for the definition of primary and secondary walls

was investigated and specified.

The methods outlined above are not suited for non-proportionate structures, especially if the floor system cannot be assumed infinitely rigid as is the case for Universal Prefab (see Section 3.2). However, proportionate analysis results provide a useful basis to which the UP structural behaviour can be compared.

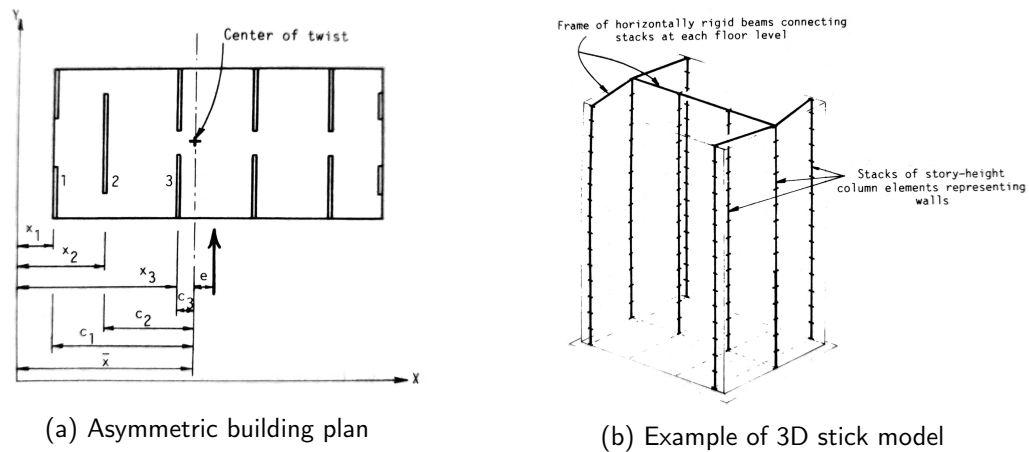


Figure 3.2: Building examples (Smith and Coull 1991)

3.1.2 | Analysis of non-proportionate structures

Accurate modelling of the behaviour of structures that see a non-proportionate change in their stability system requires a more elaborate analysis than for proportionate stability systems. As declared in the CUPD scope (Section 2.3), the intended application needs to incorporate the modelling of structures that are asymmetrical around the axis of loading. Computational software is the only practical solution for modelling such behaviour of non-proportionate structures. Smith and Coull (1991) propose a model (visualised in Figure 3.2b) in which the stability walls and floor slabs are represented by column and beam elements respectively. The stiffness properties of each wall are assigned to its corresponding column. Floor slabs linking the stability elements can be modelled as either rigid links or beam elements with finite stiffness. Subsequently, the model can be analysed with a structural analysis program. This stick-representation significantly reduces the model size with respect to a complete Finite Element model of the same building. The challenge of implementation in the proposed application lies in translation of an arbitrary building design into the stick-model: a universally applicable logic should produce an accurate representation of the lateral system.

Flat Stick model | A flat stick-model, as shown in Figure 3.3a, could simplify the representation of the lateral system by projecting all primary walls on the building's primary axis perpendicular to the axis of loading. Single beams can link the walls on neighboring grid-lines and are assigned a width equal to that of the floor-plan. The author proposes to place potentially present perpendicular walls on the primary building axis parallel to the axis of loading (see Figure 3.3b), arriving at a 'Two-dimensional Flat Stick' model.

StructuralComponents 5 & DSEM | The analysis model of Hohrath (2018) is based on the differential super elements derived by Steenbergen (2007). The major advantage of these building blocks is the non-rigid representation of the floors, which are instead represented as continuously distributed elastic springs. For the three considered structural components (visualised in Figure 2.1) the floor stiffness matrices were assembled and the differential equations

^{III}Principle: a rigid floor slab, translating and rotating.

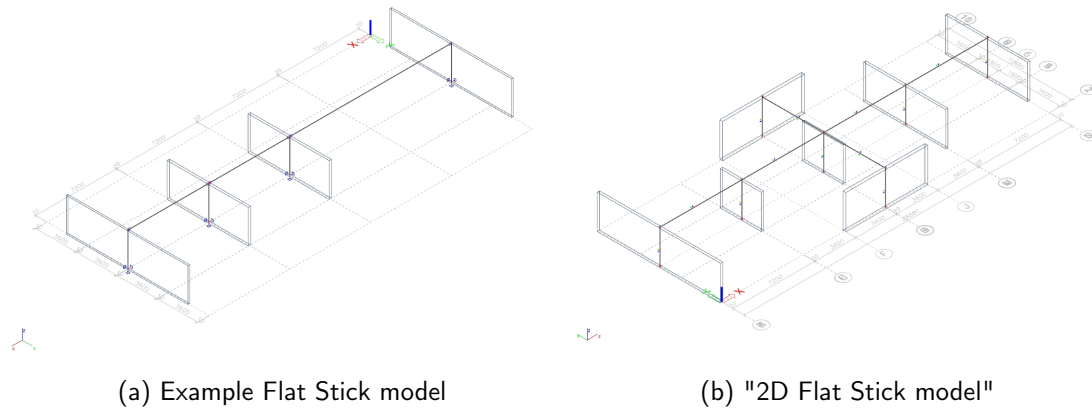


Figure 3.3

derived. From this, the element stiffness matrix of each component could be derived. In his dissertation, Steenbergen (2007) presented clear observations regarding the shear force and bending moment distributions in non-proportionate buildings and concluded that it is unacceptable to generally assume a rigid floor-system. The Differential Super Element Method provides an accurate and very rapid model for structural calculation of conceptual designs and the incorporation of non-rigid floors suits the representation of the CD20 lateral system. However, the automatisisation to allow for user-specifiable floor-plans was deemed to complex by Dierker Viik (2019), eliminating this option for the CUPD application. However, it would be interesting to discover if the ultimately implemented analysis model arrives at similar results for the shear force and bending moment distributions in non-proportionate structures. Comparison with the results of Steenbergen aids the verification (or rejection) of the CUPD analysis model and provides additional insight into the behaviour of non-proportionate structures; see Section 5.4 for this comparison.

3.2 | Structural behaviour of Universal Prefab

To guarantee lateral stability analysis with sufficient accuracy, a thorough understanding of UP behaviour is required and a basis for comparison should be established. This section outlines the definition of a detailed modelling approach for realistic Finite Element Analysis (FEA) of CD20 structures. To research the behaviour of the floor system compared to the case of rigid monolithic floor slabs, three test-cases have been analysed following said models. This provides insight into the influence of the floor-system stiffness on the redistribution of lateral loads over the stability walls. Additionally, a preliminary investigation into the accuracy of the 2D Flat Stick model (see Section 3.1.2) is performed.

3.2.1 | Reference modelling concept

A substantiated, detailed CD20 modelling method has been defined, hereinafter referred to as the 'reference' model. The decisions regarding this model have been made based on existing finite element models (courtesy of RHDHV), communication with RHDHV and TU Delft engineers and personal engineering knowledge. An example of a reference model is shown in Figure 3.4.

The grid – on which all walls and columns are placed – has x- and y-spacing corresponding to the floor-slab dimensions in x- and y-direction respectively^{IV}. On both sides of each spacing, an additional 0.01m spacing has been added for modelling purposes. The foundation is assumed to be infinitely rigid in accordance with the scope of this research: each wall and column is

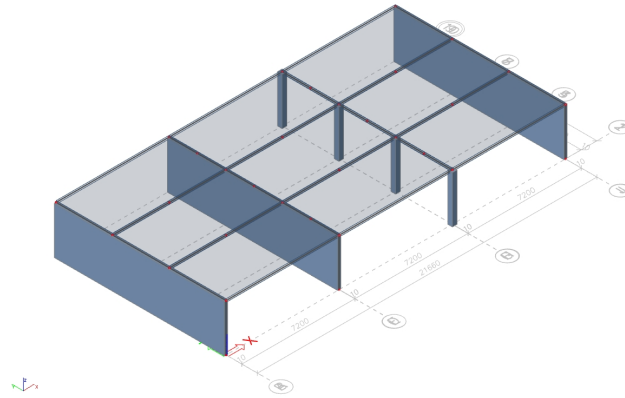


Figure 3.4: Example of reference modelling concept

clamped at the foundation, constraining every Degree of Freedom (DoF). However, all columns (of both the bottom and upper storeys) are hinged around their non-axial directions in order to prevent attracting lateral load (see Figure 3.6a). All structural elements are modelled with concrete strength class C50/60, with a Young's modulus of $37.3GPa$. The load is assumed to be a $1.45kN/m^2$ surface load on the facade (representing a wind load), which is modelled as an equivalent line load of $4.35kN/m$ on the floor slab edges. To accurately mimic the behaviour of the signature CD20 column-floor slab connection, dummy elements with specific hinges and stiffnesses have been defined (hence the additional 0.01m spacing). Their characteristics are documented in Appendix C; Figure 3.5 provides a visualisation.

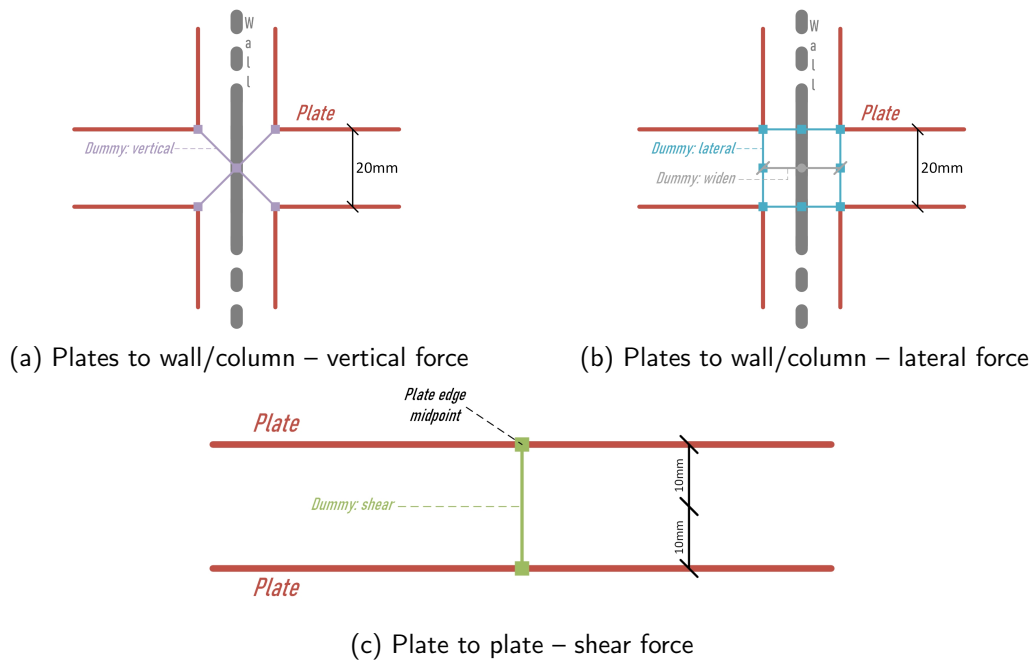


Figure 3.5: Modelled dummy elements for different connections

Monolithic model | As stated in the section's introduction, the FEM reference model behaviour is compared to a model in which the floor system is replaced with a rigid^V, monolithic slab on each grid spacing; this model is referred to as the 'monolithic' model. Rather than with dummy-elements, the slabs are connected to the walls and columns directly. The plates are

^V7.2x3.6m is a standard CD20 floor-slab size.

free to rotate in the OOP direction, as shown in Figure 3.6b.

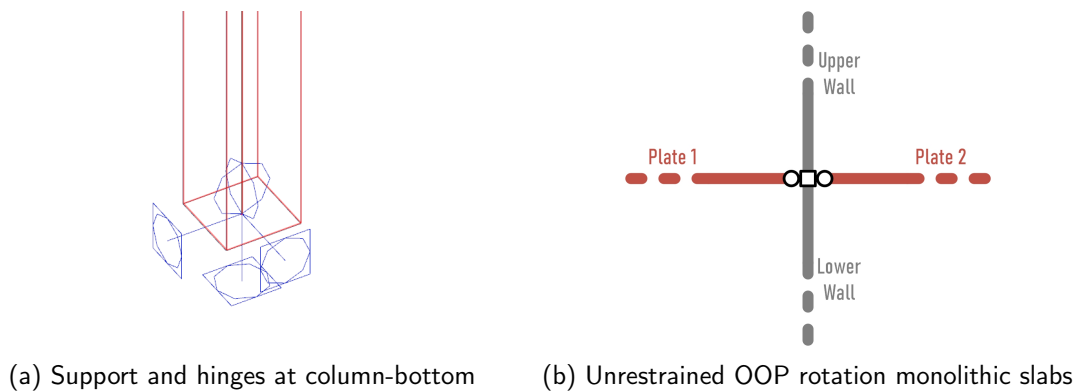


Figure 3.6

3.2.2 | Initial stick model

Based on the Universal Prefab characteristics outlined in Chapter 2 and the assessment of lateral stability analysis in Section 3.1.2, it was expected that the two-dimensional Flat Stick-model devised by the author could be suitable for implementation in the CUPD tool. To make an assessment of its suitability in the next section, a preliminary elaboration of the proposed model is provided below.

The stability walls are translated to equivalent one-dimensional (1D) column-elements with equal dimensions. Each of these stick-walls is projected on the building's principal axis perpendicular to its own in-plane direction as illustrated by Figure 3.7. The floor-system consists of 1D beam-elements as wide as the building (in their corresponding direction) with end-hinges that allow unrestrained bending in the OOP direction. Similar to the reference model, the vertical elements are clamped at the foundation. Lateral loads can be applied in both directions (X and Y); a uniformly distributed facade load is modelled as a line load along the beam elements on each floor. The composed stick representation of a building design – comprising nodes, loads, supports and one-dimensional elements – is analysed with SCIA Engineer (SCIA NV n.d.).

3D Stick Model | The section on analysis of non-proportionate buildings (3.1.2) initially introduced a three-dimensional stick representation of a building. For this, a logic would be required that is able to translate arbitrary user-input into a sufficiently accurate representation of the floor-system. A first examination of potentially valid methods showed that the resulting beam-models are likely to provide inaccurate results due to the wide envelope of potential user-input. Therefore, this model has not been subjected to further consideration.

3.2.3 | Preliminary research on UP behaviour

This section documents the analysis of six test-cases with the reference, monolithic and stick modelling concepts. This comparison aims to achieve the following:

- provide insight into lateral load redistribution in UP structures (the influence of the floor stiffness in particular),
- determine the validity of the 'rigid-floor' assumption for UP building designs,
- assess the suitability of the proposed 2D Flat Stick model

The complete results of the various test-case analyses have been documented in Appendix D

Test-cases | The defined test-cases deviate in height, proportionality and/or wall configuration. The floor-plan shown in Figure 3.8a has been analysed for one, six and ten storeys. To

^vApproximately rigid: $E=1e14$ MPa (computers do not like infinities.)

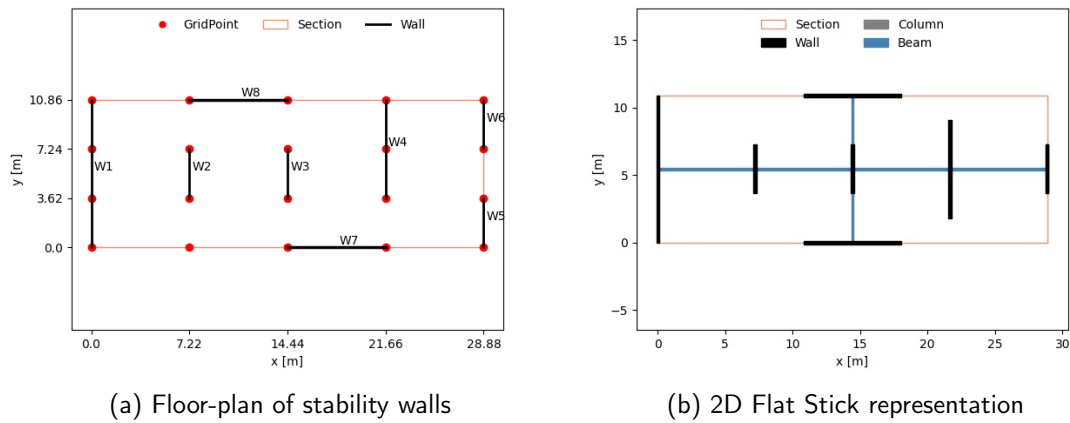


Figure 3.7: Translation of floor-plan to stick-model

investigate the addition of secondary walls the plan in 3.8b was analysed for a building with ten storeys. The six and ten storey models required additional restraining in the X-direction. On each floor, in the left front corner, a support restrains translation in the X-direction only. The effect of these lateral supports on the R_y distribution has been judged negligible. Ultimately, also a staircase-type design was modelled to investigate the

Symmetric model | To serve as a logical verification an additional symmetric test-case has been analysed; the results are presented in Table 3.1. As is required, both models show a symmetric distribution of the reaction forces in Y-direction (R_y). Furthermore, the monolithic model should (and does) equally distribute the horizontal load over all supports. The constructed models both met the symmetry conditions to a satisfactory degree.

Table 3.1: Results symmetric models

	R_y [kN]					
	Single storey			Six storey		
	Left	Middle	Right	Left	Middle	Right
Reference	-16.92	-28.97	-16.89	-117.05	-143.25	-116.49
Monolithic (Rigid)	-20.88	-20.88	-20.88	-125.47	-125.51	-125.55
Monolithic (37300MPa)	-19.60	-23.44	-19.60	-121.99	-133.17	-121.82

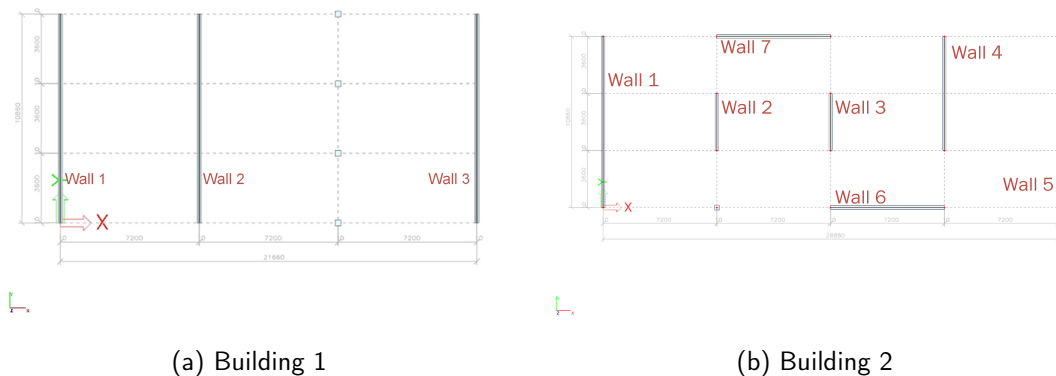


Figure 3.8

One storey building | The distribution of R_y is shown in Table 3.2, which also reports the root-mean-squared-error^{VI}(RMSE) with respect to the reference model. As expected, the monolithic model greatly overestimates the redistribution of the horizontal load: the middle wall carries more load in the reference model than in the monolithic model and vice versa for the outer walls. As a verification of the 'Monolithic-Rigid' model, the proportionate analysis (as presented in Section 3.1.1) has been performed as well. In accordance with the expected outcome, the results of both analyses match. The floor stiffness of the Monolithic model has also been decreased to illustrate its influence. The overestimation seems to reduce with decreasing stiffness of the floor-slabs. The 2D Flat Stick representation leads to very accurate results for the applied finite stiffnesses.

Table 3.2: One storey model - concise results

	R_y [kN]			RMSE [%]
	Left	Middle	Right	
Reference	-13.69	-50.33	-30.04	-
Proportionate	-26.92	-30.29	-37.02	61.82
Monolithic (Rigid)	-26.92	-30.27	-36.99	61.81
Monolithic (25000MPa)	-13.93	-49.58	-30.45	1.54
Stick (20000MPa)	-12.87	-51.23	-29.97	3.65

Six storey building | Table 3.3 shows the concise results of the analyses. The proportionate and monolithic models again produce corresponding values and overestimate the amount of redistribution, but less than for the single storey model. As was expected (see Section 2.2), the influence of the floor stiffness on the global redistribution seems smaller with increasing building height. Decreasing the E-modulus of the monolithic slabs decreases the overestimation of the redistribution, but even at $E = 5000MPa$ the outer walls still attract more load than for the reference case. The author expects this to be caused by the supports of the floor slabs; in contrast to the discrete, point-supported slabs in the reference model, the line-supported monolithic slabs restrain bending of the walls providing additional bending stiffness in this direction. For this building, the rigid floor assumption leads to acceptable results (RMSE < 20%), but is less accurate than finite stiffnesses. The 2D Flat Stick model again produces very accurate results for the applied finite stiffnesses.

Table 3.3: Six storey model - concise results

	R_y [kN]			RMSE [%]
	Left	Middle	Right	
Reference	-131.82	-218.91	-198.77	-
Proportionate	-161.52	-181.71	-222.09	17.65
Monolithic (Rigid)	-156.17	-183.07	-211.97	14.76
Monolithic (5000MPa)	-135.90	-213.08	-201.56	2.49
Stick (20000MPa)	-139.19	-215.22	-210.91	4.88

Ten storey building | The results of the ten storey building are shown in Table 3.4. The RMSE of the 'Rigid Floor' models is smaller with respect to the six and single storey designs, promoting the hypothesis that floor stiffness has less influence on the lateral redistribution in

^{VI}Root Mean Square Error (RMSE) is a standard way to measure the error of a model in predicting quantitative data.' (Moody2019)

higher buildings. For this building, the rigid floor assumption leads to acceptable results, but is less accurate than finite stiffnesses. The 2D Flat Stick model again produces very accurate results for the applied finite stiffnesses.

Table 3.4: Results ten storey models

	R_y [kN]			RMSE [%]
	Left	Middle	Right	
Reference	-243.05	-334.06	-348.20	-
Proportionate	-269.20	-302.85	-370.15	9.00
Monolithic (Rigid)	-265.97	-306.49	-362.63	7.62
Monolithic (25000MPa)	-256.27	-315.01	-356.14	3.25
Stick (Rigid)	-269.21	-302.85	-370.14	9.00
Stick (20000MPa)	-246.36	-337.14	-358.70	1.98

Ten storey building with walls in two directions | The principal results are shown in Tables 3.5 and 3.6; only the primary walls are considered. The models containing a rigid floor system show a large deviation from the reference model for wind in Y-direction, especially for the more slender walls. It seems the equal dimensions of the walls in the one-directional design, might accommodate the rigid floor assumption. This could also cause the low RMSE for wind in X-direction: the model only has two walls in this direction, of equal dimension. For wind in the Y-direction the RMSE reduces strongly with decreasing E-modulus. The 2D Flat Stick model again produces very accurate results for the applied finite stiffnesses, for both wind directions.

Table 3.5: 2D, ten storey model; wind in Y-direction - concise results

	R_y [kN]					RMSE [%]
	Wall 1	Wall 2	Wall 3	Wall 4	Wall 5	
Reference	-476.29	-72.69	-73.48	-222.64	-404.44	-
Proportionate	-563.44	-20.28	-19.69	-152.1	-499.82	49.86
Monolithic (Rigid)	-422.90	-109.69	-105.69	-240.15	-363.44	30.99
Monolithic (20000MPa)	-473.53	-73.46	-72.98	-227.63	-401.51	1.22
Stick (20000MPa)	-474.20	-74.46	-71.38	-233.66	-400.13	2.83

Table 3.6: 2D, ten storey model; wind in X-direction - concise results

	R_x [kN]		RMSE [%]
	Wall 6	Wall 7	
Reference	-235.72	-235.78	-
Proportionate	-235.75	-235.75	0.01
Monolithic (Rigid)	-229.22	-230.54	2.50
Stick (20000MPa)	-232.74	-232.74	1.27

Staircase design | To investigate the influence of a non-proportionate change in the stability system, a staircase design has been modelled as shown in Figure 3.9. The building has two 'wings' of twelve and six storeys respectively. The results of different models are shown in Table 3.7. The proportionate and monolithic models are relatively accurate compared to the previous building designs. This is not in direct accordance with the hypothesis that the floor stiffness is

of significant influence in non-proportionate designs, but can also be a result of the significantly larger height of this test-case. With decreasing floor stiffness, the deviation from the reference model reduces very slightly. The 2D Flat Stick model again produces very accurate results for the applied finite stiffnesses.

Table 3.7: Staircase model - concise results

	R_y [kN]					RMSE [%]
	Wall 1	Wall 2	Wall 3	Wall 4	Wall 5	
Reference	-301.99	-313.68	-312.35	-314.21	-263.04	-
Proportionate	-287.52	-306.67	-325.82	-344.97	-241.95	6.43
Monolithic (Rigid)	-318.31	-310.67	-303.03	-295.39	-280.12	4.84
Monolithic (20000MPa)	-304.08	-316.91	-310.64	-306.75	-269.15	1.60
Stick (Rigid)	-318.31	-310.67	-303.04	-295.40	-280.12	4.84
Stick (20000MPa)	-299.71	-319.65	-313.42	-308.36	-266.40	1.37

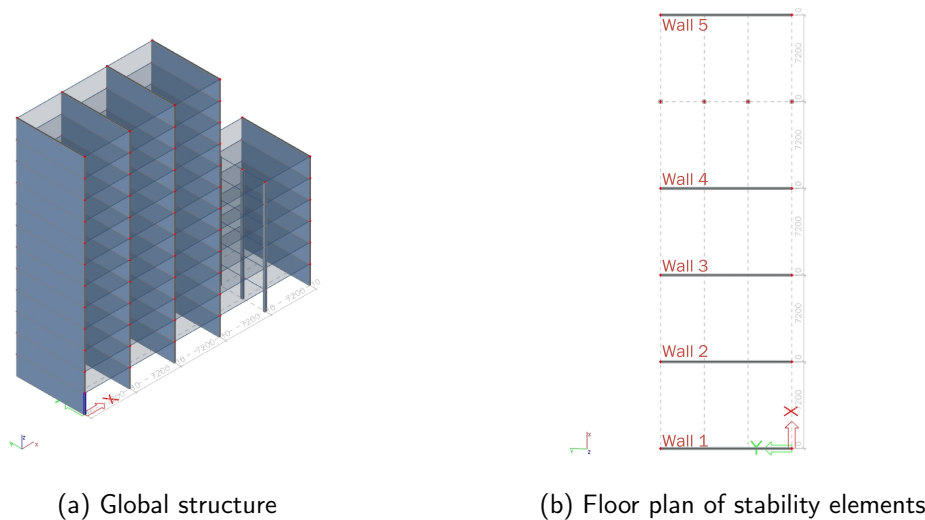


Figure 3.9: Staircase model

3.2.4 | Reflection

Based on the observations of the CD20 structural behaviour, this section reflects upon which of the lateral stability analysis models of Section 3.1 is most suitable for implementation in the CUPD-application.

The assumption of a rigid floor system simplifies the lateral stability analysis. However, this causes large overestimation of the redistribution when designing a UP structure. In accordance with the author's expectation, it was observed that lower, stockier buildings yield less accurate results than tall, slender buildings. Additionally, the model with 'perpendicular' walls illustrated that the redistribution of the load is strongly overestimated if walls of unequal dimensions are applied, even for a ten storey building. As a result, the assumption of a rigid floor is deemed invalid for conceptual design of Universal Prefab buildings.

The proposed 2D Flat Stick representation provided accurate estimation of the lateral load redistribution in the considered test-cases. Furthermore, the model is expected to meet the requirements to design freedom outlined in Chapter 2. Consequently, the '2D Flat Stick model' has been selected for implementation in the CUPD-tool prototype. Chapter 4 outlines the

model's implementation in the prototype application.

3.3 | CUPD Matrix Model

This section documents the expansion of the preliminary stick model to the ultimately implemented "Matrix Model". Named after the Matrix-Method^{VII}, this three-dimensional frame model comprises the 2D Flat Stick representation of a building design and is analysed following the frame analysis procedure outlined in Section 3.3.3. Starting with the modelling procedure, various general features are presented. Additionally, certain choices were made regarding the modelling of certain specific design cases (e.g. a core stability system or a staircase design). The research standing at the base of these choices is presented in this section. Finally, the 3D frame analysis used for calculation of the forces, moments and displacements of the stick model is elaborated upon. Section 4.3 of the next chapter describes the parametric logic that translates the designed building into the 2D Flat Stick model.

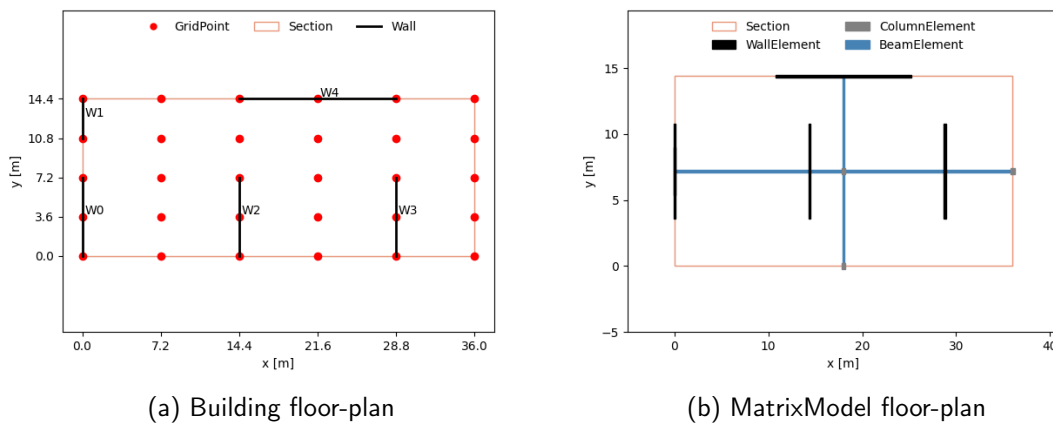


Figure 3.10: Translation from floor-plan design to stick model

The stability walls in the bottom section of the building – specified on a certain grid and with certain dimensions – are modelled as one-dimensional wall-elements and projected on the principal axes of the building (Section 3.2.2). Each wall-element has a length equal to the storey height. In case of the absence of a wall in the middle or on the borders of the section plan, a 1D column-element is generated which ensures the wind load on a section is in correspondence with its depth and width and that there always is a node at the mid-point of the building. Figure 3.10 visualises this translation.

The columns should not attract any lateral load and therefore contain several hinges at their nodes. The bottom node can freely rotate in every direction, the top node allows rotation perpendicular to central axis of the connected beam. The nodes at the ends of a beam-element are unrestrained in OOP rotation. Figure 3.11 shows the hinges and the local coordinate systems of the column- and beam-elements. The beam-elements are assigned the width of the building section in their corresponding direction.

3.3.1 | Modelling of core behaviour

The presence of a core requires a specific modelling approach. Projecting all four walls of the core separately on the primary building axes would disassemble the core; it has been established

^{VII}Also known as the matrix displacement method: "a numerical procedure to determine displacement and stress fields of a structural system under the action of applied loads. The matrix displacement method can be considered as a form of the finite element method." (Simone 2011, p.75)

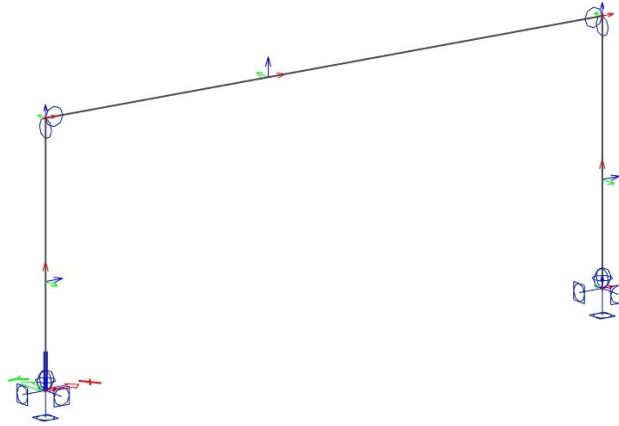
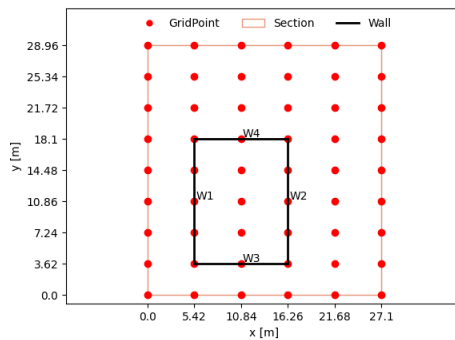
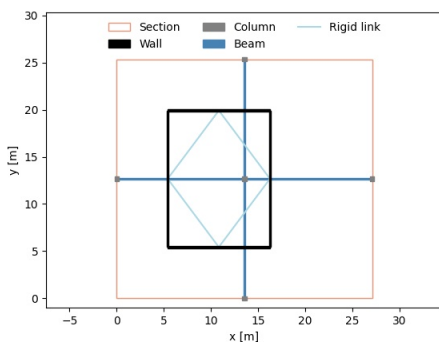


Figure 3.11: Hinges on beam- and column-ends

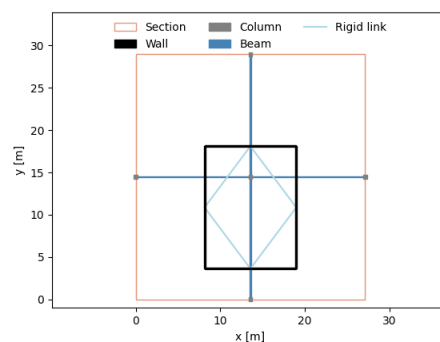
that this leads to inaccurate results. The reference modelling of a core structure as well as the investigation into different modelling approaches were documented in Appendix E. The ultimately selected modelling approach has been described below and is illustrated by Figure 3.12. It provided the most accurate results of the considered models.



(a) Core floor-plan



(b) Stick model - wind in y-dir.



(c) Stick model - wind in x-dir.

Figure 3.12: Translation from core to stick model

In accordance with standard procedure, all walls are modelled as 1D stick-elements and the primary walls of the core (the walls parallel to the axis of loading) are projected on the correct primary building axis. The secondary walls are subjected to an equal translation, preserving the size and rectangular shape of the core (i.e. the whole core is projected on the building axis perpendicular to the load). The secondary walls are not connected to the floor system of one-dimensional beam-elements. Instead, rigid links (shown in light-blue) connect the top-nodes

of the secondary wall-elements to the top-nodes of the primary ones. The rigid link end-nodes can rotate freely in the global X-Y plane.

3.3.2 | Modelling of walls on same grid-line

The building design of Figure 3.10 shows W0 and W1 on the same grid-line in Y-direction – the author proposes the term "double walls". As a consequence both stability walls are projected as wall-elements in the same location on the building's X-axis. An accurate method of redistributing lateral loads over these two walls had to be found. A study on three reference model test-cases (see Figure 3.13) showed a non-proportionate distribution over the double walls due to the limited stiffness of the lateral system and the application of the load^{VIII}: the wall in front attracts a larger portion of the load, because the load is applied on the front-side of the building only and the floor system does not act as a rigid link between the double walls. This effect decreases with increasing building height. Modelling both wall-elements on a storey with the same top- and bottom-nodes or rigidly linked top-nodes (which results in a proportionate distribution) was therefore found to be inaccurate. Therefore, a 'pseudo-beam' was added to connect the top-nodes of the double wall elements. The dimensions of this pseudo-beam were varied such that, with a stiffness equal to the stiffness of the floor-beams, the results were sufficiently accurate; the author decided upon a length and width of 1 meter and a thickness of 0.3 meters.

Table 3.8: Results double wall test-cases

	Small-small		Large-small		Small-large	
	Front	Back	Front	Back	Front	Back
2 storeys	-42.62	-23.28	-56.48	-5.26	-29.26	-21.64
4 storeys	-75.06	-54.34	-94.46	-14.63	-39.35	-61.30
8 storeys	-138.89	-117.59	-172.54	-33.44	-59.30	-137.45
12 storeys	-203.66	-182.38	-249.43	-53.51	-79.40	-214.32
20 storeys	-342.57	-321.28	-403.04	-96.42	-122.30	-368.09

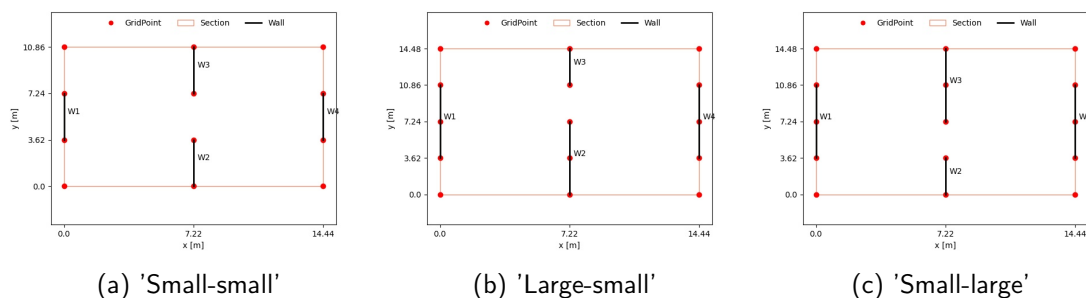


Figure 3.13: Top-views of test-cases with double walls

3.3.3 | Frame Analysis

The simplification of a building with three-dimensional prefabricated column, floor slab, and wall elements to the proposed Matrix Model allows for calculation with a three-dimensional frame analysis. The development of this analysis model, as well as its theoretical background, are the subject of this section; the analysis procedure has been realised in Python.

A proper element definition is essential for building a frame analysis program and should be used

^{VIII}A proportionate distribution over the double-walls should result in equal distributions for the 'Large-small' and 'Small-large' test-cases.

consistently. Figure 3.14 illustrates the conventions selected by the author: a local right-hand coordinate system with axes p , s , and t and a global right-hand coordinate system with axes x , y , and z . The node at each element-end (black dot) has six degrees of freedom: three displacements parallel to the local axes and three rotations around said axes. Consequently, three forces and three moments act upon each element-end, following the positive sign-convention of the coordinate system; the positive rotations and moments (following the right-hand rule) are illustrated by the axes in the upper-left corner. To describe an element with two nodes and six degrees of freedom per node, a twelve by twelve stiffness matrix is required. Below, the necessary formulas, vectors and boundary conditions are provided; the derivation of this matrix has been done with Maple (Maplesoft 2020, see Appendix F).

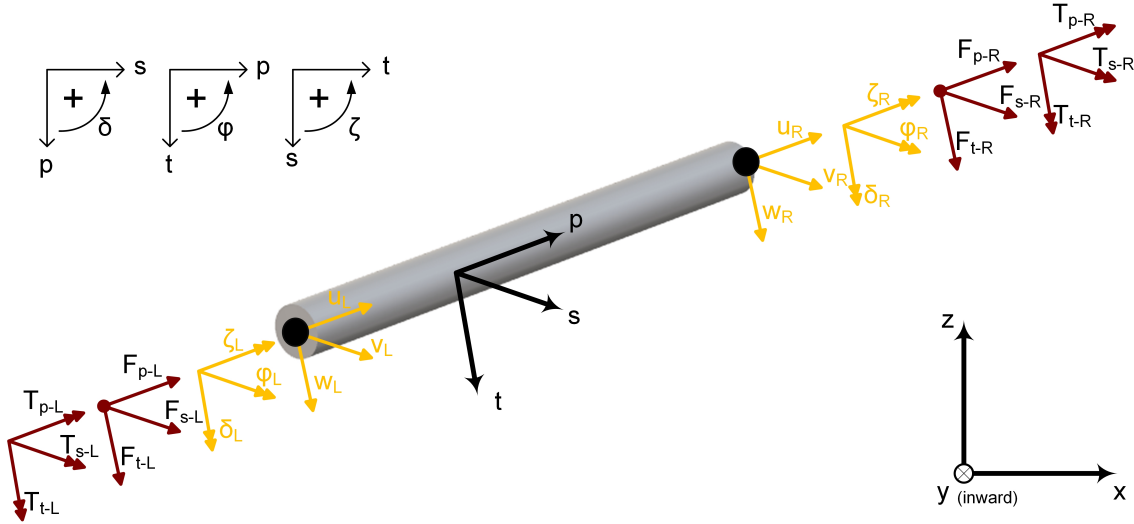


Figure 3.14: Element definition in frame analysis model

Equation 3.1 gives the element displacement vector and element force vector following from the element definition. The brackets around 'e' (for 'element') specify that the vector concerns the quantities in the Local Coordinate System (LCS).

$$\begin{aligned} \mathbf{u}^{(e)} &= \left[u_L \quad v_L \quad w_L \quad \zeta_L \quad \phi_L \quad \delta_L \quad u_R \quad v_R \quad w_R \quad \zeta_R \quad \phi_R \quad \delta_R \right]^T \\ \mathbf{f}^{(e)} &= \left[F_{pL} \quad F_{sL} \quad F_{tL} \quad T_{pL} \quad T_{tL} \quad T_{sL} \quad F_{pR} \quad F_{sR} \quad F_{tR} \quad T_{pR} \quad T_{tR} \quad T_{sR} \right]^T \end{aligned} \quad (3.1)$$

The degrees of freedom regarding axial deformation (u_L and u_R) and torsion (ζ_L and ζ_R) are uncoupled from the others. The differential equations and quantities used for the derivation of the related stiffness terms are stated below, in which I_p and m_p are the second moment of area and distributed moment around the p -axis respectively.

$$\begin{aligned} EA \cdot \frac{d^2 u}{dp^2} &= -q_p & GI_p \cdot \frac{d^2 \zeta}{dp^2} &= -m_p \\ N &= EA \cdot \frac{du}{dp} & M_p &= GI_p \cdot \frac{d\zeta}{dp} \end{aligned} \quad (3.2)$$

To incorporate both the bending and shear behaviour of the wall and floor slab elements, the remaining stiffness terms have been derived based on the Timoshenko beam theory. It was assumed that bending and shear in the p - s -plane are uncoupled from bending and shear p - t -plane. The differential equations and definitions of force- and deformation-quantities are given below (Equation 3.3: translation in the t -direction and rotation around the s -axis; Equation

3.4: translation in the s -direction and rotation around the t -axis).

$$\begin{aligned}
 \gamma_t &= \frac{dw}{dp} + \phi; & \kappa_s &= \frac{d\phi}{dp} \\
 V_t &= GA_{eff,t} \cdot \gamma_t = GA_{eff,t} \left(\frac{dw}{dp} + \phi \right) \\
 M_s &= EI_s \cdot \kappa_s = EI_s \frac{d\phi}{dp} \\
 \frac{dV_t}{dp} &= -q_t; & \frac{dM_s}{dp} &= V_t \\
 EI_s \frac{d^2\phi}{dp^2} - GA_{eff,t} \left(\frac{dw}{dp} + \phi \right) &= 0 \\
 GA_{eff,t} \left(\frac{d^2w}{dp^2} + \frac{d\phi}{dp} \right) &= -q_t
 \end{aligned} \tag{3.3}$$

$$\begin{aligned}
 \gamma_s &= \frac{dv}{dp} - \delta; & \kappa_t &= \frac{d\delta}{dp} \\
 V_s &= GA_{eff,s} \cdot \gamma_s = GA_{eff,s} \left(\frac{dv}{dp} - \delta \right) \\
 M_t &= -EI_t \cdot \kappa_t = -EI_t \frac{d\delta}{dp} \\
 \frac{dV_s}{dp} &= -q_s; & \frac{dM_t}{dp} &= V_s \\
 EI_t \frac{d^2\delta}{dp^2} + GA_{eff,s} \left(\frac{dv}{dp} - \delta \right) &= 0 \\
 GA_{eff,s} \left(\frac{d^2v}{dp^2} - \frac{d\delta}{dp} \right) &= -q_s
 \end{aligned} \tag{3.4}$$

To determine the integration constants and arrive at expressions for each nodal load, twelve boundary conditions are required; these are listed below. Additionally, the forces at each element end are defined with respect to the force quantities stated above.

$$\begin{aligned}
 (1) \rightarrow u(0) &= u_L & F_{pL} &= -N|_{p=0} & (7) \rightarrow u(L) &= u_R & F_{pR} &= N|_{p=L} \\
 (2) \rightarrow v(0) &= v_L & F_{tL} &= -V_t|_{p=0} & (8) \rightarrow v(L) &= v_R & F_{tR} &= V_t|_{p=L} \\
 (3) \rightarrow w(0) &= w_L & F_{sL} &= -V_s|_{p=0} & (9) \rightarrow w(L) &= w_R & F_{sR} &= V_s|_{p=L} \\
 (4) \rightarrow \zeta(0) &= \zeta_L & T_{pL} &= -M_p|_{p=0} & (10) \rightarrow \zeta(L) &= \zeta_R & T_{pR} &= M_p|_{p=L} \\
 (5) \rightarrow \phi(0) &= \phi_L & T_{sL} &= -M_s|_{p=0} & (11) \rightarrow \phi(L) &= \phi_R & T_{sR} &= M_s|_{p=L} \\
 (6) \rightarrow \delta(0) &= \delta_L & T_{tL} &= M_t|_{p=0} & (12) \rightarrow \delta(L) &= \delta_R & T_{tR} &= -M_t|_{p=L}
 \end{aligned} \tag{3.5}$$

Ultimately, from the expression of each of the element-end loads, the terms corresponding to a single degree of freedom are extracted and placed in the twelve-by-twelve stiffness matrix at the appropriate location. For example, the term representing the influence of a rotation of the right node around the s -axis (ϕ_R , the eleventh degree of freedom) on the force in the t -direction at the left element-end (F_{tL} , the third nodal load) is placed at the eleventh column of the third row. After assembly of the element stiffness matrix, the element is described by the following

expression:

$$\mathbf{f}^{(e)} = \mathbf{K}^{(e)} \mathbf{u}^{(e)} \quad (3.6)$$

with:

$$\mathbf{K}^{(e)} = \begin{bmatrix} \frac{EA}{L} & 0 & 0 & 0 & 0 & 0 & -\frac{EA}{L} & 0 & 0 & 0 & 0 & 0 \\ 0 & \frac{12EI_t}{L^3(\chi_v+1)} & 0 & 0 & 0 & \frac{6EI_t}{L^2(\chi_v+1)} & 0 & -\frac{6EI_t}{L^2(\chi_v+1)} & 0 & 0 & 0 & \frac{6EI_t}{L^2(\chi_v+1)} \\ 0 & 0 & \frac{12EI_s}{L^3(\chi_w+1)} & 0 & -\frac{6EI_s}{L^2(\chi_w+1)} & 0 & 0 & 0 & -\frac{12EI_s}{L^3(\chi_w+1)} & 0 & -\frac{6EI_s}{L^2(\chi_w+1)} & 0 \\ 0 & 0 & 0 & \frac{GI_p}{L} & 0 & 0 & 0 & 0 & 0 & -\frac{GI_p}{L} & 0 & 0 \\ 0 & 0 & -\frac{6EI_s}{L^2(\chi_w+1)} & 0 & \frac{(4+\chi_w)EI_s}{L(\chi_w+1)} & 0 & 0 & 0 & \frac{6EI_s}{L^2(\chi_w+1)} & 0 & \frac{(2-\chi_w)EI_s}{L(\chi_w+1)} & 0 \\ 0 & -\frac{6EI_t}{L^2(\chi_v+1)} & 0 & 0 & 0 & \frac{(4+\chi_v)EI_t}{L(\chi_v+1)} & 0 & -\frac{6EI_t}{L^2(\chi_v+1)} & 0 & 0 & 0 & \frac{(2-\chi_v)EI_t}{L(\chi_v+1)} \\ -\frac{EA}{L} & 0 & 0 & 0 & 0 & 0 & \frac{EA}{L} & 0 & 0 & 0 & 0 & 0 \\ 0 & -\frac{12EI_t}{L^3(\chi_v+1)} & 0 & 0 & 0 & -\frac{6EI_t}{L^2(\chi_v+1)} & 0 & \frac{6EI_t}{L^2(\chi_v+1)} & 0 & 0 & 0 & -\frac{6EI_t}{L^2(\chi_v+1)} \\ 0 & 0 & -\frac{12EI_s}{L^3(\chi_w+1)} & 0 & \frac{6EI_s}{L^2(\chi_w+1)} & 0 & 0 & 0 & \frac{12EI_s}{L^3(\chi_w+1)} & 0 & \frac{6EI_s}{L^2(\chi_w+1)} & 0 \\ 0 & 0 & 0 & -\frac{GI_p}{L} & 0 & 0 & 0 & 0 & 0 & \frac{GI_p}{L} & 0 & 0 \\ 0 & 0 & -\frac{6EI_s}{L^2(\chi_w+1)} & 0 & \frac{(2-\chi_w)EI_s}{L(\chi_w+1)} & 0 & 0 & 0 & \frac{6EI_s}{L^2(\chi_w+1)} & 0 & \frac{(4+\chi_w)EI_s}{L(\chi_w+1)} & 0 \\ 0 & \frac{6EI_t}{L^2(\chi_v+1)} & 0 & 0 & 0 & \frac{(2-\chi_v)EI_t}{L(\chi_v+1)} & 0 & -\frac{6EI_t}{L^2(\chi_v+1)} & 0 & 0 & 0 & \frac{(4+\chi_v)EI_t}{L(\chi_v+1)} \end{bmatrix}$$

and:

$$\chi_v = \frac{EI_t \cdot GA_{eff,s} \cdot L^2}{12}; \quad \chi_w = \frac{EI_s \cdot GA_{eff,t} \cdot L^2}{12}$$

The element load vector $\mathbf{f}^{(e)}$ contains both the loads at the nodes and equivalent loads at the nodes due to loads at the element (see Equation 3.7). Since only distributed loads are relevant for this project, only those have been considered in the derivation of the equivalent load vector.

$$\mathbf{f}^{(e)} = \mathbf{f}^{(e,nodal)} + \mathbf{f}^{(e,eq)} \quad (3.7)$$

with:

$$\mathbf{f}^{(e,eq)} = \left[\frac{1}{2}q_p L \quad \frac{1}{2}q_s L \quad \frac{1}{2}q_t L \quad 0 \quad -\frac{1}{12}q_t L^2 \quad \frac{1}{12}q_s L^2 \quad \frac{1}{2}q_p L \quad \frac{1}{2}q_s L \quad \frac{1}{2}q_t L \quad 0 \quad \frac{1}{12}q_t L^2 \quad -\frac{1}{12}q_s L^2 \right]^T$$

Each element definition can be converted to the global coordinate system with a three-dimensional transformation matrix \mathbf{T} . Rotation matrix \mathbf{R} summarizes the mutations necessary to rotate the global axes to the (local) element axes. The rotation-angles follow from the orientation of each element with respect to the global coordinate system, which have been visualised in Figure 3.15.

$$\mathbf{f}^e = \mathbf{T}^T \mathbf{f}^{(e)} \quad \text{and} \quad \mathbf{u}^e = \mathbf{T}^T \mathbf{u}^{(e)} \quad \text{and} \quad \mathbf{K}^e = \mathbf{T}^T \mathbf{K}^{(e)} \mathbf{T}^T \quad (3.8)$$

$$\mathbf{T} = \begin{bmatrix} \mathbf{R} & \mathbf{O}_{3,3} & \mathbf{O}_{3,3} & \mathbf{O}_{3,3} \\ \mathbf{O}_{3,3} & \mathbf{R} & \mathbf{O}_{3,3} & \mathbf{O}_{3,3} \\ \mathbf{O}_{3,3} & \mathbf{O}_{3,3} & \mathbf{R} & \mathbf{O}_{3,3} \\ \mathbf{O}_{3,3} & \mathbf{O}_{3,3} & \mathbf{O}_{3,3} & \mathbf{R} \end{bmatrix} \quad \text{with} \quad \mathbf{O}_{3,3} = \begin{bmatrix} 0 & 0 & 0 \\ 0 & 0 & 0 \\ 0 & 0 & 0 \end{bmatrix} \quad (3.9)$$

The wall-, column-, and beam-elements differ slightly in their characteristics. As stated in Section 2.2, the beam-elements should not resist out-of-plane bending (around their s -axis). For the derivation of the stiffness matrix, boundary conditions 5 and 11 change according to Equation 3.10.

$$(5) \rightarrow M_s|_{p=0} = 0 \quad \text{and} \quad (11) \rightarrow M_s|_{p=L} = 0 \quad (3.10)$$

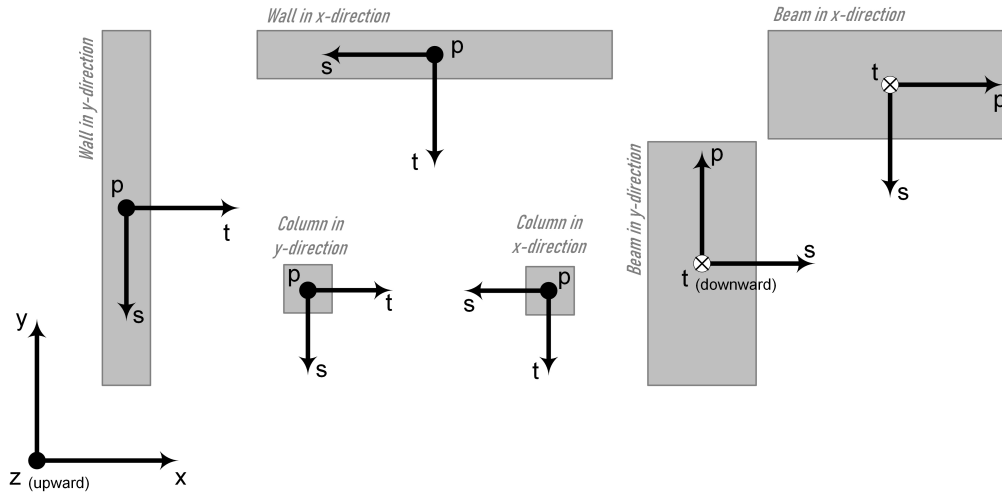


Figure 3.15: Local coordinate systems of structural elements

The bottom-node of a column-element is unrestrained in rotation the element's s - and t -axes. This changes boundary conditions 5, 6, 10 and 12 (see Equation 3.11). If a column is present in the middle of the building (at the intersection of the beams), rotation around the t -axis is not unrestrained at the top-node (condition 12 remains unchanged). This configuration of element-end hinges prevents the attraction of lateral load to the columns.

$$\begin{aligned}
 (5) &\rightarrow M_s|_{p=0} = 0 & \text{and} & \quad (6) \rightarrow M_t|_{p=0} = 0 \\
 (10) &\rightarrow M_p|_{p=L} = 0 & \text{and} & \quad (12) \rightarrow M_t|_{p=L} = 0
 \end{aligned}
 \tag{3.11}$$

From all local stiffness matrices and load vectors, the global stiffness matrix \mathbf{K} and load vector \mathbf{f} are assembled, resulting in Equation 3.12.

$$\mathbf{f} = \sum \mathbf{f}^{e,nodal} + \sum \mathbf{f}^{e,eq} = \mathbf{K} \bullet \mathbf{u}
 \tag{3.12}$$

For the restrained degrees of freedom (DoF), the corresponding row and column of the complete stiffness matrix and load vector are altered according to the procedure illustrated by Figure 3.16. The pivot element of the row corresponding to the restrained DoF is set to 1, while the other row and column terms are set to 0.

$$\begin{bmatrix} f_1 \\ f_2 \\ f_3 \\ \vdots \\ f_m \end{bmatrix} = \begin{bmatrix} k_{11} & k_{12} & k_{13} & \cdots & k_{1n} \\ k_{21} & k_{22} & k_{23} & \cdots & k_{2n} \\ k_{31} & k_{32} & k_{33} & \cdots & k_{3n} \\ \vdots & \vdots & \vdots & \ddots & \vdots \\ k_{m1} & k_{m2} & k_{m3} & \cdots & k_{mn} \end{bmatrix} \cdot \begin{bmatrix} a_1 \\ a_2 \\ a_3 \\ \vdots \\ a_m \end{bmatrix} \Rightarrow \begin{bmatrix} f_1 \\ R_2 + f_2^{eq} \\ f_3 \\ \vdots \\ f_m \end{bmatrix} = \begin{bmatrix} k_{11} & 0 & k_{13} & \cdots & k_{1n} \\ 0 & 1 & 0 & \mathbf{0}^T & 0 \\ k_{31} & 0 & k_{33} & \cdots & k_{3n} \\ \vdots & \vdots & \vdots & \ddots & \vdots \\ k_{m1} & 0 & k_{m3} & \cdots & k_{mn} \end{bmatrix} \cdot \begin{bmatrix} a_1 \\ 0 \\ a_3 \\ \vdots \\ a_m \end{bmatrix}$$

Figure 3.16: Matrix 'row-striking' procedure

The non-zero degrees of freedom can now be solved. In combination with the restrained DoFs, the complete displacement vector \mathbf{u} is found and used to calculate the nodal loads, the support reactions in particular.

$$\begin{aligned}
 \mathbf{u}_{\text{nonzero}} &= \mathbf{K}_{\text{reduced}}^{-1} \bullet \mathbf{f}_{\text{reduced}} \\
 \mathbf{u} &= \mathbf{u}_{\text{restrained}} \text{ " + " } \mathbf{u}_{\text{nonzero}} & (\text{" + " = 'combined with'}) \\
 \mathbf{f}_{\text{nodal}} &= \mathbf{K} \bullet \mathbf{u} - \mathbf{f}^{eq}
 \end{aligned}
 \tag{3.13}$$

3.4 | Conclusion of chapter

This chapter provides the following answers to research questions V to VII:

- V. For the analysis of Universal Prefab structures the 2D Flat Stick model (or 'Matrix-Model') was devised. This representation, modelling all two-dimensional elements as one-dimensional (stick-)elements, greatly reduces the number of degrees of freedom with respect to Finite Element Analysis while still offering the possibility of a non-rigid floor-system, which was found to be crucial for the modelling of Universal Prefab structures. Furthermore, its implementation in a parametric environment enables the composition of a wide envelope of stability wall configurations.
- VI. In the MatrixModel, the floor-system of slabs and hinges is represented by beams spanning from wall-column to wall-column. The beams are assigned the width of the building in their corresponding direction and their nodes do not restrain out-of-plane bending of these floor-beams. The beams are assigned a finite stiffness in the order of magnitude of the wall-stiffness. This representation has been proven to be sufficiently accurate for analysis in the conceptual design phase.
- VII. A 3D frame analysis implemented in Python scripts is sufficiently quick and well-suited for the analysis of the devised MatrixModel representation of a conceptual building design.

4 | CUPD Tool Prototype

Sub-objective 3 states the importance of the development of a prototype of the proposed application. The sections of this chapter document the development of the system architecture and user interface and the capacities and limitations of the realised tool prototype.

Ultimately, this chapter provides an answer to research questions VIII to X:

- VIII. What input-parameters are minimally required for modelling of the considered buildings in the conceptual design phase?
- IX. Based on the minimally required input, what is a sufficiently efficient procedure for the composure of conceptual Universal Prefab building designs?
- X. What procedure should be followed to generate a specific instance of the elected analysis model from the provided (limited) user input?

4.1 | System architecture

The complete application has been programmed with Python. Prior to any software development however, a conceptual outline of the software infrastructure was designed. Ultimately, a collaboration between a user-interface and a parametrically implemented frame analysis had to be realised. The object-oriented-programming paradigm was selected as the main programming strategy based on the prior experience of the author and its structured character. Following this strategy, the author defined various classes: reusable components of code which possess certain predetermined logic and require certain user-input, for example the BuildingSection class. For the generation of a BuildingSection instance (or object¹) input is required, with which the embedded logic determines the values of various attributes; such a BuildingSection represents one particular prismatic part of the building. Figure 4.1 shows three classes along with a selection of their attributes and interdependencies in a database format.

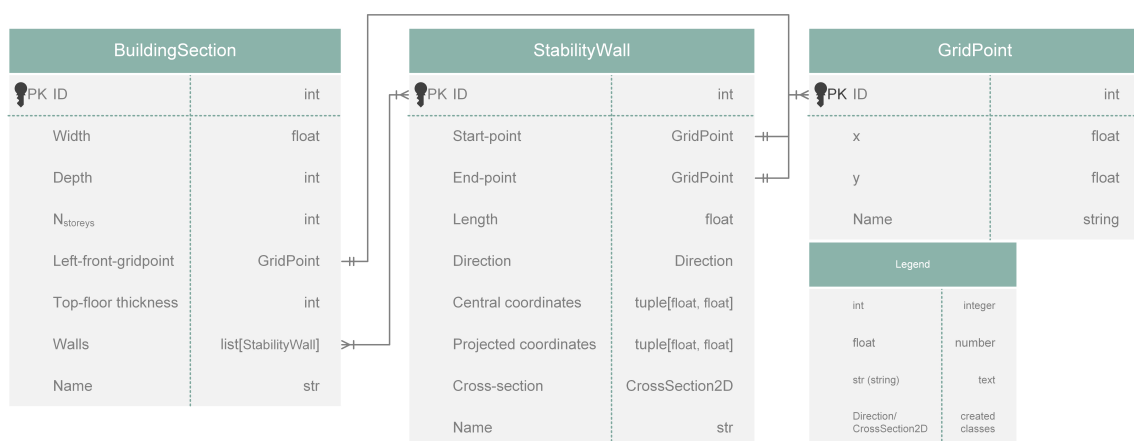


Figure 4.1: Classes with attributes

Based on the pre-determined classes, a large portion of the tool prototype was developed and the Matrix Model was implemented in a parametric environment. This enabled the generation

¹According to codementor.io (Donovan 2020): a Class is a reusable piece of code that can be used as a blueprint, creating similar Objects; an Instance is one particular Object.

and analysis of the 2D Flat Stick representation for a wide range of conceptual building designs. For various test-cases – differing in height, wall-configuration, non-proportionality, and stability system – a FEM reference model^{II} was created and analysed with SCIA Engineer. The analysis results regarding base shear and top-deflection were compared to the results of the CUPD Matrix Model to assess its accuracy. The results of this assessment can be found in Chapter 5.

Figure 4.2 visualises the system architecture of the developed tool. The three Controller entities represent the back-bone of the program. The interactions of the user with the UI are interpreted by the InterfaceController. Depending on the request, a figure is generated, a model assembled, a project saved/opened, etcetera. The Building- and AnalysisController entities contain functions (also called 'methods') with which, respectively, the Building- and MatrixModel objects can be generated and analysed. The former consists of BuildingSection and StabilityWall objects and forms a crude representation of the designed structure. The latter, the 2D Flat Stick representation of the structure, contains all one-dimensional structural elements and their definitions (stiffness and transformation matrices, load vectors, nodes, etc.). The results of the 3D frame analysis are documented in a ModelResults object and visualised on the UI. A concise documentation of the flow-of-logic in the program is given by Section 4.3.

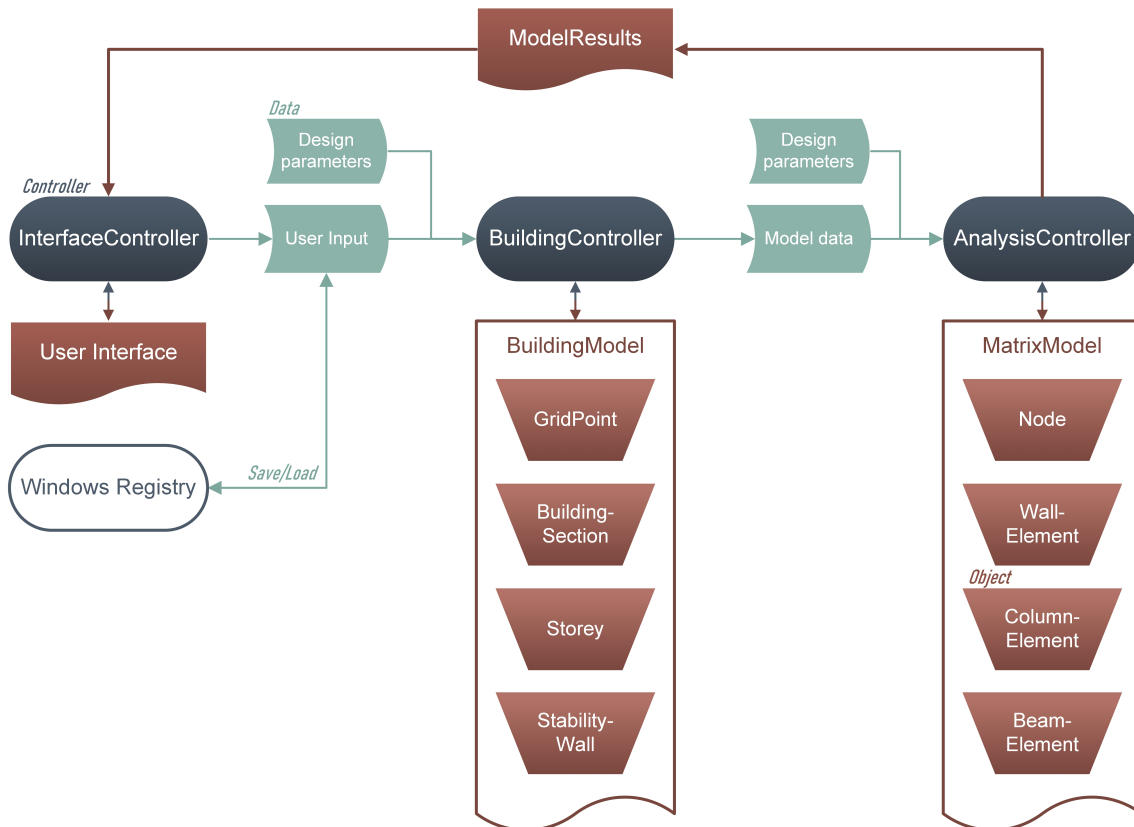


Figure 4.2: System architecture

4.2 | User-Input & -Interface

To achieve the intended expansion of StructuralComponents regarding the practical application of the conceptual design tool, a working User Interface was designed and developed. This encouraged the reflection on efficient methods for acquiring the necessary user-input and present-

^{II}The reference modelling approach was documented in Section 3.2.1

tation of the relevant results. The interface was programmed using PyQt5, a Python package for development of graphical user interfaces with the Qt libraries^{III}.

To illustrate the design of the interface, the 'Main' tab is shown in Figure 4.3; the complete UI has been visualised in Appendix G. The User Interface comprises several tabs, a menu-bar, and a toolbar. Using the menu-bar (A), the user is able to open a new or existing project, save the present input (either in the current, a new or an existing project), and delete projects. Saved input is stored as a project in the Windows Registry (see Figure 4.2). The toolbar (B) comprises several action-buttons for the addition of a new section-tab, the generation of the Building- or MatrixModel, and the execution of the analysis. The main area (C) contains input fields for general quantities. The grid table (E) and section-order table (F) are used to define the grid and the order of building sections. The grid plot (G) and section diagram (H) provide visual feedback on the user's input.

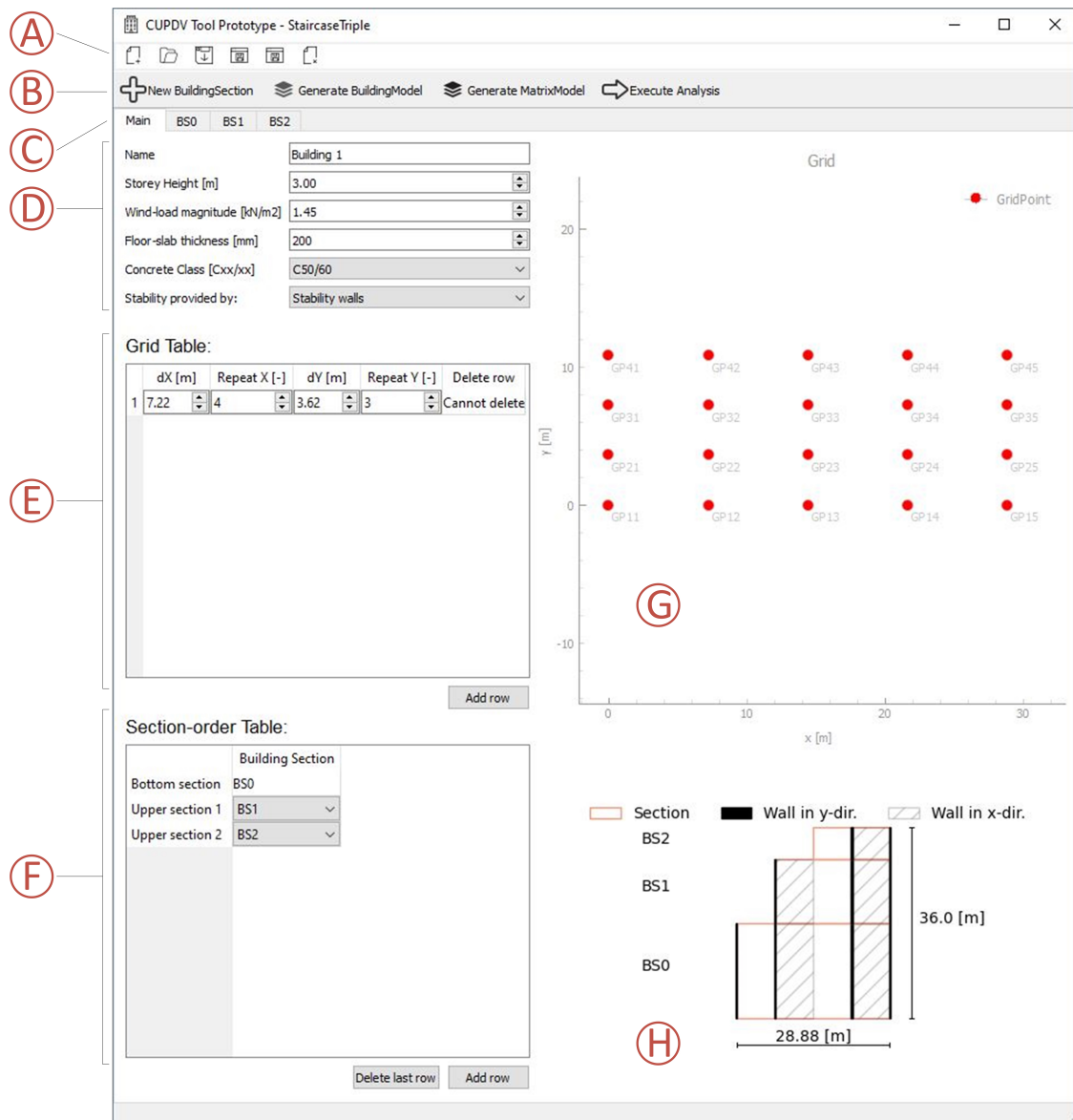


Figure 4.3: Main tab of User Interface

On the 'Main' tab the user can specify general quantities of the design (D), a grid in the XY-plane (E & G), and the stacked order of building sections (F & H). The sections themselves can be designed in each section-tab (C); Figure 4.4 visualises the input required on the section-

^{III}Qt is set of C++ libraries suitable for development of applications for various platforms (*Python bindings for the Qt cross platform application toolkit* 2021).

tabs. For the bottom-section, a user can design a floor-plan of stability walls by selecting start- and end-points (within the borders of the section) and providing thickness-values (see Figure G.2). Optionally, stiffness reduction factors due to the presence of door/window-openings can be provided. For upper stories, the bottom floor-plan can be adapted by removing walls or changing their length^{IV} (in the XY-plane), thickness and/or stiffness reduction; the direction or coordinates of the central wall axis cannot be changed (see Figure G.3 and G.4).

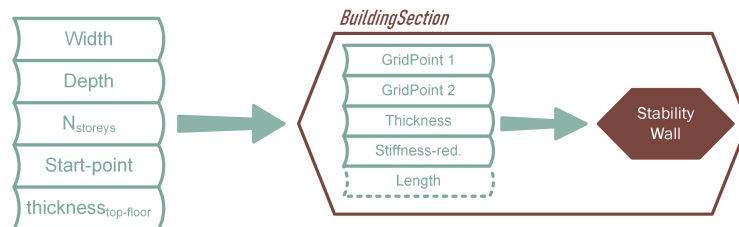


Figure 4.4: Input (green) for BuildingSection and StabilityWall objects (red)

4.2.1 | Result visualisation

The analysis results are visualised on two separate tabs. If a user re-executes the analysis for a different wind-direction, two additional tabs for that direction will be created.

The 'Result - Visual' tab shows three graphs (see Figure G.6) depicting the force and deformation distributions of the stability walls. The user can select the desired quantity and stability walls. Important to note: the prediction of the deformation distribution is not guaranteed to be sufficiently accurate (see Section 5.1.10), this has been explicitly stated on the interface.

The 'Result - Data' tab (Figure G.7) shows an annotated top-view of the stability wall floor plan along with general results (e.g. total base shear and moment). Additionally, the characteristics (cross-section, height, direction, etc.) and force/deformation vectors of a single wall are shown, which can be selected by the user. At the bottom, the direction, base shear, base moment, and top displacement are listed for each wall separately.

4.3 | System process

A request for analysis of the composed design will trigger a series of events. The input on the main-tab and section-tabs is used to generate (and visualise: Figure 4.3H) a crude model of the design; any erroneous input is brought to the attention of the user and halts the process. The BuildingModel consists of BuildingSection, StabilityWall, and sometimes Core objects (in case of a core stability system). Additionally, each section is assigned the correct number of Storey instances. The logic translating an arbitrary BuildingModel into a MatrixModel containing all required structural elements and their interdependencies required thorough consideration. Ultimately, the author arrived at the procedure described below.

For the ground-floor, each StabilityWall on the bottom-section floor-plan is used to generate a WallElement object of equal dimensions and its start- and end-Node objects. The floor-plan of stability elements is reviewed to identify whether there are no walls present on a certain border and/or in the middle of the section; if so, a ColumnElement is generated in that location as stated in Section 3.3. For the vertical elements in y- and x-direction separately, the top-nodes are stored and sorted from left to right and front to back respectively. Subsequently, BeamElement instances are created and assigned the nodes from these sequences as start- and

^{IV}The 'Length' is only specifiable for walls in upper building sections. There, the grid-points cannot be altered but the wall can be widened or narrowed.

end-Node objects. All Wall-, Column, and BeamElement instances are stored in the current Storey object. For each upper storey within the same section, the elements of the Storey below are "copied" to create corresponding elements on the current Storey, resulting in a model of stacked Wall- and ColumnElement objects, connected at their top-nodes by BeamElement instances. Figure 4.5 illustrates the creation of Wall- and BeamElement instances from stability walls; the listed object-attributes are but a small portion of the total.

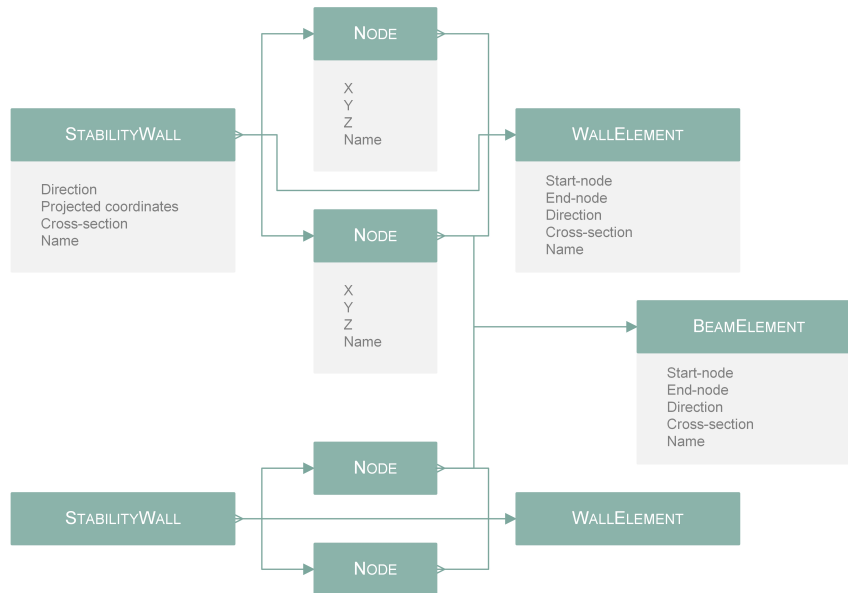


Figure 4.5: StabilityWall to Wall- and BeamElement procedure

The bottom-storey of an upper BuildingSection requires a different approach than a 'regular' upper storey. For all walls still present in the upper section, a WallElement is created according to standard procedure. This also applies for the ColumnElement instances on the previous storey. However, the discontinued walls are also continued as ColumnElement instances (and therefore do not attract any lateral load, see Section 3.3.3). Furthermore, all column-elements outside the BuildingSection boundaries are marked as 'phantom' (see Figure 4.6). Without this phantom-protocol it would not be possible to exclude the building-centre from an upper section (as for BuildingSection 2 in the figure), because this would disconnect the systems of beams in y- and x-direction. The upper storeys of the sections are generated following the standard procedure.

The wind-direction and -magnitude are provided by the user. The BeamElement instances perpendicular to this direction are loaded by an uniformly distributed line load in their local s -direction (see Figure 3.15). This line load is applied as two equivalent nodal loads according to the calculation of $f^{(e,eq)}$ in Equation 3.7. A BeamElement that is partly outside the borders of the section is assigned a line load over its complete span with a reduced magnitude, such that the *total* load on the element corresponds to reality.

The logic embedded in each structural element generates the local stiffness matrix and equivalent load vector based on the element's cross-section, material and freed DoFs. From the complete set of Node and Wall-, Column- and BeamElement instances, the global stiffness matrix \mathbf{K} and the load vector \mathbf{f} are assembled; the system is solved according to Equation 3.12 and 3.13. For each stability wall, the results of the displacement and force distributions are collected from each WallElement object comprising that wall. Subsequently, these distributions are visualised on the dashboard (Figure G.6), along with the base shear, base moment and top-displacement values (Figure G.7).

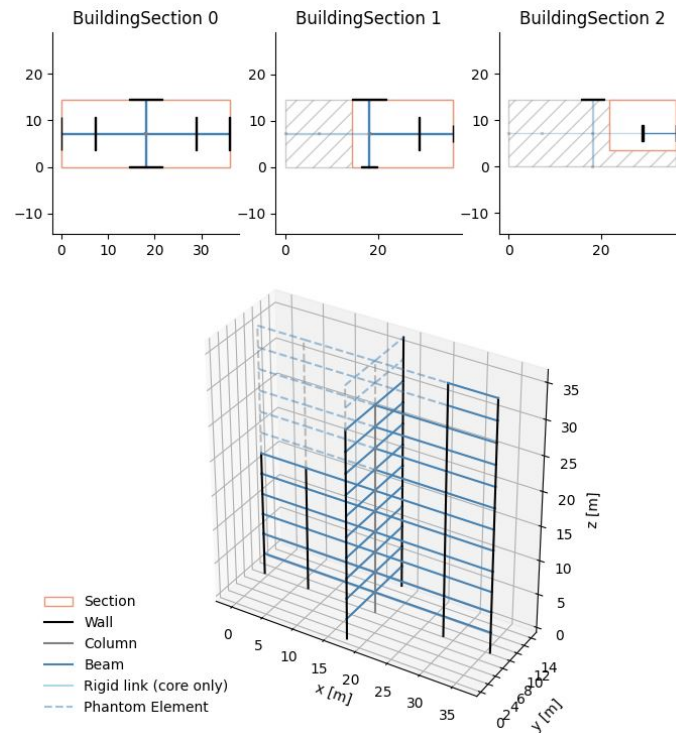


Figure 4.6: Visualisation of a non-proportionate MatrixModel

4.4 | Capacities & Limitations

This section provides an overview of the functionalities incorporated in the CUPD Tool Prototype (denoted with a '+'). However, not all intended functionalities could be implemented (completely), these limitations ('-') have also been outlined below.

- Analysis of Universal Prefab buildings:
 - + rapid analysis that provides insight in the global force distribution in the stability system,
 - + rectangular floor-plans,
 - + both core and shear wall stability systems,
 - + both proportionate and non-proportionate designs,
 - + upper sections can be reduced in size to create staircase-type designs,
 - + reduction of wall-stiffness due to door/window opening,
 - + divergent transition floor thickness between building sections,
 - + walls in two directions,
 - + walls can change in width and thickness in each consecutive section,
 - a hybrid core-shear wall stability system was excluded,
 - consecutive building sections can only become smaller or remain of equal dimensions (in the horizontal plane),
 - walls can only be placed on a (user-specifiable) grid,
 - walls cannot change in direction or location over their height,
 - walls can only be defined parallel to primary building axes,
 - constant floor thickness throughout building (except transition floors)
- Conceptual design:

- + quick design composure through vertical combining of building blocks,
- + user can design own building blocks,
- + visualisation of generated models allows verification by the user/engineer,
- + saving and loading of designs enables comparison of design alternatives and improves practical use,
- + interface is user-friendly (no Grasshopper spaghetti-monster),
- + built-in safeguards against erroneous input,
- + clear, concise visualisation of results with possibility to request complete results,
- + possibility to request very specific data like element stiffness matrices directly in back-end (Python knowledge required),
 - without knowledge of Python, program can feel like a 'black box'
 - analysis limited to redistribution of lateral load

4.5 | Conclusion of chapter

Thorough consideration of various alternatives for obtaining the required user-input and generating the MatrixModel led to the tool presented in this chapter and Appendix G. The application possesses a graphical User Interface with which a designing engineer can efficiently compose building designs using customizable building blocks. The visualisation of the composed building design and the generated MatrixModel supports corroboration of the obtained results. Additionally, projects can be saved and opened, realising even more practical value. The calculated shear force and bending moment distributions of each wall are plotted and the values are provided, offering clear insight into the lateral structural behaviour.

The answers to research questions VIII to X can be found in Sections 4.2, 4.1, and 4.3 respectively.

This page has been intentionally left blank.

5 | Result Analysis

The developed CUPD Matrix Model naturally requires validation regarding its accuracy in predicting the support reactions as a result of lateral loading. This chapter provides a description of the test-cases created to assess this accuracy. Additionally, the analysis results of the implemented modelling approach are used to identify the influence of the stiffness of the floor system and of a thick transition floor between two successive building sections. A comparison of the redistribution results to the Differential Super Element Method devised by Steenbergen (2007) provides further insight into the performance of the model. Both the 2D Flat Stick and reference modelling of the various test-cases provide insight into the consequences of selecting a Universal Prefab system, particularly regarding the expected structural behaviour.

Ultimately, this chapter provides an answer to research questions XI to XIII:

- XI. What is the accuracy of the implemented analysis model for various test-cases?
- XII. How is the force distribution effected by various characteristics of the floor- and stability-system?
- XIII. How do the results of the developed analysis model compare to existing analyses?

5.1 | CUPD analysis model accuracy

As stated in the chapter's introduction, a variety of representative designs has been composed. These test-cases comprise several building designs varying in height, non-proportionality, stability system and wall configuration. Comparison with the reference modelling results of these test-cases provides the reader with the accuracy of the Matrix Model proposed by this research.

Both prismatic and non-prismatic test-cases have been defined; a distinction was made between 'dense' and 'scattered'. The former represents floor-plans more densely populated by stability walls, while for the latter the walls are smaller in number and/or placed further apart. Two staircase designs and two core designs were used to verify the accuracy for such buildings. The symmetric building from the dissertation of Raphaël Steenbergen (2007) has been modelled to compare findings on the influence of the non-proportionate change in the stability system. The floor-plans of all test-case can be found in Figure 5.2 and 5.3. Subsequently, the results of each design are concisely documented. The full results, top-views of the 2D Flat Stick representations, and a table containing the considered number of storeys per test-case can be found in Appendix H.



Figure 5.1: Simple-Scattered test-case top-view

All test-case designs have been modelled for a varying number of storeys (see Table H.1) and an E -modulus assigned to the beam-elements varying between $12.5GPa$ and $40GPa$. Ultimately, $E = 20GPa (= 20 * 10^9 N/m^2)$ was found to provide the best estimation for the base shear of the primary walls. The sections below, documenting each test-case and its results, show the error of the base shear prediction versus the number of storeys for each primary wall separately, applying a global BeamElement stiffness of $20GPa$. In these figures, a positive error represents an overestimation of the Matrix Model regarding the base shear of that wall with respect to the reference model. Appendix H provides plots of the RMSE versus storey-count and floor-beam stiffness.

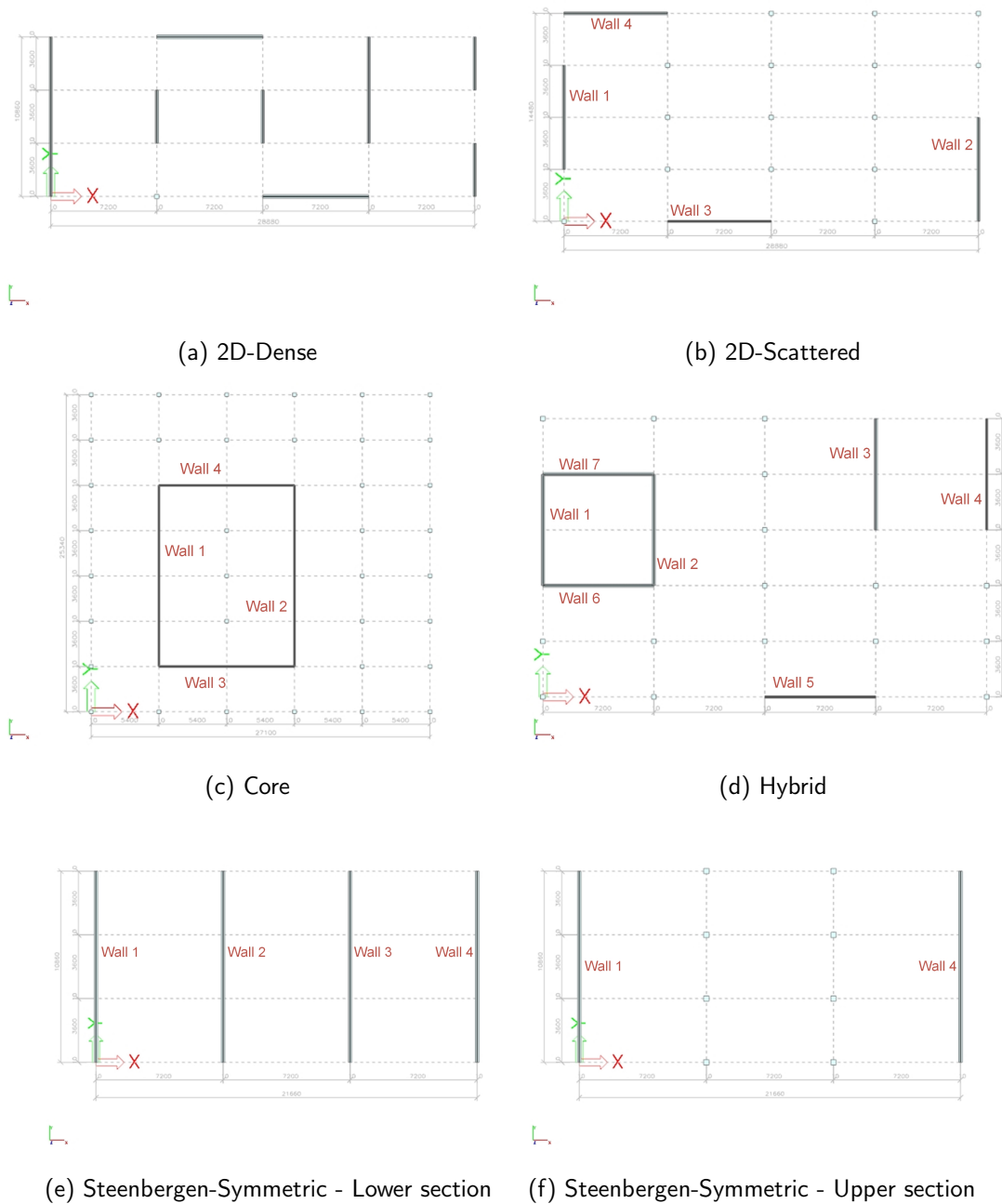


Figure 5.2: Reference model top-views of test-cases (1)

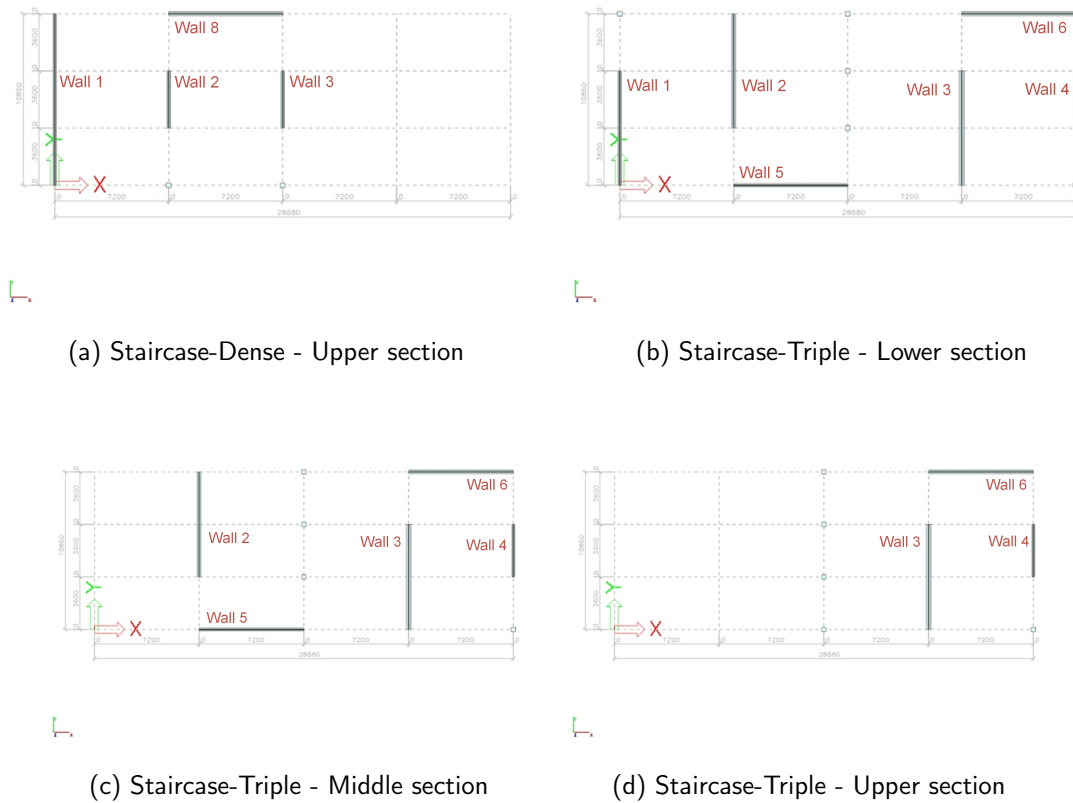


Figure 5.3: Reference model top-views of test-cases (2)

5.1.1 | Simple-Dense

One of the test-cases used for the exploratory research on UP behaviour was also used for this assessment. Figure 3.8a shows the actual floor-plan, Figure H.1a shows a top-view of the 2D Flat Stick representation. Due to the singular direction of the walls, only loading in y-direction is considered. The accuracy of the redistribution analysis performed on this test-case is visualised by Figure 5.4a. The error is within the accepted range of 20% for all walls.

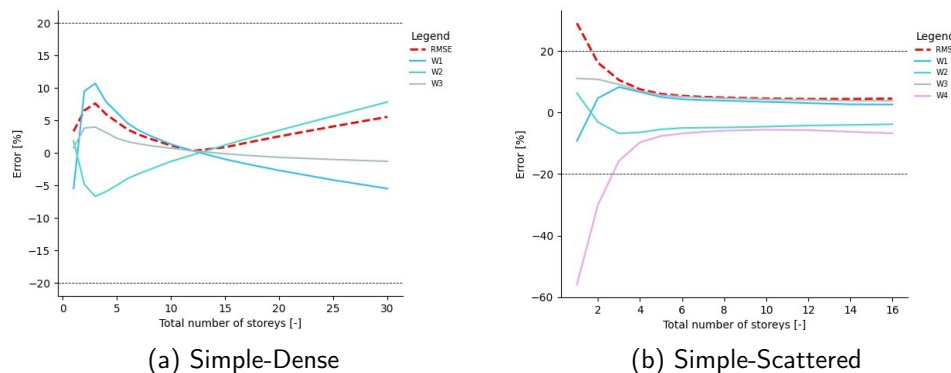


Figure 5.4: Base shear *Error* vs. $N_{storeys}$ for $E_{beam} = 20GPa$

5.1.2 | Simple-Scattered

The second test-case with walls in a single direction is shown in Figures 5.1 and H.1b. This test-case has a less dense distribution of shear walls. Additionally, a 'double-wall' configuration (see Section 3.3.2) has been incorporated in this design. Due to the singular direction of the

walls, only loading in y-direction is considered. Figure 5.4b illustrates the accuracy of the Matrix Model for this specific test-case. For buildings with more than two storeys the deviation from the reference model is within the acceptable limit.

5.1.3 | 2D-Dense

Additional to the prismatic test-cases above, also prismatic test-cases with walls in two directions (hence the name '2D') were created. This test-case also incorporates a double-wall configuration. The floor-plan in Figures 5.2a and H.1c is also the bottom-section floor-plan of the Staircase-Dense test-case. Figure 5.5 shows that for buildings higher than a single storey the primary base shear results were sufficiently accurate, for both loading directions. However, it was found that the developed model is not able to accurately predict the base shear of the secondary walls. Fortunately, loading perpendicular to a wall's direction does not produce the governing load situation for that wall. For the full results, consult Figure H.4.

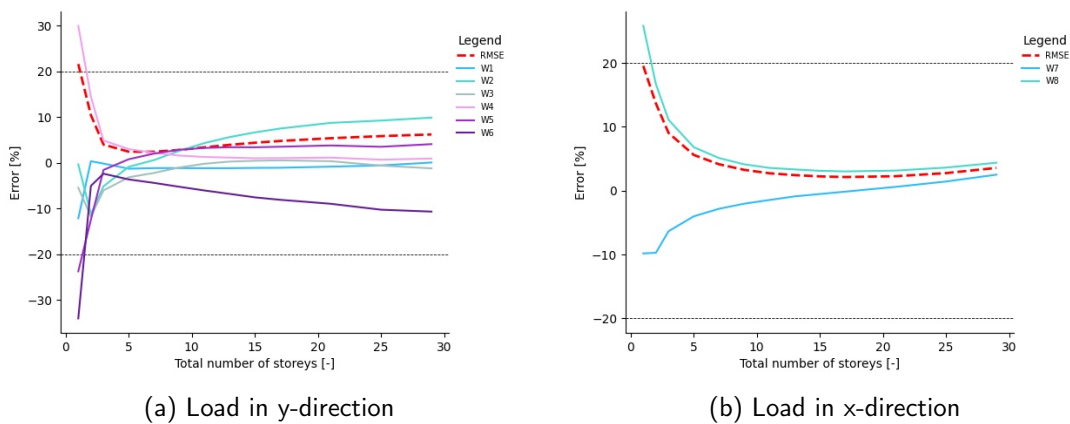


Figure 5.5: 2D-Dense Base shear - $Error$ vs. $N_{storeys}$ for $E_{beam} = 20GPa$

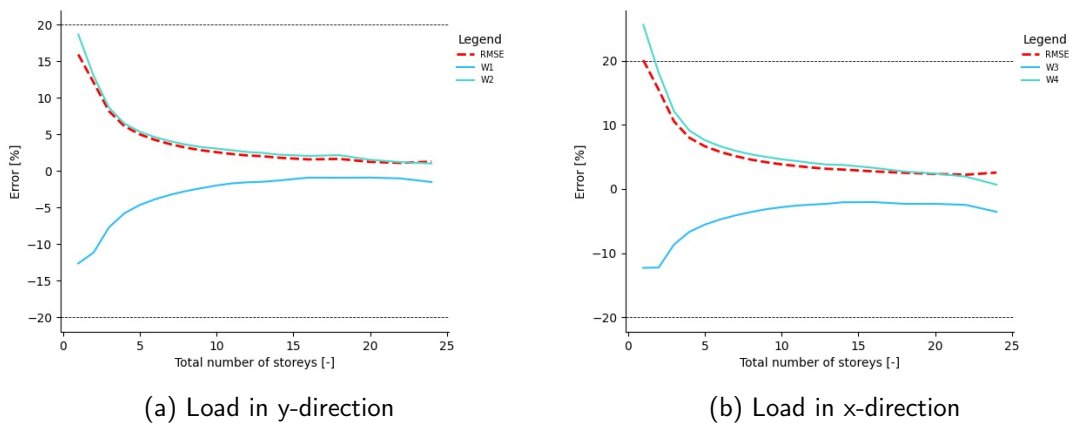


Figure 5.6: 2D-Scattered Base shear - $Error$ vs. $N_{storeys}$ for $E_{beam} = 20GPa$

5.1.4 | 2D-Scattered

The second two-directional test-case is presented by Figures 5.2b and H.1d. Again, the density of the walls has been decreased with respect to the dense design. It was found that the redistribution in buildings with more than a single storey could be predicted sufficiently accurate (see Figure 5.6). The floor-plan of the 2D Flat Stick representation illustrates the challenge of accurately predicting the loads on the secondary walls for an arbitrary configuration. Due to the projection of the walls on the primary building axes, the stick model of this test-case is

symmetric around the axis of loading and no twisting occurs¹, resulting in zero base shear for the perpendicular walls. The reference model does model some twisting, albeit a small amount, which naturally results in an error of 100%. Interesting to note is the irrelevance of the stick model floor-stiffness regarding the redistribution, due to the symmetric wall configuration (see Figure H.6b).

5.1.5 | Core

To investigate the model performance regarding a core stability system, the floor-plan design of Figures 5.2c and H.1e was composed. The reference model was created according to the procedure outlined in Appendix E. Figure 5.7 visualises the accuracy of the CUPD Matrix Model analysis: the base shear prediction of the primary walls is more than adequate for both loading directions. For the full results, consult Figure H.7.

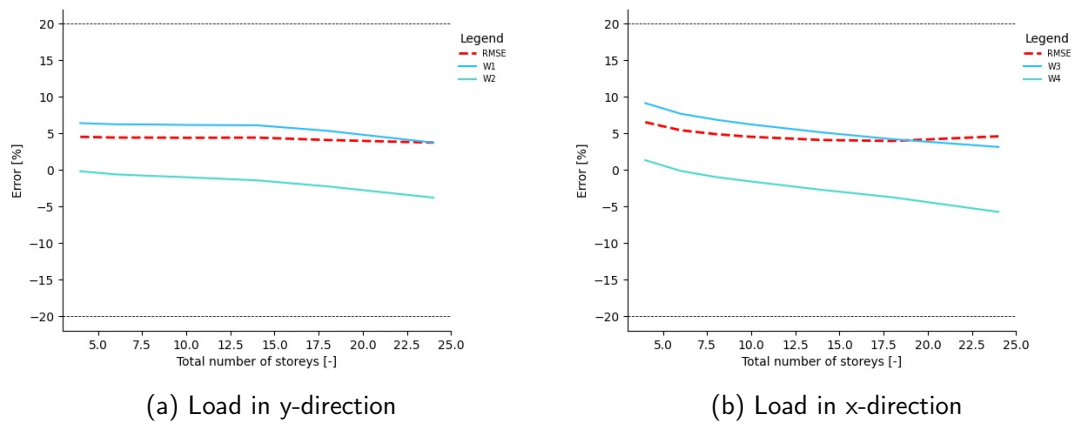


Figure 5.7: Core Base shear - *Error* vs. $N_{storeys}$ for $E_{beam} = 20GPa$

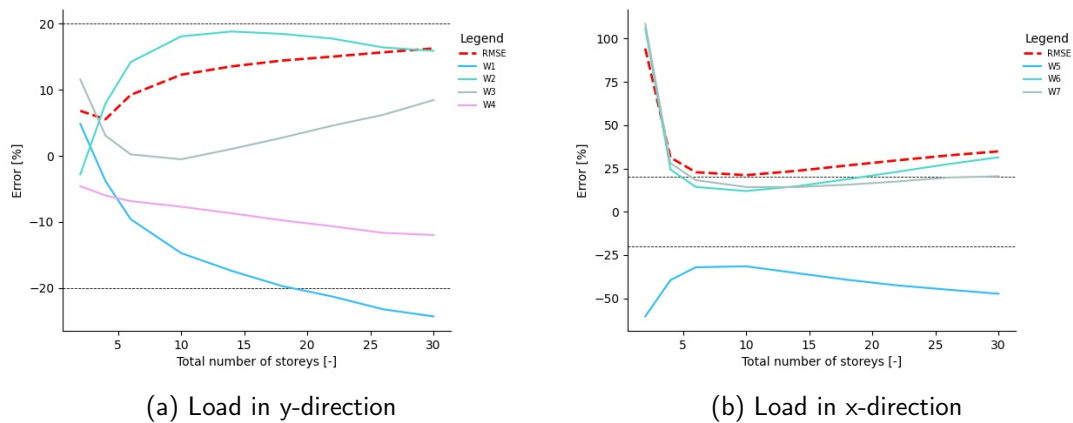


Figure 5.8: Hybrid Base shear - *Error* vs. $N_{storeys}$ for $E_{beam} = 20GPa$

5.1.6 | Hybrid

The accuracy regarding a hybrid (core-shear wall) stability system was investigated through modelling of the test-case presented in Figures 5.2d and H.1f. The building's core was modelled according to the procedure outlined in Appendix E. As stated in Appendix E, multiple modelling approaches were investigated. This investigation presented a trade-off between accurate results for the walls comprising the core or accurate results for the additional (primary) walls. Furthermore, the presence of additional walls can decrease the validity of the 2D Flat

¹For loading in the x-direction a slight twisting does occur, because the thickness of Wall 3 is smaller than that of Wall 4.

Stick representation of an arbitrary floor-plan, as shown in Figure 3.12). As a result, the accuracy of the CUPD Matrix Model analysis was insufficient for the Hybrid test-case (see Figures 5.8 and H.8).

5.1.7 | Staircase-Dense

This test-case has a floor-plan equal to the 2D-Dense design (Figures 5.2a and H.1c). However, somewhere along the height a non-proportionate change in the stability system occurs, resulting in the floor-plan of Figures 5.3a and H.2a. The number of storeys of both sections of the building were the subject of variation. This leads to the analysis accuracy presented by Figures 5.9^{II} and H.9. The highest error occurs for the building with two sections of both 5 storeys (5-5), a building of equal height but with an 8-2 distribution shows a significantly smaller error.

The Staircase-Dense design has also been modelled with a thick (1m) transition floor between the bottom- and upper-section for certain distributions of $N_{storeys}$; the RMSE's of the results are presented by Figures H.10c and H.10d.

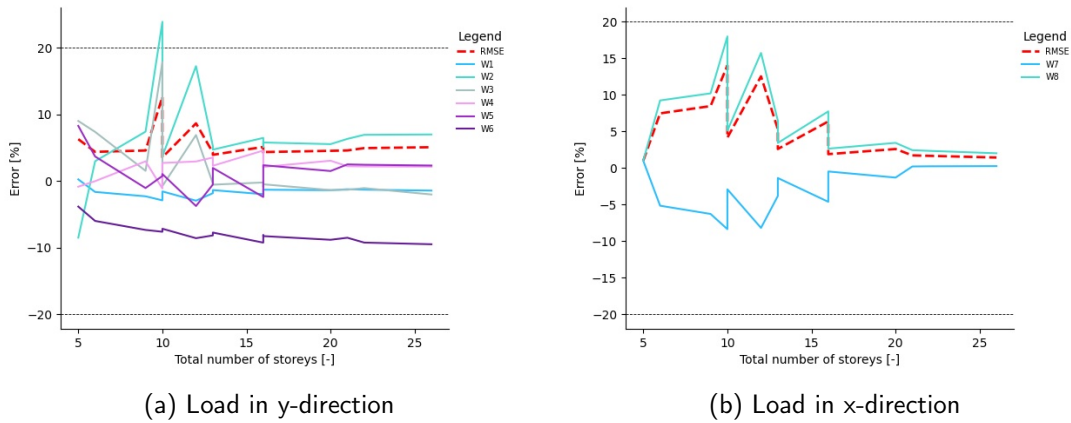


Figure 5.9: Staircase-Dense Base shear - *Error vs. $N_{storeys}$ for $E_{beam} = 20GPa$*

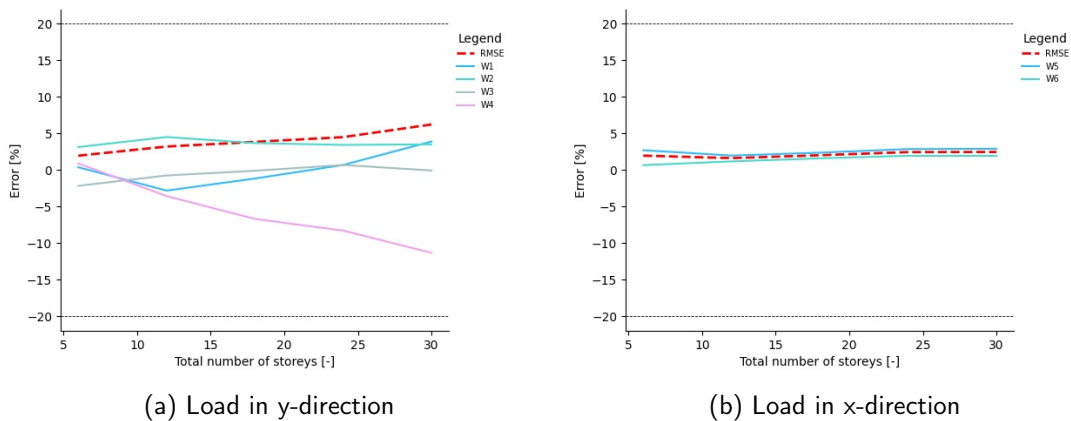


Figure 5.10: Staircase-Triple Base shear - *Error vs. $N_{storeys}$ for $E_{beam} = 20GPa$*

5.1.8 | Staircase-Triple

This test-case incorporates two non-proportionate jumps in the stability system. All three floor-plans are visualised in Figures 5.3 and H.2. The ratio between the number of storeys of the building sections has been kept constant at 3:2:1 (see Table H.1). The accuracy of

^{II}The x-axis of the figures below denotes the total number of storeys (i.e. the building height), explaining the occurrence of the vertical increments/reductions.

the redistribution prediction (see Figures 5.10 and H.11) of this test-case is well within the acceptable limit for both wind-directions.

The Staircase-Triple design has also been modelled with a thick (1m) transition floor between the bottom- and upper-section for certain distributions of $N_{storeys}$; the RMSE's of the results are presented by Figure H.12.

5.1.9 | Steenberg-Symmetric

As stated, also the symmetric building design of Steenberg (2007) has been used as a test-case. Figures 5.2 and H.2 show the floor-plans of the two building sections and its Matrix Model respectively; the accuracy of the modelled redistribution is visualised by Figures 5.11 and H.13. The accuracy is within the acceptable limits for all considered building heights. The right plot of the figure below illustrates the influence of the magnitude of the non-proportionate change in the stability system. In accordance with the findings for the Staircase-Dense design, a smaller jump leads to a more accurate prediction of the base shear.

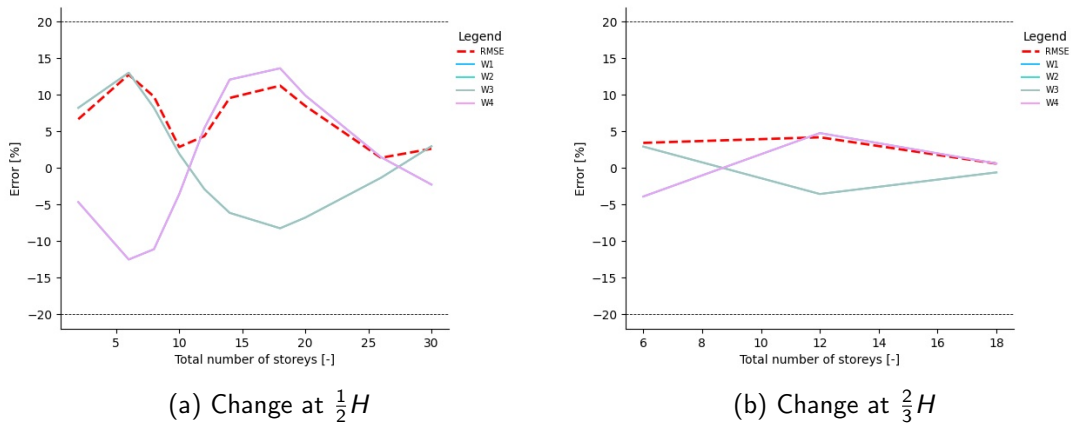


Figure 5.11: Steenberg-Symmetric Base shear - Error vs. $N_{storeys}$ for $E_{beam} = 20GPa$

5.1.10 | General

Figure 5.12 summarizes the RMSE versus the total number of storeys for all test-cases in the same plot. Important to note is the absence of the test-cases with walls in only y-direction from the plot on the right. From the same plot, the Hybrid test-case was excluded because its high inaccuracy reduced the readability.

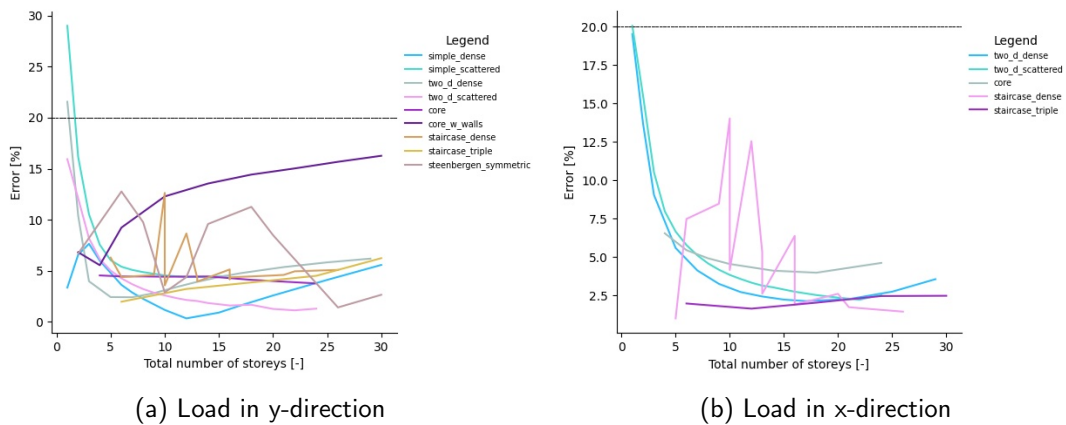


Figure 5.12: All test-cases - RMSE vs. $N_{storeys}$ for $E_{beam} = 20GPa$

The displacement at the top of the stability walls is also calculated by the Matrix Model analysis. However, the accuracy of these predictions proved to be inconsistent. The displacement parallel to the axis of loading is overestimated significantly (with more than 20%) except for the Core test-case in which a large underestimation occurs. The reference model appears to behave more stiff than the Matrix Model (except for the Core test-case). To accurately model the deformation – possibly with the developed 2D Flat Stick representation, further research is required.

5.2 | Influence of the floor stiffness

The lateral system of hinged connections and thin, discrete floor-slabs is characteristic for the Universal Prefab structural system. Chapter 3 concluded that this system cannot be assumed to behave rigidly, especially for non-proportionate building designs. Consequently, the influence of the floor stiffness on the redistribution of lateral load was of special relevance for this research. This section inspects the behaviour of the non-proportionate test-cases for a varying stiffness of the beam-elements representing the lateral system.

Additional to the figures presented below, several graphs are presented in Appendix J to ensure the report's continuity.

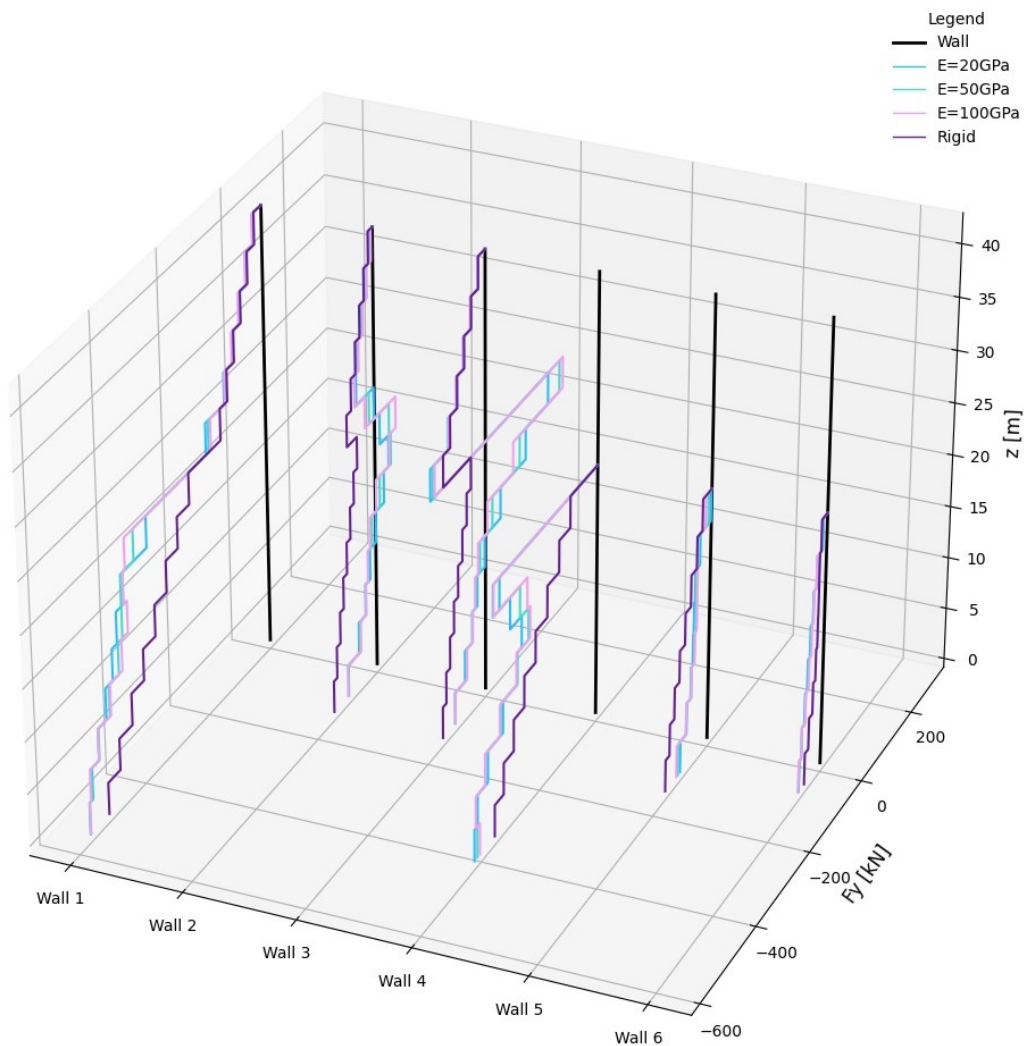


Figure 5.13: Staircase-Dense: 8-6 - F_y distributions for varying E_{beam} (primary walls only)

5.2.1 | Staircase-Dense

It is intriguing to see that the stiffness assigned to the floor-beams of the stick model has little influence on the base shear predictions for a number of storey configurations; Figures H.9b and H.9d show only a small curvature for the higher buildings. This was to be expected for loading in the x-direction due to the stability wall symmetry around the x-axis. However, for loading in the y-direction the occurrence of a non-proportionate change the stability system was expected to require accurate representation of the lateral structural system with a non-finite floor stiffness. Figure 5.13 provides additional insight into the influence of the floor stiffness on the shear force distribution of each wall; the model has 8 bottom-section and 6 upper-section storeys. The floor stiffness mainly seems to influence the shear force and moment distributions of the storeys surrounding the non-proportionality. For the walls present in both sections (W1-W3), a higher floor-stiffness increases the magnitude of the 'jump' in the force distribution. For the walls discontinued at the transition (W4-W6), the upper storeys show divergent behaviour of the shear force distribution compared to the lower storeys (and the case of a rigid floor). For a higher stiffness the magnitude of this deviation is larger than for lower stiffnesses. The effects are small for walls 5 and 6 due to them being double-walls (see floor-plan). For storeys further from the non-proportionality the distribution differences seem to dissipate; the dissipation of the disturbance seems to progress more rapidly for buildings with a higher floor-stiffness. At ground level the differences between the finite stiffnesses are negligible, explaining the floor-stiffness' lack of influence on the base shear distribution. Figures H.10a and H.10b show the RMSE for an expanded range of considered stiffnesses. Due to the dissipation of the disturbance in the force distribution, a stiffness variation between 10 and 40 GPa may not be of significant influence on the results. However, it would be unacceptable to assume a system of rigid floors.

Figure J.1 visualises the shear force distribution for a Staircase-Dense building of equal height, but with a smaller non-proportionality (11-3 storeys); the figure shows a significantly smaller disturbance but otherwise similar results.

5.2.2 | Staircase-Triple

Figures J.2 to J.4 show the shear force distribution of the four walls in y-direction for varying floor-stiffness for three Staircase-Triple designs. Similar as for the Staircase-Dense design, a high stiffness results in a larger jump in the distribution at transition level. However, for the walls present in *all* sections (W3 & W4) the lower disturbance, at the transition from bottom to middle section, is distorted by the not yet dissipated upper disturbance at the upper transition. This does not occur for the walls spanning only one or two sections. For the 6-4-2 building the plotted disturbances are somewhat small and difficult to interpret, but the 9-6-3 and 12-8-4 designs clearly support the findings of the Staircase-Dense test-case.

5.2.3 | Steenbergen-Symmetric

Figure 5.14 illustrates the influence on the shear force distribution of the beam-element stiffness in the Matrix Model of the Steenbergen-Symmetric test-case. The quantity displayed on the horizontal axis is the relative shear force, representing the portion of the total applied load and multiplied with a factor 2 (because there are two outer and two inner walls). The disturbance due to the non-proportionate change corresponds to the findings for the Staircase test-cases: a higher floor stiffness results in a larger disturbance that dissipates more quickly over the adjacent storeys; for the considered building and stiffness-range the disturbance has fully dissipated at ground level. At a certain stiffness – disproportionate to the stiffness of the walls ($E_{beam} > 100 GPa$) – the effect reverses, subsequently arriving at the distribution in case of a rigid floor-system.

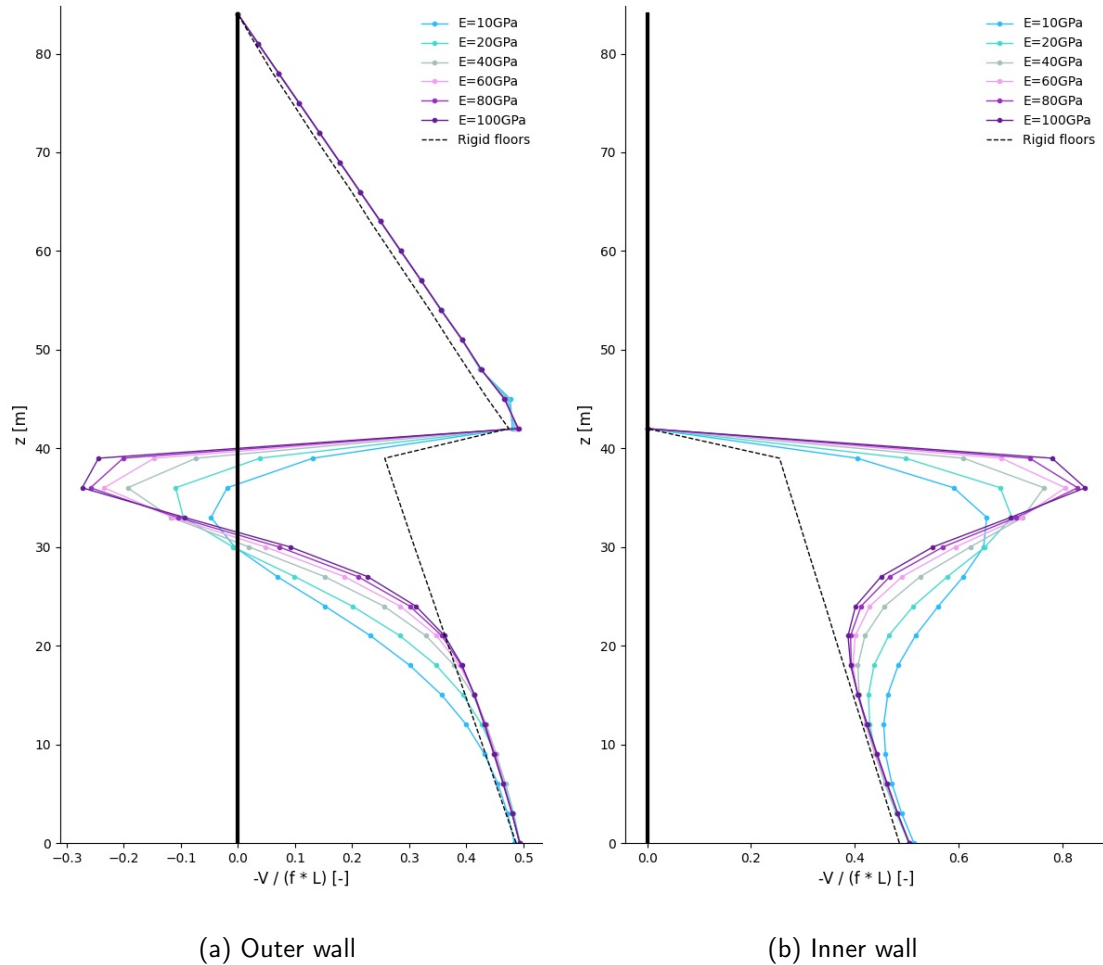


Figure 5.14: Steenberg-Symmetric - Interpolated relative distribution F_y for varying E_{beam}

From the test-case assessments it can be concluded that the magnitude of the disturbance caused by the changing stability system is influenced by the stiffness of the floor-system. A higher stiffness results in more redistribution and therefore causes a larger disturbance in the force distributions at the transition with respect to the case of a rigid floor-system. However, the effect on the force distributions seems to reverse at excessively large stiffnesses (with respect to the wall stiffness) which then gradually progress to the distributions found for a rigid floor-system. The occurring disturbance dissipates gradually over the storeys below the transition; a higher floor-beam stiffness accelerates this dissipation. Whether the disturbance has fully dissipated at ground level depends on the floor-system stiffness, the magnitude of the non-proportionality and the building height.

5.3 | Influence of the transition-floor thickness

Often in building practice, the floor-system between two successive building sections has a higher stiffness than on the 'regular' storeys to allow more redistribution of the load on the upper section over the walls present in the bottom section (ir. S. Pasterkamp, personal communication, June 17, 2021). Generally, the increased stiffness is achieved by applying a higher thickness or opting for a cast in-situ slab instead of prefabricated floor-plates. In the CUPD Tool, the designing engineer can provide a divergent thickness for the top-floor of a building section. This section reflects on the influence of the thickness of this transition-floor by means of the non-proportionate test-cases.

Additional to the figures presented below, several graphs were presented in Appendix K to ensure the report's continuity.

Both the Staircase-Dense and -Triple test-cases have been modelled with divergent transition-floor thicknesses; Table H.1 lists the considered storey-configurations. Similar to the general floor-stiffness and the magnitude of the non-proportionality, the thickness of the transition floor influences the shear force and moment distributions around the non-proportionality. The figure below and Figures K.1 to K.4 visualise the F_y distribution of each wall separately for a number of building designs. At the change-level, a thicker floor results in a larger jump in the force distribution, similar to the influence of a higher general floor stiffness. The effect seems to reverse at a certain floor thickness. This turning point differs from wall to wall and from test-case to test-case, as visualised by the highlighted parts of the shear force distribution in Figure K.2.

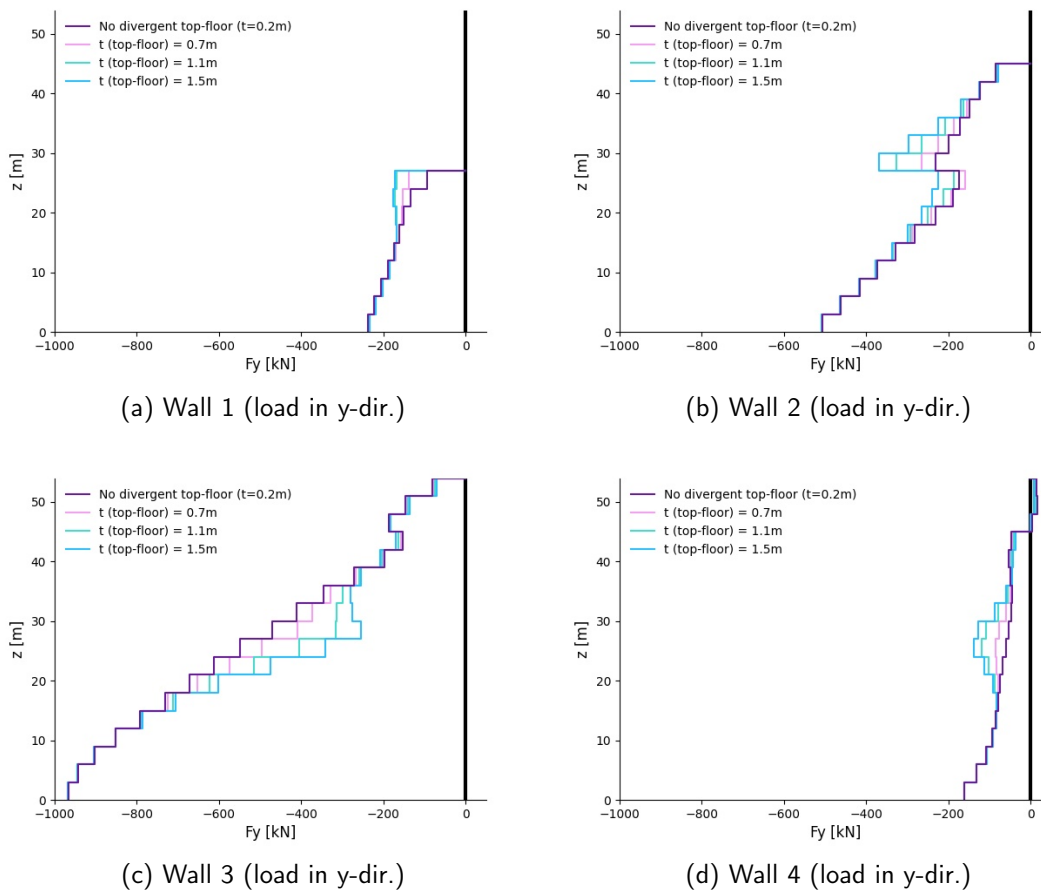


Figure 5.15: Staircase-Triple - F_y distributions for varying $t_{top-floor}$ (primary walls only))

5.4 | Non-proportionality and comparison with DSEM

As introduced in Sections 2.1.2 and 3.1.2, Steenbergen (2007) developed a method for quick structural analysis of mid- and high-rise buildings. A model comprising certain 'super elements', which modelled the floors as elastic springs instead of assuming a rigid floor system. This model was used, amongst other things, to investigate the distributions of the shear force and bending moment in a building similar to the Steenbergen-Symmetric test-case; this building is portrayed in Figure 5.16. The distributions found by Steenbergen were compared to the results of the CUPD Matrix Model.

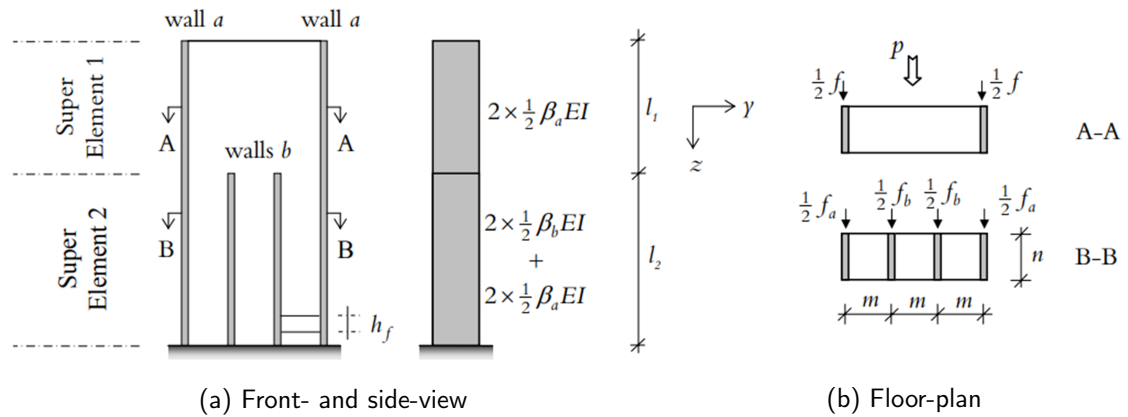


Figure 5.16: Symmetric building of Steenbergen (2007)

The shear force and bending moment distributions found by Steenbergen are presented in Figures 5.17 and 5.18, along with the CUPD predictions. The case in which the floors are modelled as rigid links is represented by the dashed lines. As shown by Figures 5.17a-c, the non-proportionate change does not necessarily influence the base shear, but does cause a disturbance spreading a number of storeys. L_{char} represents the characteristic length of this disturbance; this length can be clearly recognized in the graphs. Steenbergen provides the following formula for calculating the characteristic length:

$$L_{char} = \left(4\beta_a\beta_b\frac{EI}{k}\right)^{\frac{1}{4}} \quad (5.1)$$

with β_a and β_b according to Figure 5.16. For a higher L_{char}/L_1 ratio (Figures 5.17d-f), the non-proportionate change in the stability system does cause a divergence at ground level.

The figures show a strong correlation in predictions on structural behaviour of the considered models. As previously concluded by Steenbergen, the finite floor stiffness causes a lower shear force in the outer walls on the storeys below the non-proportionate change with respect to a rigid floor system. Correspondingly, the inner walls are subject to an increase of the shear force.

For the Staircase-Dense, -Triple and Steenbergen-Symmetric test-cases it was observed that a smaller jump in the stability system leads to a smaller disturbance in the force distributions. Additionally, it seems the CUPD analysis model can provide more accurate predictions for buildings with a smaller proportionality (see Sections 5.1.7 and 5.1.9). In a building with a larger non-proportionality, the specific configuration of stability walls has a larger influence on the redistribution of the lateral load. This increased complexity is more more difficult to model accurately for a wide span of arbitrary building designs.

To provide insight in the influence of the building height and non-proportionality, the shear force distribution of 14 Steenbergen-Symmetric designs has been plotted in Figures 5.19a and 5.19b; similar plots for the moment distribution are shown in Figure H.14. The z-coordinate, denoting the height along the building (specified on the vertical axis), has been standardized through a division by the total building height L . For the 1-1 and 2-2 buildings, the storeys below the transition fail to redistribute sufficient load over the inner walls: the relative base shear of an outer wall is larger than 0.5. Between configurations of 3-3 and 12-12 storeys, the redistribution results in a relative outer-wall base shear lower than 0.5 as a result of the not fully dissipated disturbance. From 14-14 storeys and upward, the jump in the stability system has no significant influence on the base shear distribution. Note: this graph shows the distributions for one specific design of the test-case, with specific dimensions.

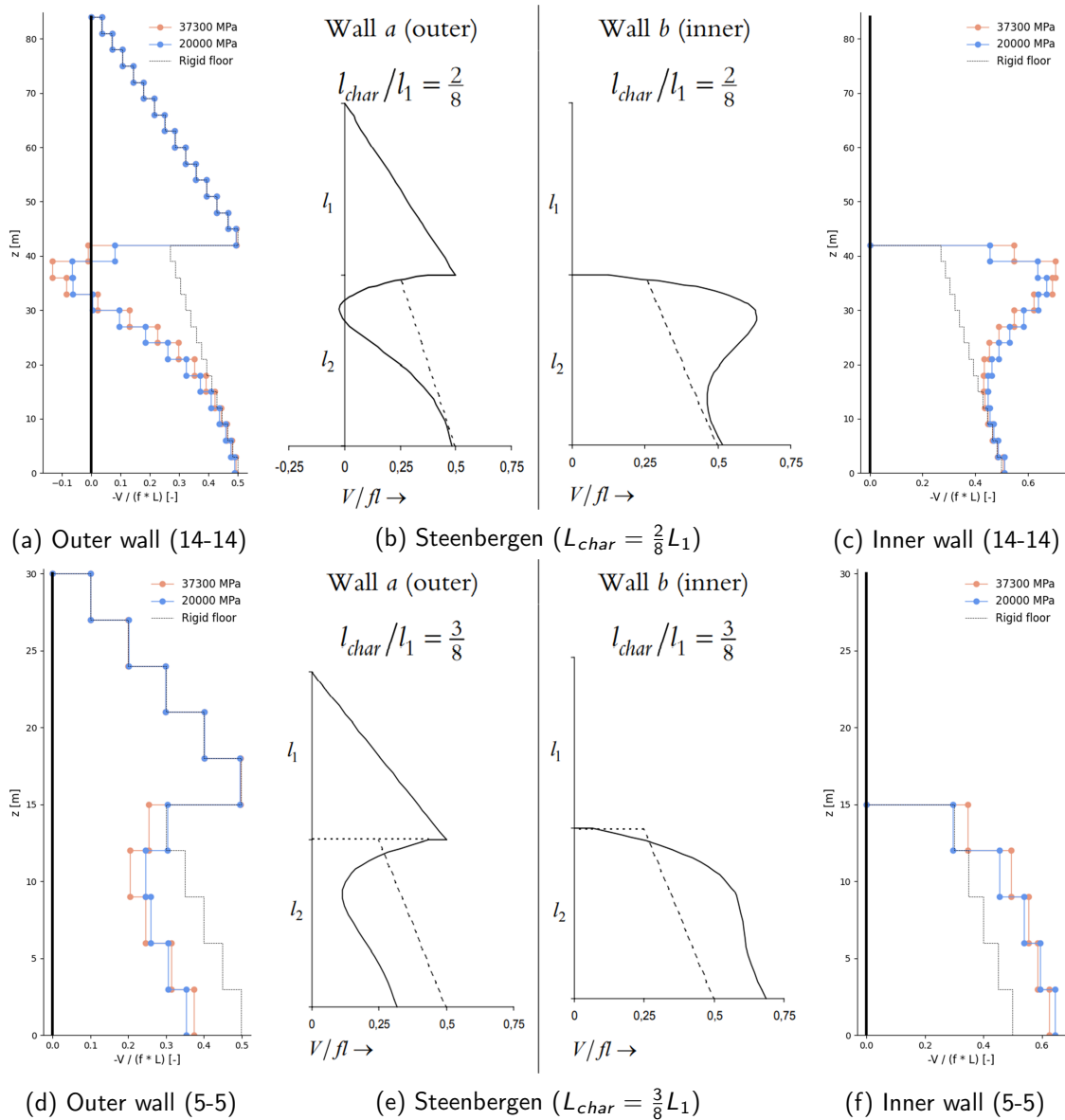


Figure 5.17: Relative shear force distributions of Steenbergen (2007) and CUPD Matrix Model

Similar plots of relative height versus relative shear force have been produced for a varying height of the top section only (see Figures 5.19c and 5.19d), changing the magnitude of the structure's non-proportionality (i.e. the 14-2 design has a smaller non-proportionality than the 14-14 design). Conform the expectations a more slender buildings sees a larger disturbance of the shear force, representing more redistribution at the transition level.

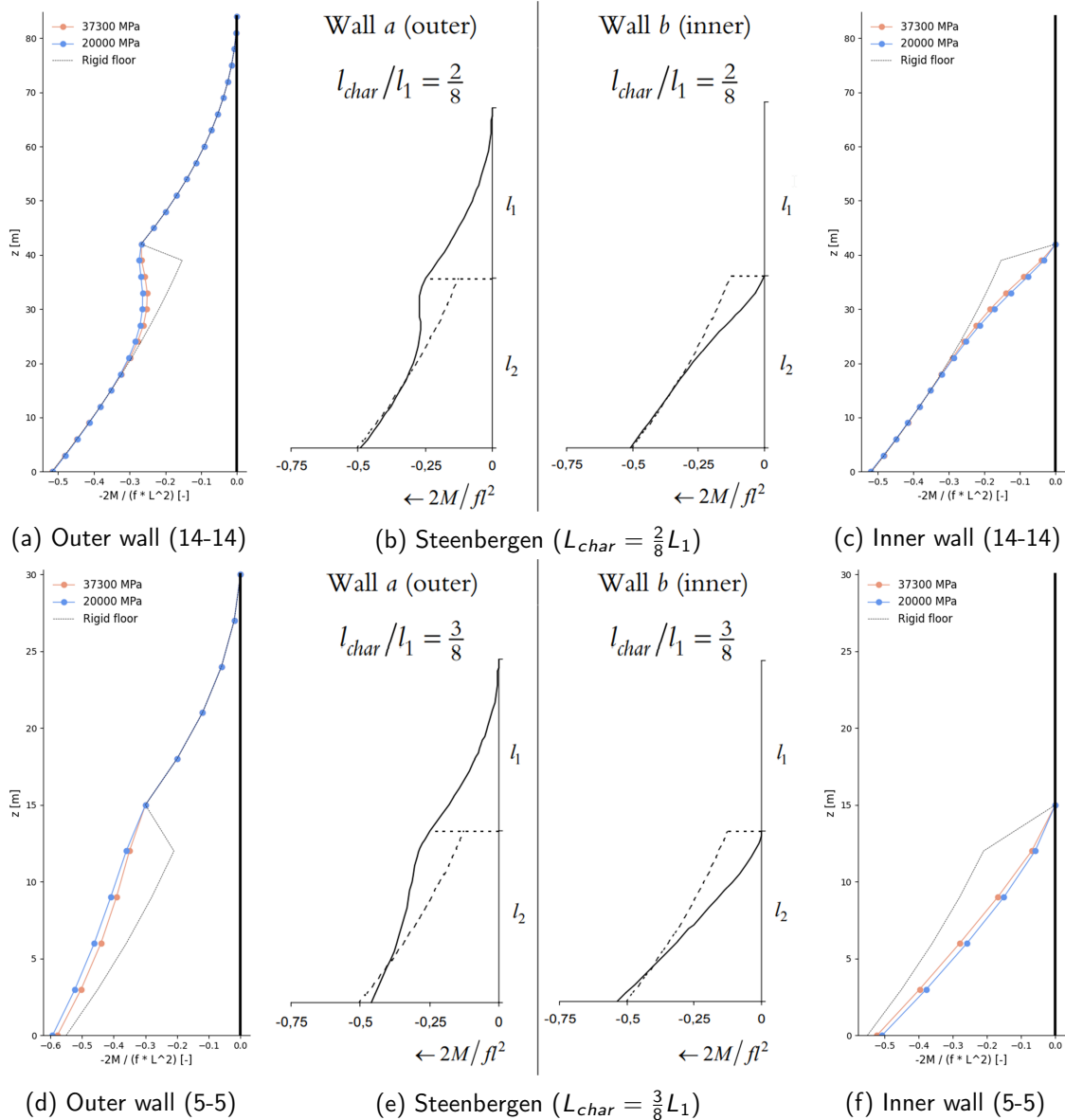


Figure 5.18: Bending moment distributions of Steenbergen (2007) and CUPD analysis model

5.5 | Conclusion of chapter

This chapter provides the following answers to research questions XI to XIII:

- XI. From the test-case assessments it can be concluded that for conceptual designs of proportionate, non-proportionate and core stability systems – ranging from three to thirty storeys – the primary force distribution can be predicted with sufficient accuracy by the developed Matrix Model. Walls can be placed both parallel and perpendicular to the axis of loading and may change in thickness and width over the height of the building. Sufficient accuracy cannot be guaranteed for the force distributions of hybrid core-shear wall systems and the walls perpendicular to the axis of loading and the deformation distribution in general.
- XII. The CUPD structural analysis results showed a disturbance in the shear force and bending moment distributions caused by a non-proportionate change in the stability system, in accordance with the Differential Super Element Method developed by Raphaël Steenbergen. It was established that the magnitude of this disturbance is influenced by the floor-beam stiffness: a higher, finite stiffness allows for more redistribution, thus causing a larger

disturbance in the force distributions at the transition with respect to the case of a rigid floor-system. Applying an increased thickness for the floor-system at transition-level has a comparable effect. For excessively large stiffnesses (with respect to the wall stiffness) the disturbance reduces; for a rigid floor-system the lateral load is proportionately distributed over all walls at each storey.

- XIII. The shear force and bending moment distributions found with the Differential Super Element Method developed by Raphaël Steenbergen (2007) show a large resemblance with the distributions found with the MatrixModel.

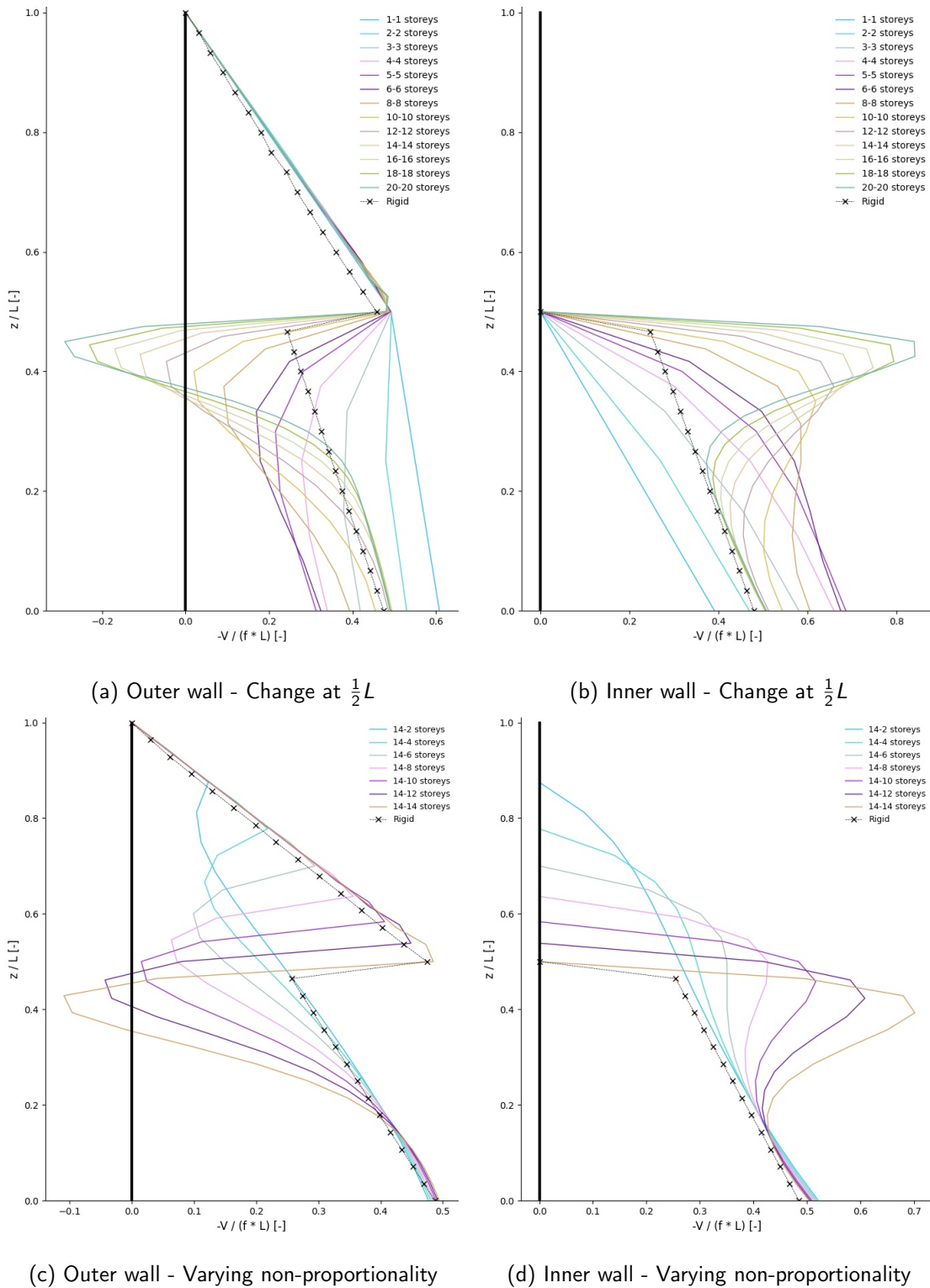


Figure 5.19: Steenberg-Symmetric - Interpolated distribution F_y over relative height according to the CUPD Matrix Model ($E_{beam} = 20GPa$)

6 | Discussion

The chapter reflects on the completion of the defined sub-objectives and examines the validity of the performed research.

Sub-objective 1 | Conceptual Design of UP Apartment Buildings

Determine the capabilities a parametric tool requires to enable (more efficient) conceptual design of UP apartment buildings.

An investigation into the existing StructuralComponents toolbox led to a focus on combining the advantages of SC5 – composure and analysis of non-proportionate designs – with that of SC6 – customizable building blocks. Additionally, the author determined an emphasised consideration regarding the user-friendliness of the tool prototype as a personal objective to increase the value of this research’s final product. A study on the structural characteristics of the Universal Prefab system identified the importance of lateral stability analysis in the conceptual design phase, the relevant stability systems to consider and that the modelling of the connections and floor-slabs should be subject to scrutiny. Additionally, a comprehensive understanding of the UP structural system and elements was established. The considerations listed above formed a crucial guideline for the realization of the intended research objective.

All previous research on SC was considered briefly, but thorough examination was limited to the reports treated in Section 2.1. While the identified opportunities were sufficient challenges for this project, it should be noted that there is undoubtedly more potential for expansion of StructuralComponents.

No comprehensive assessment was made of the current conceptual design tools in the civil engineering industry. The relevance of development of such tools was presumed based on consideration of the previous reports on StructuralComponents, consultation with the thesis committee and the interest expressed by Royal HaskoningDHV.

Sub-objective 2 | Structural Analysis Model

Define a suitable analysis model for providing quick structural validation of the considered assortment of conceptual designs.

A preparatory literature study on (general) lateral stability analysis was documented in Chapter 3. The consideration of various analysis methods helped identify models potentially suitable for structural analysis of UP structures. The applicability of the considered models was assessed through the analysis of six test-buildings and focused on comparison of the modelled lateral load redistribution over the stability walls at ground level. This preliminary investigation led to the selection of the 2D Flat Stick representation for implementation in the CUPD tool prototype; the 'Proportionate' and 'Monolithic' analysis models did not offer sufficient accuracy, even for the relatively simple buildings under consideration. For both non-proportionate and two-dimensional¹ building designs the Matrix Model accurately predicted the base shear distribution due to lateral loads. As a result, the preliminary stick model was expanded and refined into the CUPD Matrix Model.

The defined reference modelling approach formed the basis for the preliminary assessment of

¹ *Two-dimensional* refers to a building design with stability walls both parallel and perpendicular to the axis of loading.

the various models' suitability. While this approach was carefully established and refined, its results were not compared to experimental research on UP structural systems. Whether the adopted approach sufficiently represents reality cannot be guaranteed. However, the author is confident the established practice is well-founded. Engineers inclined to use the CUPD tool could assess the validity of the reference modelling approach using the provided substantiation.

Initially, the intended purpose of the application was to provide full (to a certain degree naturally) structural validation of conceptual building designs, comprising force distribution due to both lateral and gravity loads and unity checks. This goal was modified to calculation of the redistribution of lateral load only. The incorporation of core and double-wall behaviour (Sections 3.3.1 and 3.3.2) as well as the development of the system processes (Section 4.3) required significant effort. The author felt that investigation into accurate modelling of the lateral force distribution in a wide range of building designs contributed more to scientific advancement than the incorporation of relatively standard unity checks.

Sub-objective 3 | CUPD Tool Prototype

Develop a prototype of the proposed tool.

As intended, a functioning tool prototype was successfully created; its development was characterised by two main challenges: development of a process (or: "logic") that can generate an analysable stick model from the relatively limited provided input parameters, and the development of a functioning UI. Implementation of the frame analysis discussed in Section 3.3.3 was relatively straightforward, assuming possession of the required programming skills. Both the "model-assembly logic" and the User Interface are the product of thorough brainstorming and experimentation. A balance was sought between limiting the required input and maximizing design freedom.

Python was used for the development of the tool prototype. While undoubtedly other programming languages also would have been suitable, the author's prior Python programming skills saved time and increased the quality of the final product.

A beta-test, in which the tool prototype would be subject to review by designing engineers, could be used to thoroughly assess the efficiency of the implemented design principles. Based on an example-design and a questionnaire, the participants could provide insight in the strengths and weaknesses of the application. Due to time-constraints an extensive beta-test was not performed. Consequently, qualitative evaluation of the implemented design functionalities was substantiated through the feedback of supervisors and rational assessment by the author.

Optimisation of the collaboration between engineers and architects in the conceptual design phase is one of the key objectives of the StructuralComponents concept. While the UI was designed in a way that the user can efficiently provide the necessary input, the specific input parameters that are required were almost completely dictated by the analysis model. Although the choice for, and the development of this model reflected the need for a limited user-input and rapid analysis, no thorough assessment was made of the requirements imposed by this multidisciplinary process. Nevertheless, the tool prototype does provide quick insight into the force distribution and is at least a good step towards optimal collaboration.

Sub-objective 4 | Result Analysis

Assess the accuracy of the implemented structural analysis model and examine the observed Universal Prefab structural behaviour.

The assessment of the model's accuracy was based on the analysis of nine test-case designs varying in wall configuration, non-proportionality and stability system. For each test-case mul-

tiple buildings with a varying amount of storeys (i.e. height) were modelled with Finite Element software (SCIA Engineer). The base shear distributions were compared to that of the CUPD Matrix Model. Additional to the varying building height, the assessment of the analysis accuracy considered numerous different stiffnesses for the beam-elements comprising the floor-system to arrive at the optimal representation. The Result Analysis continued with an investigation into the influence of the floor-stiffness, a divergent transition floor-thickness and a non-proportionality on the shear force distribution in non-proportionate designs. Both the analysis of the test-cases as well as the investigation into non-proportionate buildings provided a comprehensive understanding of Universal Prefab structural behaviour.

Naturally, the number of considered test-cases was limited. It can be concluded that the analysis model provides estimates of the base shear distribution below an error of 20% for the considered designs. For buildings with a similar floor-plan, this can be assumed as well; there will always be exceptional designs for which the model is not valid. Based on the considered test-cases, the model can be expected to provide sufficiently accurate results for the shear force distributions of the primary walls in following types of building designs:

- proportionate, only parallel walls, three to thirty storeys;
- proportionate, walls in both primary directions, two to thirty storeys;
- proportionate, stability provided by a core, two to thirty storeys;
- non-proportionate interior (change within façade), up to termination of half the stability walls (or less) at $\frac{1}{2}H$ (or above), two to thirty storeys;
- non-proportionate interior and exterior (staircase), up to termination of half the stability walls (or less) at $\frac{1}{2}H$ (or above), mind the results for jumps at $\frac{1}{2}H$ if $N_{storeys} < 10$;

The stability core in the Core test-case was placed with a small eccentricity from the building centre. The twist generated by a large eccentricity could result in inaccuracies regarding the shear distribution in the primary walls. The peaks in the plots of Figure 5.9 (Staircase-Dense test-case) are expected to be caused by the relatively large non-proportionality in a relatively low building. The results for these types of designs should be used with caution. Fortunately, the inaccuracies outside the 20% limit are caused by overestimation of the shear force.

This page has been intentionally left blank.

7 | Conclusion

This chapter presents several concise conclusions regarding the performed research; elaboration of these conclusions can be found at the end of each chapter.

- The developed Conceptual Universal Prefab Design Application increases the design efficiency of Universal Prefab apartment buildings through the combination of a simplified structural representation – allowing for quick analysis – and a graphical User Interface.
- The realised combination of non-proportionate stability systems with user-customisable floor-plans was essential for conceptual design of the considered structures and provided a significant expansion of the StructuralComponents toolbox.
- Accurate prediction of the redistribution of lateral (façade) loads over the stability walls for a wide range of building designs was considered more relevant for conceptual design exploration and validation than providing full design justification based on codes or regulations.
- A finite stiffness of the floor-system leads to more complex redistribution of lateral loads over the stability walls with respect to a rigid floor-system.
- Generally, the assumption of a rigid floor-system is invalid for conceptual design of Universal Prefab structures.
- The devised 2D Flat Stick representation (or 'MatrixModel') proved to be sufficiently flexible for the design and analysis of proportionate, non-proportionate, and core stability systems of Universal Prefab stability systems.
- The devised 2D Flat Stick representation proved to be sufficiently accurate for analysis of proportionate, non-proportionate, and core stability systems of Universal Prefab stability systems.
- A non-proportionate change in a structure with a finite floor-system stiffness causes a disturbance – with respect to a rigid-floor – in the force distributions of the stability system occurs.
- The magnitude of the aforementioned disturbance is larger for a higher floor-stiffness. At excessively high stiffnesses (with respect to the wall stiffness) this effect reverses and converges to the 'rigid-floor' force distributions.
- In a more slender building, a higher disturbance occurs in contrast to more stockier buildings.
- A smaller non-proportionate change (relative to the global building size) leads to a smaller disturbance in the force distributions.
- The force distributions found through analysis of the MatrixModel match the results found by the Differential Super Element Method of Steenbergen (2007).
- Consideration and development of a user-friendly interface provided the developed tool prototype with additional value and demonstrated the feasibility of this feature.

To conclude, the expansion of StructuralComponents was accomplished through the realisation of a tool prototype with significant practical value along with the addition of Universal Prefab structural analysis to the existing toolbox and the combination of user-customisable floor-plans for non-proportionate buildings. The Conceptual Universal Prefab Design Application enhances

the conceptual design efficiency of Universal Prefab buildings and provides rapid and clear insight into their lateral structural behaviour. In doing so, more extensive exploration of the conceptual design space and collaboration between designing engineers and other parties are encouraged. The heightened early-stage design efficiency provides incentive for increased construction of Universal Prefab apartment buildings and can consequently lead to a reduction in residential shortage.

8 | Recommendations

This project investigated the requirements for a conceptual design tool for Universal Prefab structures and realised a prototype of the intended application. This chapter provides several recommendations for successive and related research.

Finite Element Analysis

A potentially suitable analysis procedure for the conceptual design phase could be to make use of existing Finite Element software programs (e.g. SCIA Engineer), controlled by a User Interface through Python scripts, for analysis of a (somewhat) simplified representation of a structure. Advantages of using comprehensive Finite Element software are the accuracy of the analysis and the possibility to create a detailed model of a structure – in contrast to a simpler frame model for example. In the past, speed was one of the main limiting factors for making use of "external" analysis software: it takes additional time to direct an external program, create a model following its exact format, and to interpret its results – which are often not optimal for acquiring the specific results desired. Additionally, calculation can take significant time, depending on the model size. However, FEA-programs (and software in general) are increasing in speed. Conceptual design tools for a specific type of construction could provide the appropriate demarcation of the design space and reduce the input required from the user through assumptions made in the back-end code. Through (Python-)scripts the model is created (from the limited input) and analysed with an external FE-program; only the appropriate results are presented to the user. While this kind of tool may not provide real-time results, it could help designing engineers to verify more design alternatives.

The use of external FEA software requires comprehensive Python bindings to that specific software, which not all companies/institutes possess.

Study on multidisciplinary collaboration

As mentioned in the discussion, this project did not make an extensive assessment of the requirements posed by multidisciplinary collaboration in conceptual design. Whereas the StructuralComponents projects up to and including this research focused mainly on quick and accurate modelling and analysis, it could be interesting to perform a qualitative assessment of the conceptual design practice. Below, various potentially relevant topics have been listed:

- clear visualisation of the appropriate results,
- requirements regarding design composure (e.g. flexibility regarding global structural system versus flexibility regarding singular irregularities in the structural system),
- simultaneous comparison of alternatives: what data makes for relevant comparison

Improvement CUPD Tool

This section offers recommendations on the improvement of the CUPD Tool developed for this project.

Hybrid stability system | The developed tool prototype allows the analysis of shear wall and core stability systems; the 2D Flat Stick representation proved unsuitable for the analysis of their combination – a hybrid system. However, additional research on modelling of the behaviour of UP cores could lead to an improvement on the currently adopted representation: rigid links

to the secondary walls of the core, placement on the building axis perpendicular to the axis of loading. A refinement of the core modelling could increase the accuracy of the MatrixModel for hybrid systems. Since this kind of stability system is regularly applied for UP apartment buildings, its incorporation in the current application would be a significant improvement.

Representation of floor-system | The currently applied representation for the floor-system – beam-elements as wide as the building with unrestrained out-of-plane bending – performed well for the considered test-cases. However, it was observed that the optimum for the beam stiffness varied between test-cases and thus presumably depends on the specific wall configuration. The analysis accuracy is expected to benefit from a representation in which the walls "remain" in their individual locations and are not projected on the primary axes. This would require a different representation of the floor system, suitable for appropriate connection of arbitrary located walls; in Chapter 3 this was regarded unfavourable for this project. However, successive research could focus on the development of an accurate representation of the floor-stiffness with arbitrary located walls and by doing so increase the accuracy of the analysis model. Potentially, a more precise representation could lead to accurate predictions of the hybrid core-shear wall system and/or the upper-floor wall deflections.

Design justification | This research focused on accurate modelling of the force distribution due to lateral loading. The incorporation of gravity loads and design validation based on codes and regulations would further improve the practical value of the tool and thus increase design efficiency for UP apartment buildings. The justification of a design could be focused on capacity checks of the discrete structural elements comprising the UP structure and global checks on stability. Additionally, incorporation of the foundation stiffness would increase the practical relevance of the tool.

Modelling of adjoining walls | In general building practice it can occur that adjacent walls are joined together, forming a T-, U-, or I-shape (or others). The behaviour of these assemblies has not been studied; their incorporation would broaden the applicability of the tool.

Beta-test of design functionalities | As discussed, it would be interesting to perform a qualitative assessment of the design principles implemented in the tool prototype. This could identify opportunities for improvement and, more general, reveal whether the developed tool sufficiently meets the requirements posed by the conceptual design phase.

References

- ABF Research (2020). *Primos 2020 - Prognose van bevolking, huishoudens en woningbehoefte tot 2050*. Research rep.
- Belzen, Thomas van (Oct. 2019). "Revolutionaire bouwers dolblij met stikstof: 'Dit kan weleens dé motor van verandering zijn'". In: *Cobouw*. URL: <https://www.cobouw.nl/duurzaamheid/nieuws/2019/10/van-stikstofnegatief-naar-biobased-en-modulair-dit-kan-weleens-de-motor-van-verduurzaming-zijn-uw-101277340> (visited on 01/11/2021).
- Breach, Mark (2009). *Dissertation Writing for Engineers and Scientists*. Pearson Education Limited. ISBN: 978-1-4058-7278-2.
- CD20 Bouwsystemen (n.d.). *Bouwperspectief*. Brochure.
- Concrete Building Structures* (Nov. 2016). TU Delft.
- Dierker Viik, Leah (Sept. 2019). "StructuralComponents6 - An early-stage design tool for flexible topologies of mid-rise concrete buildings". MA thesis. TU Delft.
- Doherty, Erin (Apr. 2020). *What is Object Oriented Programming? OOP Explained in Depth*. Website. URL: <https://www.educative.io/blog/object-oriented-programming#what-is> (visited on 08/27/2021).
- Dong, Ya Hong et al. (Nov. 2015). "Comparing carbon emissions of precast and cast-in-situ construction methods – A case study of high-rise private building". In: *Construction and Building Materials* 99, pp. 39–53.
- Donovan, Steve (Mar. 2020). *Class vs Object vs Instance*. Website. URL: <https://www.codementor.io/@stevedonovan/class-vs-object-vs-instance-14i2s2lu6r> (visited on 09/07/2021).
- Egeland, Olav and Per O. Araldsen (1974). "SESAM-69 - A General Purpose Finite Element Method Program". In: *Computers & Structures* 4, pp. 41–68.
- Flager, Forest et al. (Aug. 2009). "MULTIDISCIPLINARY PROCESS INTEGRATION AND DESIGN OPTIMIZATION OF A CLASSROOM BUILDING". In: *Journal of Information Technology in Construction* 14, pp. 595–612. ISSN: 1874-4753.
- Groothuisbouw (n.d.). *Wat is Systeembouw?* Website. URL: <https://www.groothuisbouw.nl/vraag-antwoord/systeembouw> (visited on 02/05/2021).
- Hohrath, Babette L. (Apr. 2018). "StructuralComponents5.0 - Super element based tool for early design collaboration applied to mid-rise buildings". MA thesis. TU Delft.
- Jorritsma Bouw (n.d.). *Design / Engineering & Build*. Website. URL: <https://www.jorritsmabouw.nl/utiliteit/expertises/design-engineering-build/> (visited on 02/12/2021).

- Kennisportaal Constructieve Veiligheid (n.d.). *Ontwerpend constructeur*. Website. URL: <https://kpcv.nl/definitie/ontwerpend-constructeur/> (visited on 02/12/2021).
- Maplesoft (2020). *Maple*. Software. Version 2020. URL: <https://www.maplesoft.com/products/Maple/>.
- Ministry of the Interior and Kingdom Relations (2020). *Staat van de Woningmarkt - Jaarrapportage 2020*. Tech. rep.
- NEN-EN 1991-1-4 (2005).
- Projectburo B.V. (2015). *UAV-GC contracten*. Website. URL: <http://uavgc2005.nl/> (visited on 02/12/2021).
- Python (n.d.). Software. URL: python.org.
- Python bindings for the Qt cross platform application toolkit (Mar. 2021). Website. URL: <https://pypi.org/project/PyQt5/> (visited on 09/07/2021).
- Remkes, J.W. et al. (June 2020). *Niet alles kan overal - Eindadvies over structurele aanpak op lange termijn*. Tech. rep. Adviescollege Stikstofproblematiek.
- Robert McNeel & Associates (n.d.). *Grasshopper*. Software. URL: <https://www.rhino3d.com/6/new/grasshopper/>.
- Rolvink, Anke (2010). "StructuralComponents2.0 - A Parametric and Associative Toolbox for Conceptual Design of Tall Building Structures". MA thesis. TU Delft.
- Romero, David Niño (2019). "StructuralComponents 7". MA thesis. TU Delft.
- SCIA NV (n.d.). *SCIA Engineer*. Software. Version 18.1. URL: <https://www.scia.net/en>.
- Simone, Angelo (2011). *An Introduction to the Analysis of Slender Structures*. Tech. rep. Delft University of Technology.
- Smith, Bryan Stafford and Alex Coull (1991). *Tall Building Structures: Analysis and Design*. John Wiley & Sons, INC. ISBN: 0-471-51237-0.
- Steenbergen, Raphaël (2007). "Super Elements in High-Rise Buildings under Stochastic Wind Load". PhD thesis. Technische Universiteit Delft.
- Steenbergen, Raphaël and Johan Blaauwendraad (Jan. 2007). "Closed-form super element method for tall buildings of irregular geometry". In: *International Journal of Solids and Structures* 44, pp. 5576–5597.

List of Figures

1	Characteristic CD20 column-plate connection (CD20 Bouwsystemen n.d.)	v
2	Translation from original design to stick model	vi
3	Relative shear-force distribution in walls of non-proportionate building.	vii
1.1	Expected residential shortage by 2025 (ABF Research 2020)	1
1.2	Potential solution - 'Universal Prefab' apartment buildings	2
1.3	CD20 column-floor connection (CD20 Bouwsystemen n.d.)	3
1.4	Stability system of Fridtjof Nansenhof - Amsterdam	3
1.5	Visualisation of the conceptual design space	5
1.6	The problem definition	6
1.7	Visualisation of key challenges within the problem context	7
1.8	The research objective	8
1.9	The defined sub-objectives	9
1.10	The research process	10
2.1	Structural components of SC5 (Hohrath 2018)	14
2.2	Procedure for traditional SEM (Hohrath 2018)	14
2.3	Rectangular, prismatic floor plan of SC6 case study	15
2.4	Timoshenko representation of rigid frame mid-rise building (Romero 2019)	15
2.5	Hinged versus rigid connection of floor-slabs	16
2.6	Wall elements forming a continuous shear wall, with corresponding shear force distribution	17
2.7	General characteristics of prefab CD20 elements	18
3.1	Proportionality of shear walls (Smith and Coull 1991)	22
3.2	Building examples (Smith and Coull 1991)	23
3.3	24
3.4	Example of reference modelling concept	25

3.5	Modelled dummy elements for different connections	25
3.6	26
3.7	Translation of floor-plan to stick-model	27
3.8	27
3.9	Staircase model	30
3.10	Translation from floor-plan design to stick model	31
3.11	Hinges on beam- and column-ends	32
3.12	Translation from core to stick model	32
3.13	Top-views of test-cases with double walls	33
3.14	Element definition in frame analysis model	34
3.15	Local coordinate systems of structural elements	37
3.16	Matrix 'row-striking' procedure	37
4.1	Classes with attributes	39
4.2	System architecture	40
4.3	Main tab of User Interface	41
4.4	Input (green) for BuildingSection and StabilityWall objects (red)	42
4.5	StabilityWall to Wall- and BeamElement procedure	43
4.6	Visualisation of a non-proportionate MatrixModel	44
5.1	Simple-Scattered test-case top-view	47
5.2	Reference model top-views of test-cases (1)	48
5.3	Reference model top-views of test-cases (2)	49
5.4	Base shear <i>Error</i> vs. $N_{storeys}$ for $E_{beam} = 20GPa$	49
5.5	2D-Dense Base shear - <i>Error</i> vs. $N_{storeys}$ for $E_{beam} = 20GPa$	50
5.6	2D-Scattered Base shear - <i>Error</i> vs. $N_{storeys}$ for $E_{beam} = 20GPa$	50
5.7	Core Base shear - <i>Error</i> vs. $N_{storeys}$ for $E_{beam} = 20GPa$	51
5.8	Hybrid Base shear - <i>Error</i> vs. $N_{storeys}$ for $E_{beam} = 20GPa$	51
5.9	Staircase-Dense Base shear - <i>Error</i> vs. $N_{storeys}$ for $E_{beam} = 20GPa$	52
5.10	Staircase-Triple Base shear - <i>Error</i> vs. $N_{storeys}$ for $E_{beam} = 20GPa$	52

5.11	Steenbergen-Symmetric Base shear - $Error$ vs. $N_{storeys}$ for $E_{beam} = 20GPa$	53
5.12	All test-cases - $RMSE$ vs. $N_{storeys}$ for $E_{beam} = 20GPa$	53
5.13	Staircase-Dense: 8-6 - F_y distributions for varying E_{beam} (primary walls only)	54
5.14	Steenbergen-Symmetric - Interpolated relative distribution F_y for varying E_{beam}	56
5.15	Staircase-Triple - F_y distributions for varying $t_{top-floor}$ (primary walls only)	57
5.16	Symmetric building of Steenbergen (2007)	58
5.17	Relative shear force distributions of Steenbergen (2007) and CUPD Matrix Model	59
5.18	Bending moment distributions of Steenbergen (2007) and CUPD analysis model	60
5.19	Steenbergen-Symmetric - Interpolated distribution F_y over relative height according to the CUPD Matrix Model ($E_{beam} = 20GPa$)	62
B.1	Stability elements	80
C.1	LCS of dummy end-connections (courtesy of SCIA Engineer)	82
E.1	Design of core in reference model	88
E.2	Initial (a & b) and ultimate (c) designs of core model	89
G.1	Main tab of UI	93
G.2	Bottom section tab of UI	94
G.3	Upper section tab 1 of UI	95
G.4	Upper section tab 2 tab of UI	96
G.5	MatrixModel tab of UI	97
G.6	Results-Visual tab of UI	98
G.7	Results-Data tab of UI	99
H.1	MatrixModel top-views of test-cases (1)	101
H.2	MatrixModel top-views of test-cases (2)	102
H.3	RMSE results Simple-Dense	103
H.4	RMSE results 2D-Dense (primary walls only)	103
H.5	RMSE results Simple-Scattered	104
H.6	RMSE results 2D-Scattered (primary walls only)	104

H.7	RMSE results Core (primary walls only)	105
H.8	RMSE results Hybrid (primary walls only)	106
H.9	RMSE results Staircase-Dense (primary walls only)	107
H.10	Additional RMSE results Staircase-Dense (primary walls only; load in y-dir.)	108
H.11	RMSE results Staircase-Triple (primary walls only)	109
H.12	RMSE results Staircase-Triple - 1m thick transition floor (primary walls only)	109
H.13	RMSE results Steenbergen-Symmetric	110
H.14	Steenbergen-Symmetric - Interpolated distribution M_x over relative height according to the CUPD Matrix Model ($E_{floor} = 20GPa$)	111
J.1	Staircase-Dense: 11-3 - F_y distributions for varying E (primary walls only)	113
J.2	Staircase-Triple: 6-4-2 - F_y distributions for varying E (primary walls only)	113
J.3	Staircase-Triple: 9-6-3 - F_y distributions for varying E (primary walls only)	114
J.4	Staircase-Triple: 12-8-4 - F_y distributions for varying E (primary walls only)	114
K.1	Staircase-Dense 8-6 - F_y distributions for varying $t_{top-floor}$ (primary walls only)	115
K.2	Staircase-Dense 8-6 - F_y around non-proportionality for varying $t_{top-floor}$	116
K.3	Staircase-Dense: 11-3 - F_y distributions for varying $t_{top-floor}$ (primary walls only)	116
K.4	Staircase-Triple: 6-4-2 - F_y distributions for varying $t_{top-floor}$ (primary walls only)	117

List of Tables

3.1	Results symmetric models	27
3.2	One storey model - concise results	28
3.3	Six storey model - concise results	28
3.4	Results ten storey models	29
3.5	2D, ten storey model; wind in Y-direction - concise results	29
3.6	2D, ten storey model; wind in X-direction - concise results	29
3.7	Staircase model - concise results	30
3.8	Results double wall test-cases	33
C.1	Vertical dummy element specifications	82
C.2	Lateral dummy element specifications	83
C.3	Shear dummy element specifications	83
C.4	Widener dummy element specifications	83
D.1	One storey model - complete results	84
D.2	Six storey model - complete results	85
D.3	Ten storey model - complete results	85
D.4	2D, ten storey model; wind in Y-direction - complete results	86
D.5	2D, ten storey model; wind in X-direction - complete results	86
D.6	Staircase model - complete results	87
E.1	Initial results - core model Figure E.2b	89
H.1	Considered number of storeys per test-case	100

This page has been intentionally left blank.

A | Semantics

The special concept of prefab construction outlined in Section 1.2.1 is generally called "systeembouw" in Dutch (EN: system-construction). It is often wrongfully assimilated to "regular" prefab construction. In essence it represents a method of building construction in which a single, particular approach is followed for a whole building. Generally (but not necessarily), only prefabricated elements are applied (Groothuisbouw n.d.). In English, the most similar definition would be that of "Total Precast", which represents 'a construction system approach where architectural & structural precast and prestressed concrete components can be combined to create an entire building'¹. To make a slight distinction, the author has decided on the term "Universal Prefab" for the representation of the system introduced in Section 1.2.1.

¹This definition is not universally accepted however, others can be found.

B | Stability Systems

This appendix gives a concise summary of the principles of two stability systems which serve as a basis for a multitude of mid- and high-rise Universal Prefab apartment building designs. Further elaboration of lateral stability and its analysis is presented in Chapter 3.

Shear wall structures | A shear wall structure is a structure in which the lateral stability is mainly ensured by vertical walls. These walls, with very high in-plane stiffness, act as vertical cantilevers clamped at the foundation (see Figure B.1a) and 'deform predominantly in flexure' (Smith and Coull 1991, p.184). The behaviour of a *single* shear wall can be roughly described with the 4th-order differential equation for bending. For a *system* of shear walls, the calculation is somewhat more complicated due to the coupling between the walls. Important to note is the necessity of at least three walls in order to ensure stability in every direction, since a shear wall only contributes 'to the rigidity of the building within the plane of the wall' (*Concrete Building Structures* 2016, p.4.21). Additionally, the planar axes of all shear walls may not converge at a single point (*Concrete Building Structures* 2016). When composing the floor plan, it can be beneficial to distribute the walls such that the gravitational loading suppresses the lateral load tensile stresses. For residential buildings, the floor plan restrictions introduced by the solid walls do not, in general, pose a significant problem by functioning as stability and partition walls between apartments simultaneously (Smith and Coull 1991).

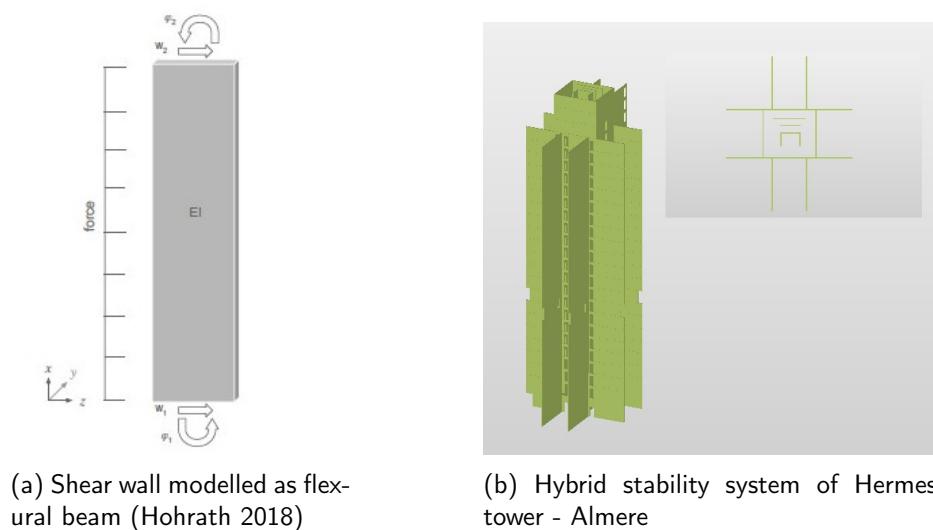


Figure B.1: Stability elements

Core structures | In a 'classical' core structure, a single continuous core is responsible for providing lateral stability as well as carrying the entire gravity load. Either all or some floors or one single floor just above ground are supported by cantilevers from the core¹. In general, 'the moments of inertia of a reinforced concrete core are invariably large' (Smith and Coull 1991, p.308) and the relatively high torsional stiffness of the core supplies 'a significant part of the total torsional resistance of the building' (Smith and Coull 1991, p.308).

¹The floors not supported by cantilevers are supported by columns, which terminate on the cantilever supports below.

Hybrid structures | Possessing a basic understanding of the stability systems mentioned above, the concept of a hybrid system can now be introduced. There are cases in which it can be beneficial to combine multiple stability or load bearing systems (Smith and Coull 1991). In apartment buildings, this combination generally consists of a core surrounding the stairwells and elevators and shear walls providing additional stability (see Figure B.1b), while simultaneously functioning as partition walls. As stated above, the stabilisation due to a core works similar to a shear wall system, as does the hybrid system.

C | Reference Modelling - Dummy Elements

This appendix documents the specifications of the modelled dummy-elements. The Local Coordinate System (LCS) of the elements (and their end-connections) is shown in Figure C.1. ϕ_x represents a rotation around the x-axis of the dummy-element, ϕ_y around the y-axis, etcetera.

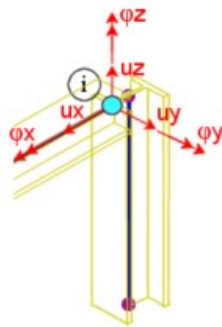


Figure C.1: LCS of dummy end-connections (courtesy of SCIA Engineer)

The stiffness of the 'vertical' and 'lateral' dummy elements has been adopted from existing FE-models and is in accordance with the stiffness of the actual CD20 column-floor slab connection. This connection can be considered virtually rigid in comparison to the floor slabs and their seam-joints. The E-modulus of the 'shear' dummy elements is such that the EA of a seam joint is equal to the EA of its corresponding dummy bar. Since the seam between two plates in Y-direction ($B = 7.2m$, $t = 200mm$) is wider than between plates in X-direction ($B = 3.6m$, $t = 200mm$), the dummy bar connecting plates in Y-direction has a higher stiffness.

Table C.1: Vertical dummy element specifications

Function	Transfer of vertical force from floor slabs to vertical elements
Joint	Models characteristic CD20 column-floor slab connection, in combination with 'lateral' dummy elements
Cross-section	Circular steel bar; $\varnothing 50$ mm
E-modulus	$2.1e10$ MPa
DoFs plate-side	u_z and ϕ_y are restrained; remaining DoFs are free
DoFs column/wall-side	All DoFs are restrained

Table C.2: Lateral dummy element specifications

Function	Transfer of lateral force from floor slabs to vertical elements
Joint	Models characteristic CD20 column-floor slab connection, in combination with 'vertical' dummy elements
Cross-section	Circular steel bar; $\varnothing 50$ mm
E-modulus	2.1e10 MPa
DoFs plate-side	u_x and u_y are restrained; remaining DoFs are free
DoFs column/wall-side	ϕ_z is free; remaining DoFs are restrained

Table C.3: Shear dummy element specifications

Function	Transfer of shear force from floor slab to floor slab
Joint	Models seam joint between floor slabs
Cross-section	Circular steel bar; $\varnothing 50$ mm
E-modulus in y-direction	2.74e7 MPa
E-modulus in x-direction	1.37e7 MPa
DoFs side 1	u_y and ϕ_z are restrained; remaining DoFs are free
DoFs side 2	All DoFs are restrained

Table C.4: Widener dummy element specifications

Function	Widens columns/walls for connection to 'lateral' dummies
Joint	-
Cross-section	Circular steel bar; $\varnothing 50$ mm
E-modulus	1e14 MPa (maximum value in SCIA Engineer; virtually rigid)
DoFs free-side	All DoFs are restricted
DoFs column/wall-side	All DoFs are restricted

D | Preliminary Research on UP Behaviour - Results

This appendix documents the complete results of the preliminary research on the redistribution of lateral loads in UP structures and the performance of the preliminary 2D flat stick model regarding this behaviour.

Table D.1: One storey model - complete results

	R_y [kN]			RMSE [%]
	Left	Middle	Right	
Reference	-13.69	-50.33	-30.04	-
Proportionate	-26.92	-30.29	-37.02	61.82
Monolithic (Rigid)	-26.92	-30.27	-36.99	61.81
Monolithic (37300MPa)	-15.27	-47.57	-31.12	7.66
Monolithic (30000MPa)	-14.51	-48.71	-30.74	4.15
Monolithic (25000MPa)	-13.93	-49.58	-30.45	1.54
Monolithic (20000MPa)	-13.29	-50.54	-30.10	1.71
Monolithic (15000MPa)	-12.59	-51.59	-29.78	4.88
Stick (Rigid)	-26.92	-30.28	-37.01	61.82
Stick (37300MPa)	-14.98	-48.19	-31.03	6.26
Stick (30000MPa)	-14.17	-49.40	-30.62	2.55
Stick (25000MPa)	-13.55	-50.33	-30.61	0.79
Stick (20000MPa)	-12.87	-51.23	-29.97	3.65
Stick (15000MPa)	-12.11	-52.50	-29.61	7.16

Table D.2: Six storey model - complete results

	R_y [kN]			RMSE [%]
	Left	Middle	Right	
Reference	-131.82	-218.91	-198.77	-
Proportionate	-161.52	-181.71	-222.09	17.65
Monolithic (Rigid)	-156.17	-183.07	-211.97	14.76
Equivalent (37300MPa)	-149.91	-191.95	-208.79	10.35
Equivalent (30000MPa)	-148.99	-193.33	-208.32	9.80
Equivalent (20000MPa)	-146.92	-196.45	-207.26	9.21
Equivalent (15000MPa)	-145.15	-199.13	-206.35	8.13
Equivalent (10000MPa)	-142.18	-203.61	-204.81	5.89
Equivalent (5000MPa)	-135.90	-213.08	-201.56	2.49
Stick (Rigid)	-161.52	-181.71	-222.09	17.65
Stick (37300MPa)	-145.51	-205.75	-214.07	8.23
Stick (30000MPa)	-143.44	-208.84	-213.04	7.08
Stick (25000MPa)	-141.60	-211.61	-212.11	6.09
Stick (20000MPa)	-139.19	-215.22	-210.91	4.88
Stick (15000MPa)	-135.85	-220.23	-209.24	3.53
Stick (10000MPa)	-130.66	-228.03	-206.64	3.36

Table D.3: Ten storey model - complete results

	R_y [kN]			RMSE [%]
	Left	Middle	Right	
Reference	-243.05	-334.06	-348.20	-
Proportionate	-269.20	-302.85	-370.15	9.00
Monolithic (Rigid)	-265.97	-306.49	-362.63	7.62
Monolithic (37300MPa)	-257.84	-312.68	-356.92	3.77
Monolithic (30000MPa)	-257.04	-313.86	-356.53	3.51
Monolithic (25000MPa)	-256.27	-315.01	-356.14	3.25
Monolithic (20000MPa)	-255.19	-316.63	-355.60	4.35
Monolithic (15000MPa)	-253.55	-319.10	-354.76	3.75
Stick (Rigid)	-269.21	-302.85	-370.14	9.00
Stick (37300MPa)	-253.03	-327.14	-361.04	3.51
Stick (30000MPa)	-250.88	-330.37	-360.96	2.89
Stick (25000MPa)	-248.93	-333.29	-359.99	2.41
Stick (20000MPa)	-246.36	-337.14	-358.70	1.98
Stick (15000MPa)	-242.76	-342.55	-356.90	2.06

Table D.4: 2D, ten storey model; wind in Y-direction - complete results

	R_y [kN]					RMSE [%]
	Wall 1	Wall 2	Wall 3	Wall 4	Wall 5	
Reference	-476.29	-72.69	-73.48	-222.64	-404.44	-
Proportionate	-563.44	-20.28	-19.69	-152.1	-499.82	49.86
Monolithic (Rigid)	-422.90	-109.69	-105.69	-240.15	-363.44	30.99
Monolithic (37300MPa)	-473.52	-74.16	-73.06	-224.71	-403.26	1.07
Monolithic (20000MPa)	-473.53	-73.46	-72.98	-227.63	-401.51	1.22
Stick (Rigid)	-423.73	-112.91	-108.74	-244.46	-363.45	33.72
Stick (37300MPa)	-478.13	-73.20	-69.00	-227.25	-406.30	2.91
Stick (30000MPa)	-477.09	-73.48	-69.62	-299.14	-404.54	2.73
Stick (25000MPa)	-475.95	-73.84	-70.31	-231.01	-402.75	2.66
Stick (20000MPa)	-474.20	-74.46	-71.38	-233.66	-400.13	2.83
Stick (15000MPa)	-471.35	-75.57	-73.12	-237.66	-396.07	3.66

Table D.5: 2D, ten storey model; wind in X-direction - complete results

	R_x [kN]		RMSE [%]
	Wall 6	Wall 7	
Reference	-235.72	-235.78	-
Proportionate	-235.75	-235.75	0.01
Monolithic (Rigid)	-229.22	-230.54	2.50
Monolithic (37300MPa)	-236.66	-229.12	2.02
Monolithic (20000MPa)	-238.05	-227.07	2.70
Stick (Rigid)	-232.32	-232.32	1.45
Stick (37300MPa)	-232.66	-232.66	1.31
Stick (30000MPa)	-232.69	-232.69	1.30
Stick (25000MPa)	-232.71	-232.71	1.29
Stick (20000MPa)	-232.74	-232.74	1.27
Stick (15000MPa)	-232.77	-232.77	1.26

Table D.6: Staircase model - complete results

	R_y [kN]					RMSE [%]
	Wall 1	Wall 2	Wall 3	Wall 4	Wall 5	
Reference	-301.99	-313.68	-312.35	-314.21	-263.04	-
Proportionate	-287.52	-306.67	-325.82	-344.97	-241.95	6.43
Monolithic (Rigid)	-318.31	-310.67	-303.03	-295.39	-280.12	4.84
Monolithic (37300MPa)	-311.35	-315.83	-304.80	-299.81	-275.74	3.47
Monolithic (30000MPa)	-307.94	-317.09	-307.25	-302.15	-273.10	3.47
Monolithic (25000MPa)	-304.53	-318.22	-309.78	-304.63	-270.38	2.03
Monolithic (20000MPa)	-304.08	-316.91	-310.64	-306.75	-269.15	1.60
Monolithic (15000MPa)	-296.92	-318.86	-316.09	-312.69	-262.98	1.20
Stick (Rigid)	-318.31	-310.67	-303.04	-295.40	-280.12	4.84
Stick (37300MPa)	-311.35	-315.83	-304.80	-299.81	-275.74	3.47
Stick (30000MPa)	-307.94	-317.09	-307.25	-302.15	-273.10	2.72
Stick (25000MPa)	-304.53	-318.22	-309.78	-304.63	-270.38	2.03
Stick (20000MPa)	-299.71	-319.65	-313.42	-308.36	-266.40	1.37
Stick (15000MPa)	-292.58	-321.43	-318.87	-314.42	-260.22	2.07

E | Reference Modelling - Core

This appendix documents the reference modelling approach of a core system and the investigation into various stick-representations of a core structure.

E.1 | Reference model

The discrete wall elements forming a core are not to be modelled as rigidly connected at the corners of the core (J. Brouns, personal communication, June 15, 2021). The connection between two perpendicular walls can be considered hinged. To assume a full shear transfer, sufficient vertical load is required to activate the connecting reinforcement. In the conceptual design phase, this cannot be assumed outright. To arrive at a conservative model for the core behaviour, the shear wall elements have been placed and connected as follows:

- vertically stacked wall elements are connected rigidly through dummy elements (a gap is needed between two storeys, see third item),
- the width of the walls in a certain direction alternates per storey (see Figure E.1): the walls in one direction are slightly longer than in the other direction, but on the floors below and above this is the other way around,
- a wall in x-direction is connected to the walls in y-direction on the adjacent storeys with a dummy element (as shown in the figure) that only transfers normal force,
- perpendicular walls on the same level are not connected directly.

The modelling approach outlined above has been approved by RHDHV engineer J. Brouns. As was the intent, this model is expected to be quite conservative.



Figure E.1: Design of core in reference model

E.2 | 2D Flat Stick representation

The method of projecting the complete core on one primary building axis (see Section 3.3.1) was applied for all models considered. Various methods of connecting the secondary to the primary walls were analysed.

Initially, the secondary core walls were connected to a column in the centre of the core with beams similar to the floor-beams, creating a cross-like system as shown in Figure E.2. These beams were assigned a width equal to that of the core. Comparison to the reference model

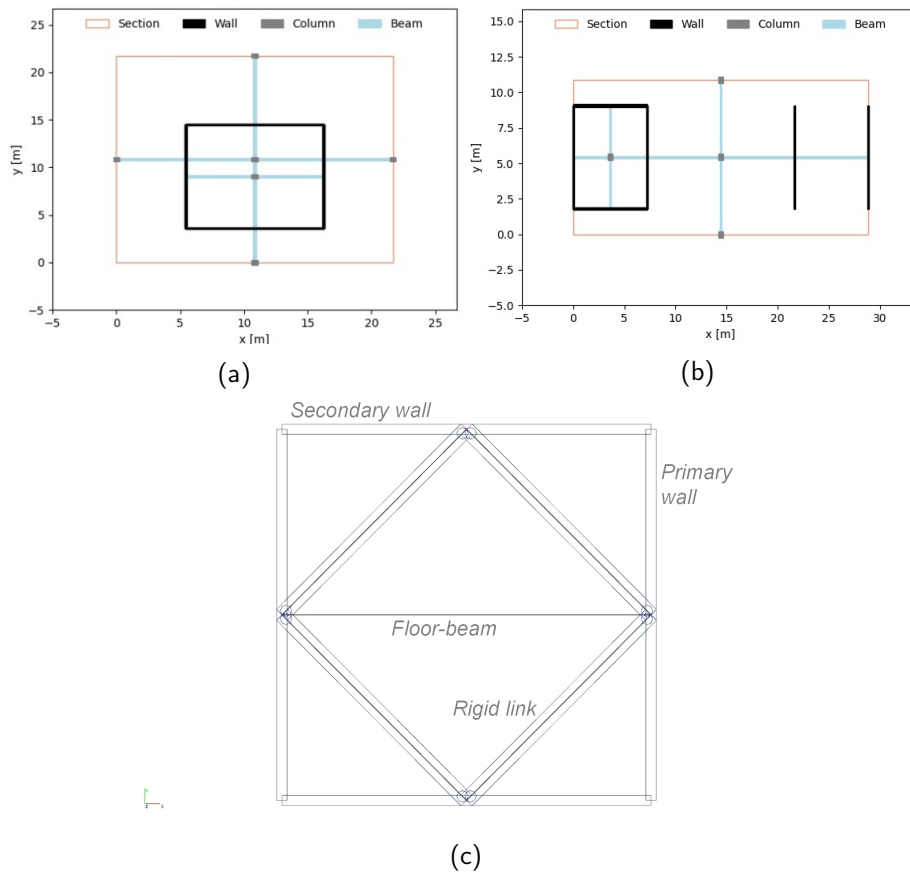


Figure E.2: Initial (a & b) and ultimate (c) designs of core model

showed inaccurate results. Consequently, the stiffness of the secondary and eventually also primary beams was varied, without success. Too little lateral load was redistributed to the walls in secondary direction (W5 to W7), as Table E.1 illustrates.

Table E.1: Initial results - core model Figure E.2b

	Wall base shear [kN] (in direction of wall)						
	Wall 1	Wall 2	Wall 3	Wall 4	Wall 5	Wall 6	Wall 7
Reference	-250.61	-444.02	-306.54	-238.58	-42.63	-76.03	114.36
Cross - Rigid secondary	-302.29	-323.62	-324.04	-301.13	-0.43	-7.49	-7.07
Cross - Rigid both	-304.72	-320.70	-323.52	-301.69	-0.65	-7.67	8.30
Rigid links	-273.83	-392.40	-296.86	-282.00	-25.62	-47.65	72.82
Rigid links (w/ hinges)	-258.49	-416.65	-295.02	-274.82	-18.53	-69.85	88.08

The results of the ultimately selected approach, connecting the secondary walls through rigid links, are also given in the table above. Both alternatives redistributed more of the lateral load to the secondary walls, improving the estimation of the base shear of the primary walls. While the error is still significant for the secondary walls (which are not governing), this approach provided the best primary wall result of a wide variety of considered options. The hinged rigid links performed best and the model has been explained in detail in Section 3.3.1.

F | Element stiffness matrix - Maple

```

> restart;
> ODE1 :=  $\frac{\chi[s] \cdot kt \cdot L^2}{12} \cdot \text{diff}(\text{phi}(p), p) - kt \cdot (\text{diff}(w(p), p) + \text{phi}(p)) = 0$  : ODE2 :=  $kt$ 
     $\cdot (\text{diff}(w(p), p) + \text{diff}(\text{phi}(p), p)) = -qt$  :
> ODE3 :=  $\frac{\chi[t] \cdot ks \cdot L^2}{12} \cdot \text{diff}(\text{delta}(p), p) + ks \cdot (\text{diff}(v(p), p) - \text{delta}(p)) = 0$  : ODE4 :=  $ks$ 
     $\cdot (\text{diff}(v(p), p) - \text{diff}(\text{delta}(p), p)) = -qs$  :
> ODE5 :=  $EA \cdot \text{diff}(u(p), p) = -qp$  : ODE6 :=  $GIp \cdot \text{diff}(zeta(p), p) = 0$  :
>
> sol := dsolve( {ODE1, ODE2, ODE3, ODE4, ODE5, ODE6}, {w(p), phi(p), v(p), delta(p),
    u(p), zeta(p)} ) : assign(sol) :
>
> u := u(p) : zeta := zeta(p) :
v := v(p) : delta := delta(p) :
w := w(p) : phi := phi(p) :
>
> Ms :=  $EIs \cdot \text{diff}(\text{phi}, p)$  : Vt :=  $\text{diff}(Ms, p)$  :
Mt :=  $-EIt \cdot \text{diff}(\text{delta}, p)$  : Vs :=  $\text{diff}(Mt, p)$  :
Mp :=  $GIp \cdot \text{diff}(zeta, p)$  : Vp :=  $EA \cdot \text{diff}(u, p)$  :
>
> p := 0 :
eq1 :=  $u = u1$  : eq2 :=  $zeta = zeta1$  : Fp1 :=  $-Vp$  : Tp1 :=  $-Mp$  :
eq3 :=  $w = w1$  : eq4 :=  $\text{phi} = \text{phi1}$  : Ft1 :=  $-Vt$  : Ts1 :=  $-Ms$  :
eq5 :=  $v = v1$  : eq6 :=  $\text{delta} = \text{delta1}$  : Fs1 :=  $-Vs$  : Tt1 :=  $Mt$  :
>
> p := L :
eq7 :=  $u = u2$  : eq8 :=  $zeta = zeta2$  : Fp2 :=  $Vp$  : Tp2 :=  $Mp$  :
eq9 :=  $w = w2$  : eq10 :=  $\text{phi} = \text{phi2}$  : Ft2 :=  $Vt$  : Ts2 :=  $Ms$  :
eq11 :=  $v = v2$  : eq12 :=  $\text{delta} = \text{delta2}$  : Fs2 :=  $Vs$  : Tt2 :=  $-Mt$  :
>
> sol := solve( {eq1, eq2, eq3, eq4, eq5, eq6, eq7, eq8, eq9, eq10, eq11, eq12}, {_C1, _C2, _C3,
    _C4, _C5, _C6, _C7, _C8, _C9, _C10, _C11, _C12} ) : assign(sol) :
>

```

```

> K := Matrix( [
  [coeff( collect(Fp1, u1), u1), coeff( collect(Fp1, v1), v1), coeff( collect(Fp1, w1), w1),
    coeff( collect(Fp1, zeta1), zeta1), coeff( collect(Fp1, phi1), phi1), coeff( collect(Fp1,
    delta1), delta1), coeff( collect(Fp1, u2), u2), coeff( collect(Fp1, v2), v2),
    coeff( collect(Fp1, w2), w2), coeff( collect(Fp1, zeta2), zeta2), coeff( collect(Fp1, phi2),
    phi2), coeff( collect(Fp1, delta2), delta2) ],

  [coeff( collect(Fs1, u1), u1), coeff( collect(Fs1, v1), v1), coeff( collect(Fs1, w1), w1),
    coeff( collect(Fs1, zeta1), zeta1), coeff( collect(Fs1, phi1), phi1), coeff( collect(Fs1,
    delta1), delta1), coeff( collect(Fs1, u2), u2), coeff( collect(Fs1, v2), v2),
    coeff( collect(Fs1, w2), w2), coeff( collect(Fs1, zeta2), zeta2), coeff( collect(Fs1, phi2),
    phi2), coeff( collect(Fs1, delta2), delta2) ],

  [coeff( collect(Ft1, u1), u1), coeff( collect(Ft1, v1), v1), coeff( collect(Ft1, w1), w1),
    coeff( collect(Ft1, zeta1), zeta1), coeff( collect(Ft1, phi1), phi1), coeff( collect(Ft1,
    delta1), delta1), coeff( collect(Ft1, u2), u2), coeff( collect(Ft1, v2), v2), coeff( collect(Ft1,
    w2), w2), coeff( collect(Ft1, zeta2), zeta2), coeff( collect(Ft1, phi2), phi2),
    coeff( collect(Ft1, delta2), delta2) ],

  [coeff( collect(Tp1, u1), u1), coeff( collect(Tp1, v1), v1), coeff( collect(Tp1, w1), w1),
    coeff( collect(Tp1, zeta1), zeta1), coeff( collect(Tp1, phi1), phi1), coeff( collect(Tp1,
    delta1), delta1), coeff( collect(Tp1, u2), u2), coeff( collect(Tp1, v2), v2),
    coeff( collect(Tp1, w2), w2), coeff( collect(Tp1, zeta2), zeta2), coeff( collect(Tp1, phi2),
    phi2), coeff( collect(Tp1, delta2), delta2) ],

  [coeff( collect(Ts1, u1), u1), coeff( collect(Ts1, v1), v1), coeff( collect(Ts1, w1), w1),
    coeff( collect(Ts1, zeta1), zeta1), coeff( collect(Ts1, phi1), phi1), coeff( collect(Ts1,
    delta1), delta1), coeff( collect(Ts1, u2), u2), coeff( collect(Ts1, v2), v2), coeff( collect(Ts1,
    w2), w2), coeff( collect(Ts1, zeta2), zeta2), coeff( collect(Ts1, phi2), phi2),
    coeff( collect(Ts1, delta2), delta2) ],

  [coeff( collect(Tt1, u1), u1), coeff( collect(Tt1, v1), v1), coeff( collect(Tt1, w1), w1),
    coeff( collect(Tt1, zeta1), zeta1), coeff( collect(Tt1, phi1), phi1), coeff( collect(Tt1, delta1),
    delta1), coeff( collect(Tt1, u2), u2), coeff( collect(Tt1, v2), v2), coeff( collect(Tt1, w2),
    w2), coeff( collect(Tt1, zeta2), zeta2), coeff( collect(Tt1, phi2), phi2), coeff( collect(Tt1,
    delta2), delta2) ],

  [coeff( collect(Fp2, u1), u1), coeff( collect(Fp2, v1), v1), coeff( collect(Fp2, w1), w1),
    coeff( collect(Fp2, zeta1), zeta1), coeff( collect(Fp2, phi1), phi1), coeff( collect(Fp2,
    delta1), delta1), coeff( collect(Fp2, u2), u2), coeff( collect(Fp2, v2), v2),
    coeff( collect(Fp2, w2), w2), coeff( collect(Fp2, zeta2), zeta2), coeff( collect(Fp2, phi2),
    phi2), coeff( collect(Fp2, delta2), delta2) ],

  [coeff( collect(Fs2, u1), u1), coeff( collect(Fs2, v1), v1), coeff( collect(Fs2, w1), w1),
    coeff( collect(Fs2, zeta1), zeta1), coeff( collect(Fs2, phi1), phi1), coeff( collect(Fs2,
    delta1), delta1), coeff( collect(Fs2, u2), u2), coeff( collect(Fs2, v2), v2),
    coeff( collect(Fs2, w2), w2), coeff( collect(Fs2, zeta2), zeta2), coeff( collect(Fs2, phi2),
    phi2), coeff( collect(Fs2, delta2), delta2) ],

  [coeff( collect(Ft2, u1), u1), coeff( collect(Ft2, v1), v1), coeff( collect(Ft2, w1), w1),
    coeff( collect(Ft2, zeta1), zeta1), coeff( collect(Ft2, phi1), phi1), coeff( collect(Ft2,

```

$\text{coeff}(\text{collect}(Ft2, u2), u2), \text{coeff}(\text{collect}(Ft2, v2), v2), \text{coeff}(\text{collect}(Ft2, w2), w2), \text{coeff}(\text{collect}(Ft2, zeta2), zeta2), \text{coeff}(\text{collect}(Ft2, phi2), phi2), \text{coeff}(\text{collect}(Ft2, delta2), delta2)]$,

$[\text{coeff}(\text{collect}(Tp2, u1), u1), \text{coeff}(\text{collect}(Tp2, v1), v1), \text{coeff}(\text{collect}(Tp2, w1), w1), \text{coeff}(\text{collect}(Tp2, zeta1), zeta1), \text{coeff}(\text{collect}(Tp2, phi1), phi1), \text{coeff}(\text{collect}(Tp2, delta1), delta1), \text{coeff}(\text{collect}(Tp2, u2), u2), \text{coeff}(\text{collect}(Tp2, v2), v2), \text{coeff}(\text{collect}(Tp2, w2), w2), \text{coeff}(\text{collect}(Tp2, zeta2), zeta2), \text{coeff}(\text{collect}(Tp2, phi2), phi2), \text{coeff}(\text{collect}(Tp2, delta2), delta2)]$,

$[\text{coeff}(\text{collect}(Ts2, u1), u1), \text{coeff}(\text{collect}(Ts2, v1), v1), \text{coeff}(\text{collect}(Ts2, w1), w1), \text{coeff}(\text{collect}(Ts2, zeta1), zeta1), \text{coeff}(\text{collect}(Ts2, phi1), phi1), \text{coeff}(\text{collect}(Ts2, delta1), delta1), \text{coeff}(\text{collect}(Ts2, u2), u2), \text{coeff}(\text{collect}(Ts2, v2), v2), \text{coeff}(\text{collect}(Ts2, w2), w2), \text{coeff}(\text{collect}(Ts2, zeta2), zeta2), \text{coeff}(\text{collect}(Ts2, phi2), phi2), \text{coeff}(\text{collect}(Ts2, delta2), delta2)]$,

$[\text{coeff}(\text{collect}(Tt2, u1), u1), \text{coeff}(\text{collect}(Tt2, v1), v1), \text{coeff}(\text{collect}(Tt2, w1), w1), \text{coeff}(\text{collect}(Tt2, zeta1), zeta1), \text{coeff}(\text{collect}(Tt2, phi1), phi1), \text{coeff}(\text{collect}(Tt2, delta1), delta1), \text{coeff}(\text{collect}(Tt2, u2), u2), \text{coeff}(\text{collect}(Tt2, v2), v2), \text{coeff}(\text{collect}(Tt2, w2), w2), \text{coeff}(\text{collect}(Tt2, zeta2), zeta2), \text{coeff}(\text{collect}(Tt2, phi2), phi2), \text{coeff}(\text{collect}(Tt2, delta2), delta2)]$

]) :

$\Rightarrow \text{simplify}(K)$

\Rightarrow

G | User Interface - Figures

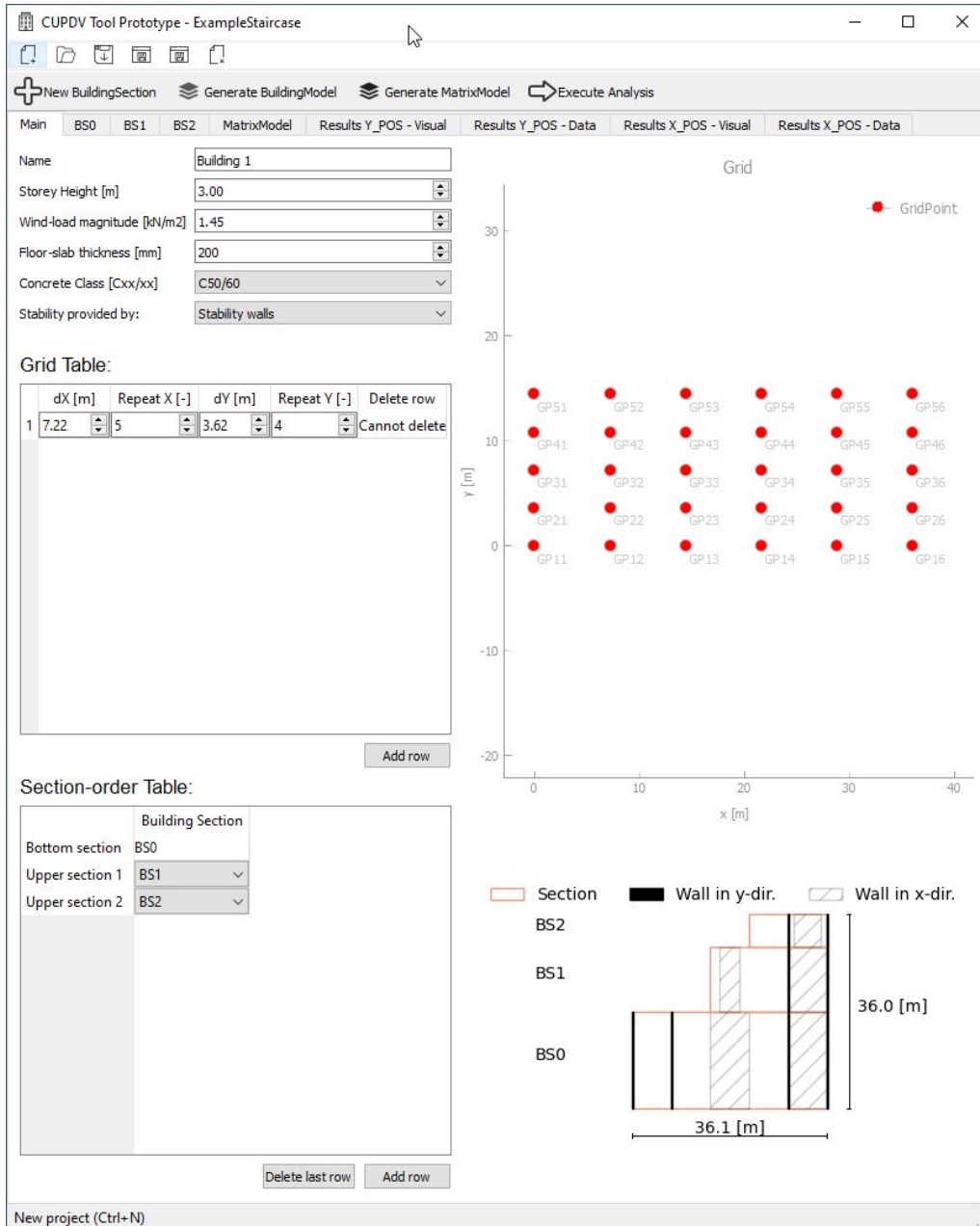


Figure G.1: Main tab of UI

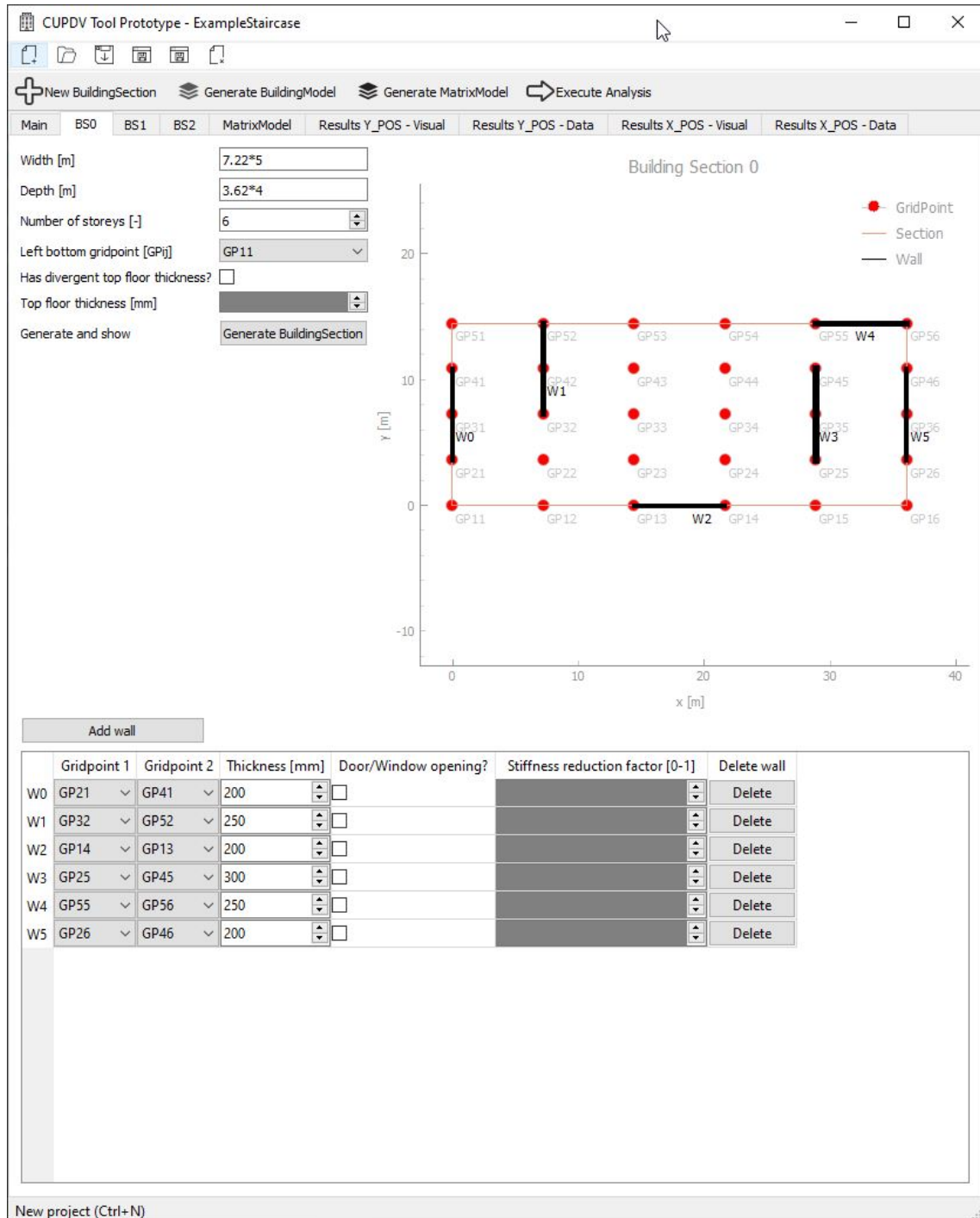


Figure G.2: Bottom section tab of UI

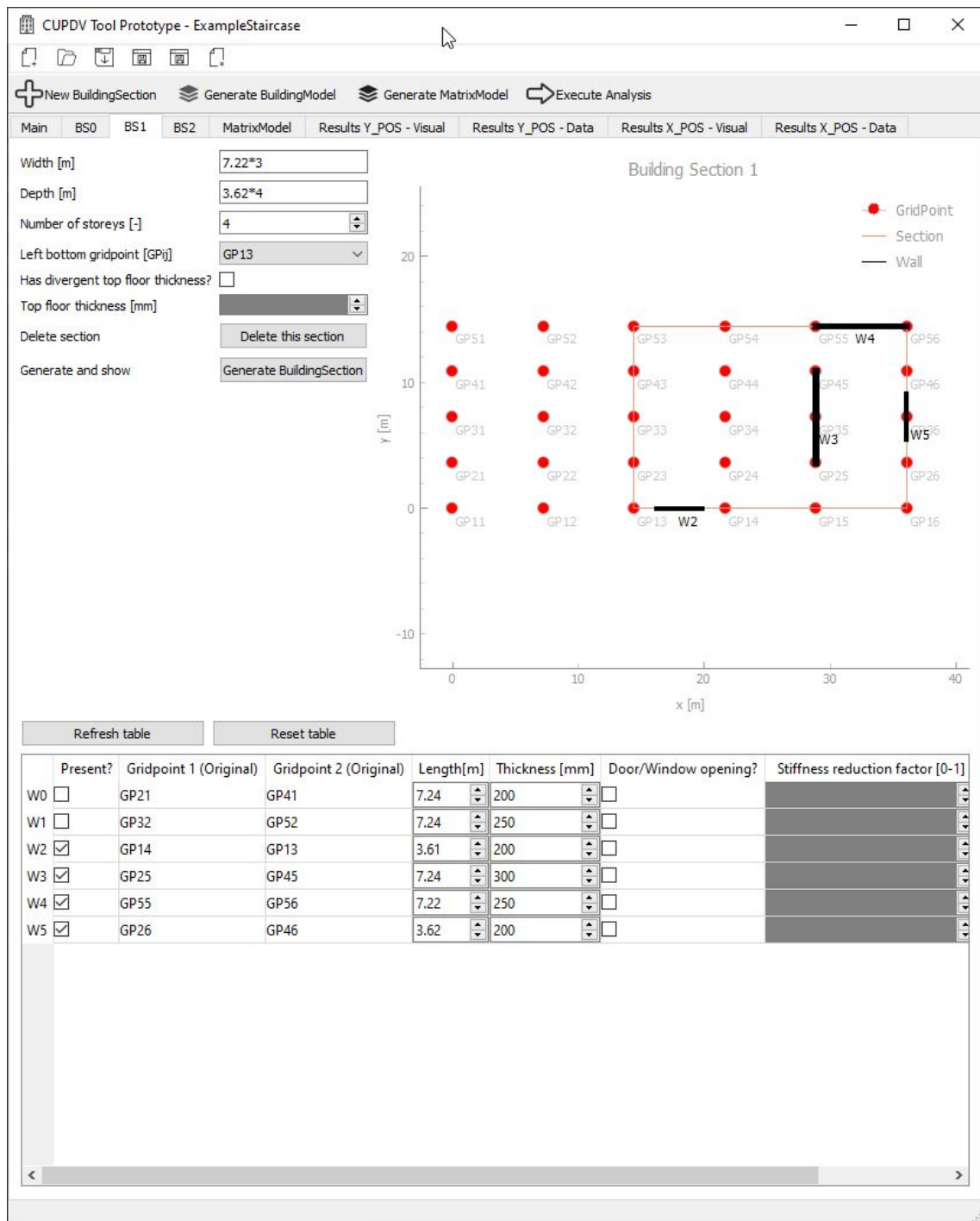


Figure G.3: Upper section tab 1 of UI

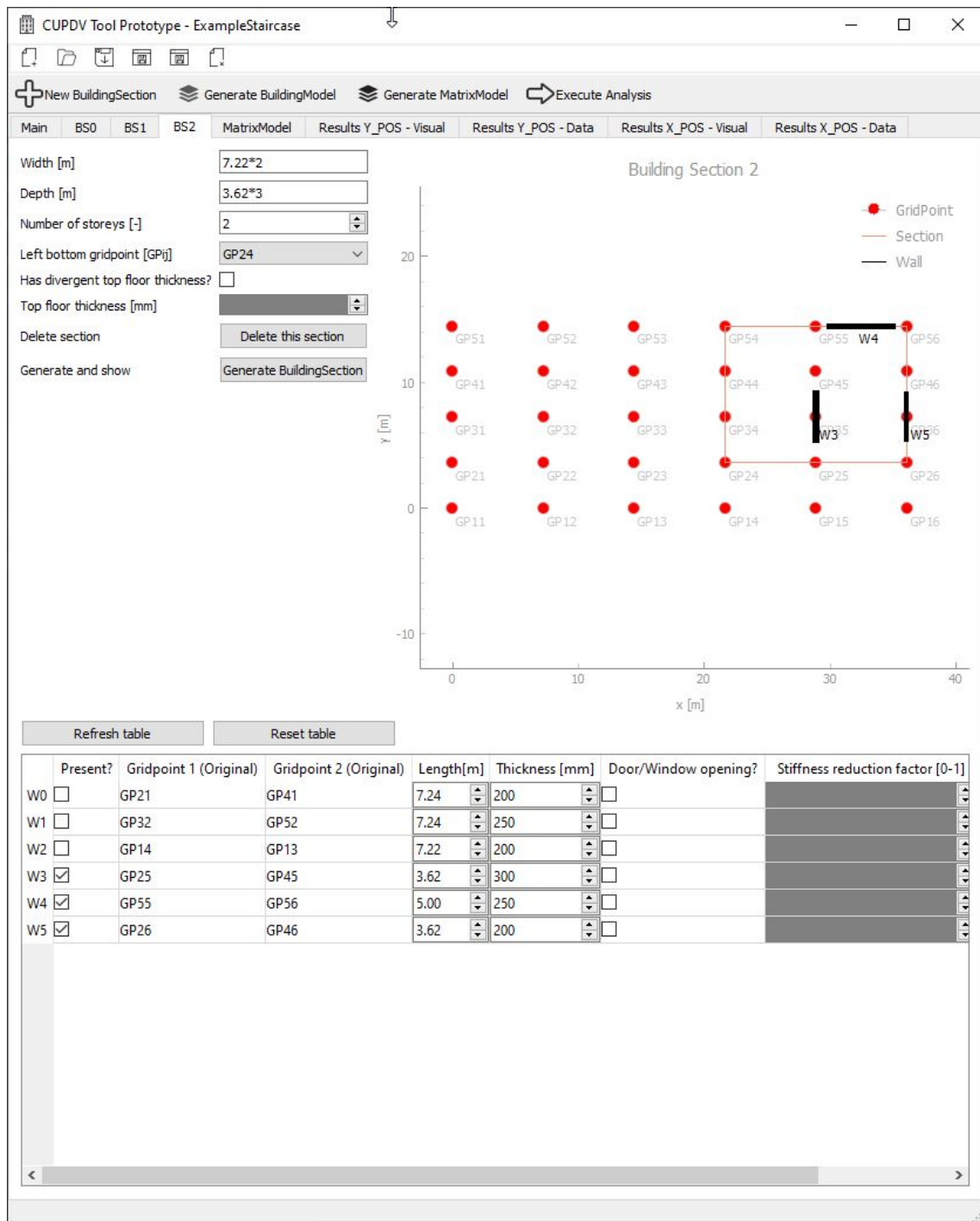


Figure G.4: Upper section tab 2 tab of UI

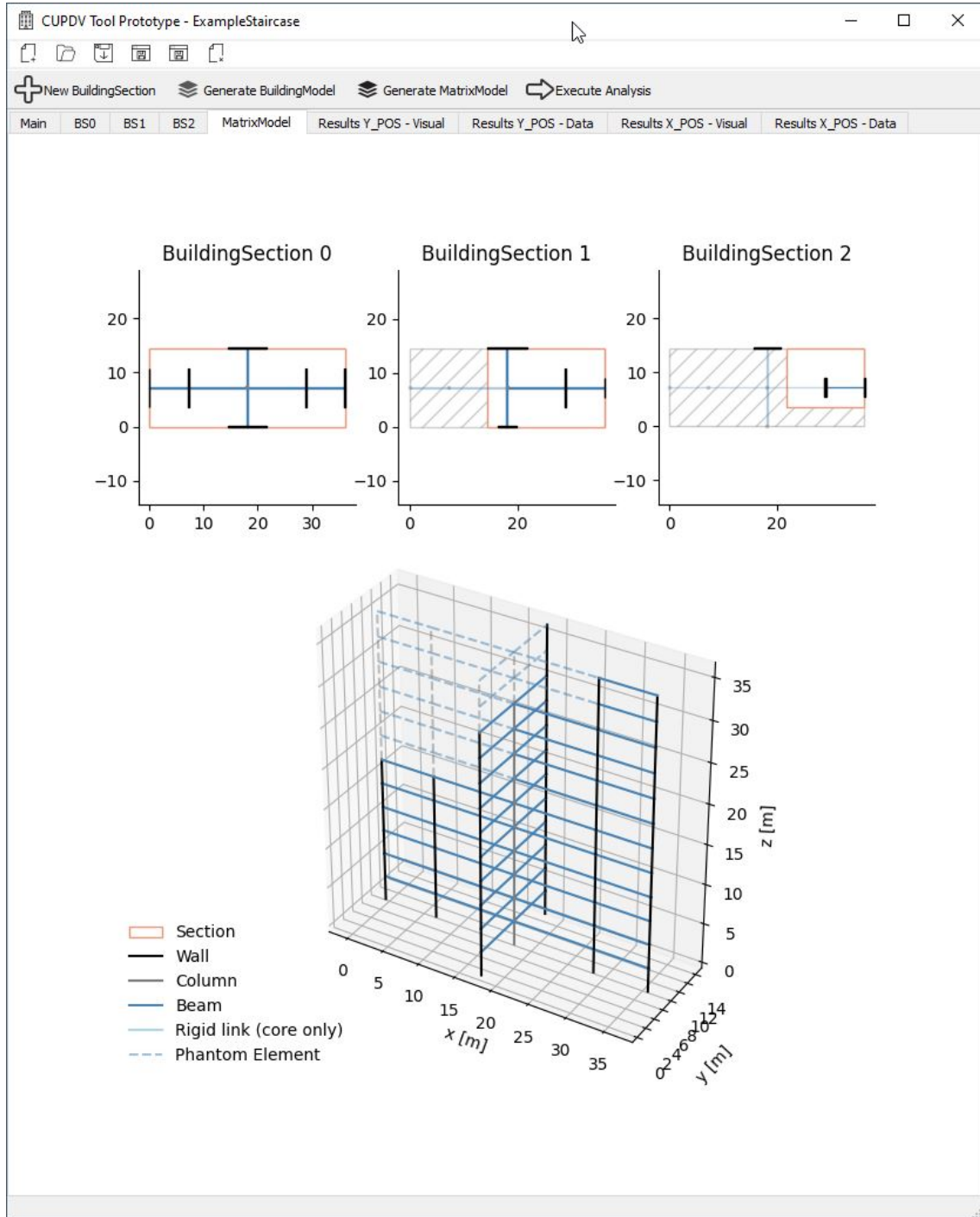


Figure G.5: MatrixModel tab of UI

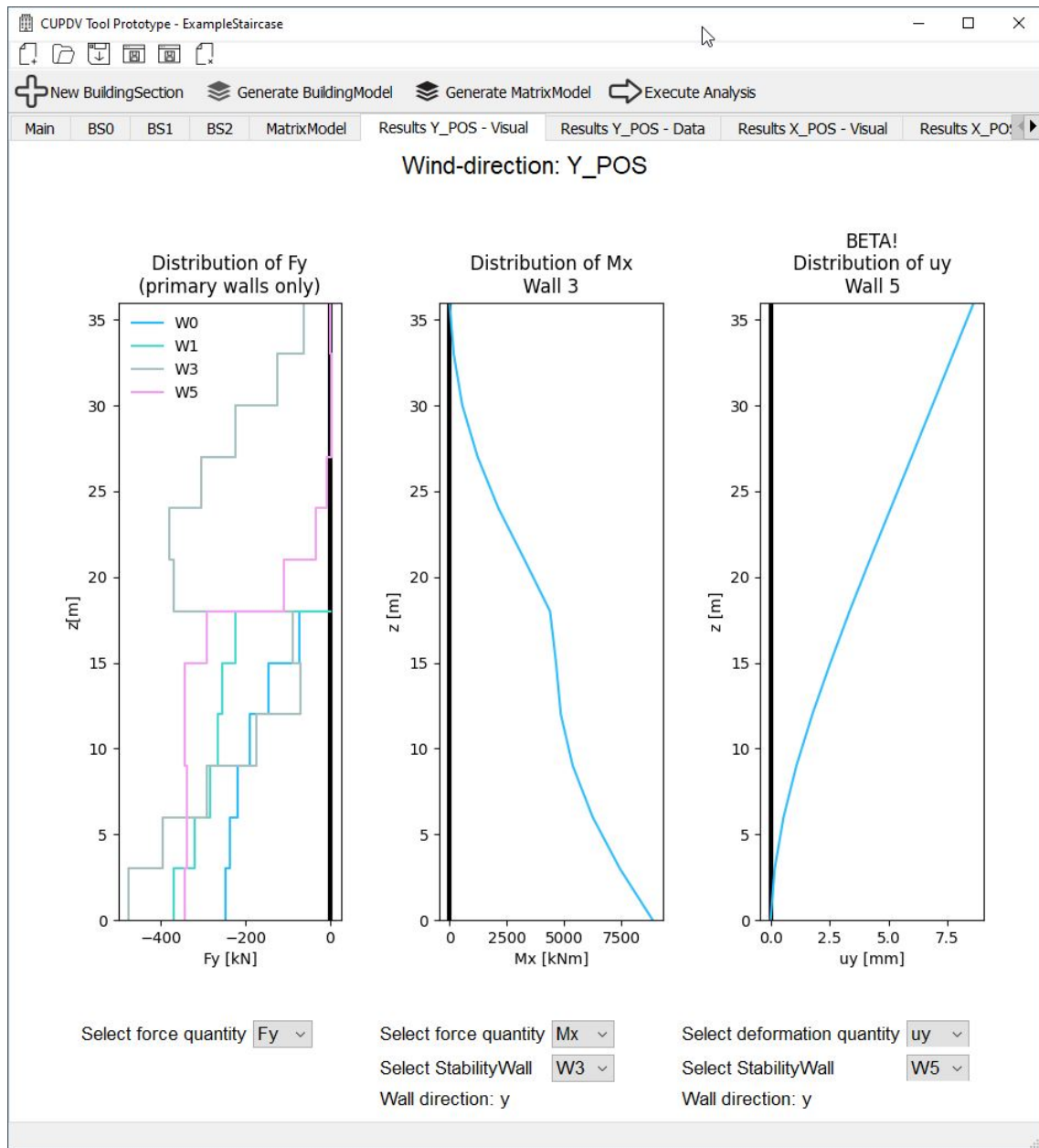


Figure G.6: Results-Visual tab of UI

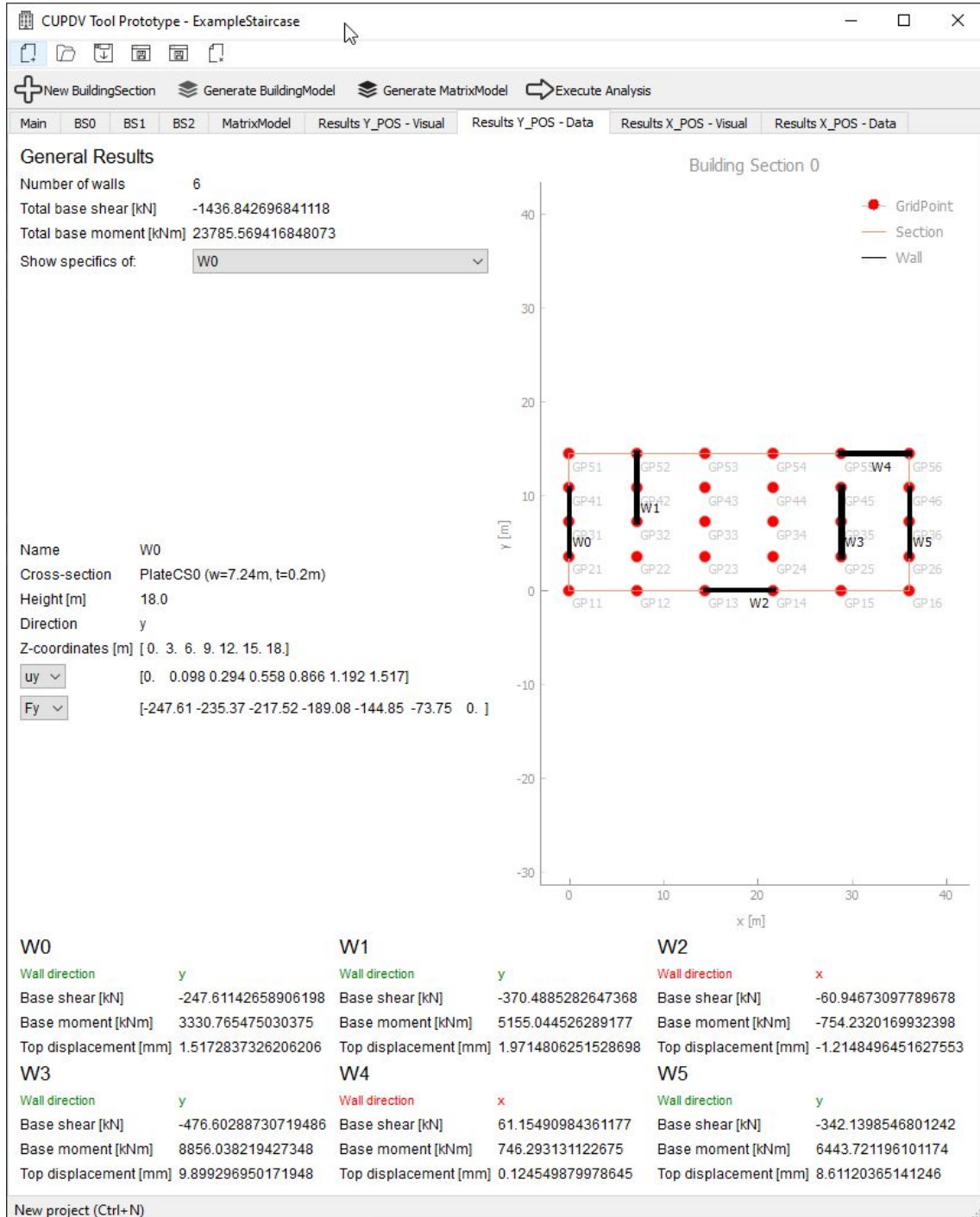


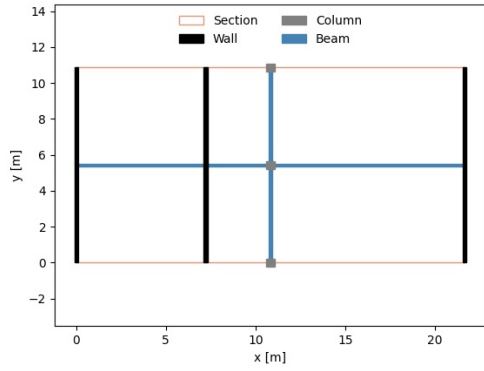
Figure G.7: Results-Data tab of UI

H | CUPD Analysis Accuracy

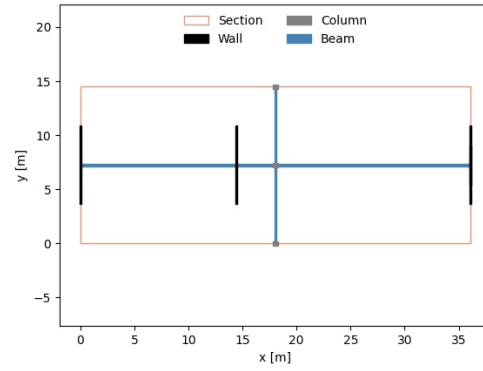
The figures below show the MatrixModel floor-plans of the test-cases introduced in Chapter 5. This appendix will also provided the full results of the redistribution analysis performed on said test-cases. Table H.1 states the modelled number of storeys per test-case. For the non-proportionate test-cases, the '-' delimits the storey-count per section while the ',' separates the different models.

Table H.1: Considered number of storeys per test-case

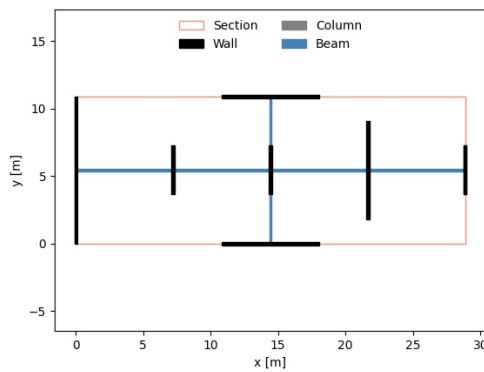
Test-case	Number of storeys [-]
Simple-Dense	1, 2, 3, 4, 5, 6, 7, 8, 10, 12, 15, 17, 20, 25, 30
Simple-Scattered	1, 2, 3, 4, 5, 6, 7, 8, 10, 12, 14, 16
2D-Dense	1, 2, 3, 5, 7, 9, 11, 13, 15, 17, 21, 25, 29
2D-Scattered	1, 2, 3, 4, 5, 6, 7, 8, 9, 10, 11, 12, 13, 14, 16, 18, 20, 22, 24
Core	4, 6, 8, 10, 14, 18, 24
Hybrid	2, 4, 6, 10, 14, 18, 22, 26, 30
Staircase-Dense	3-2, 4-2, 5-5, 6-3, 6-6, 8-2, 8-5, 8-8, 10-3, 10-6, 10-10, 12-4, 12-9, 15-7, 15-11 <i>Additionally:</i> 4-2, 6-3, 10-3, 12-5, 15-7
Staircase-Triple	3-2-1, 6-4-2, 9-6-3, 12-8-4, 15-10-5 <i>Additionally:</i> 3-2-1, 6-4-2, 9-6-3, 12-8-4, 15-10-5
Steenbergen-Symmetric	1-1, 3-3, 4-4, 5-5, 6-6, 7-7, 9-9, 10-10, 13-13, 15-15, <i>Additionally:</i> 4-2, 8-4, 12-6



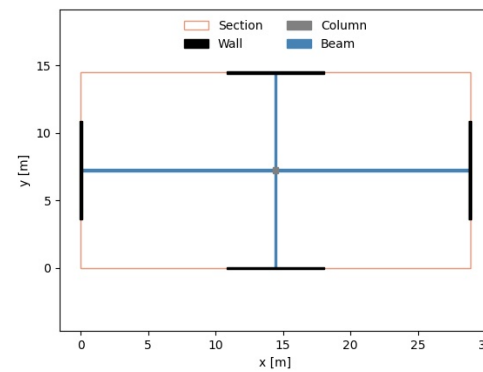
(a) Simple-Dense



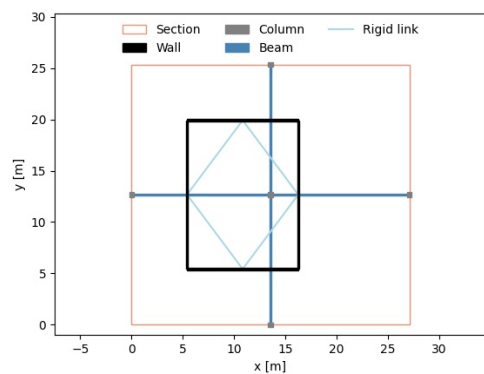
(b) Simple-Scattered



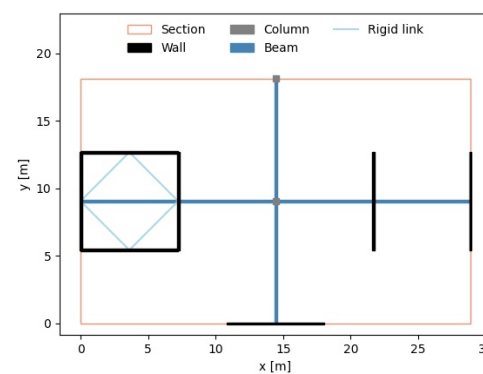
(c) 2D-Dense



(d) 2D-Scattered

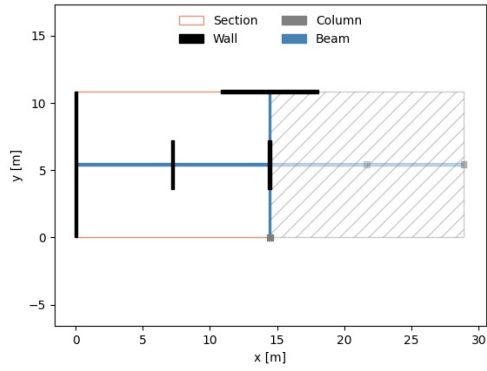


(e) Core (wind in y-dir.)

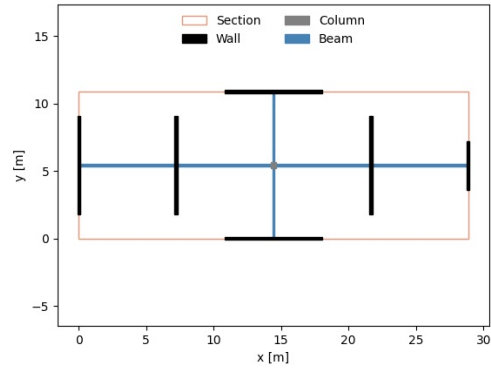


(f) Hybrid (wind in y-dir.)

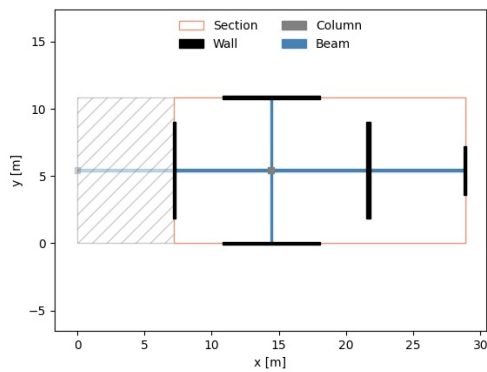
Figure H.1: MatrixModel top-views of test-cases (1)



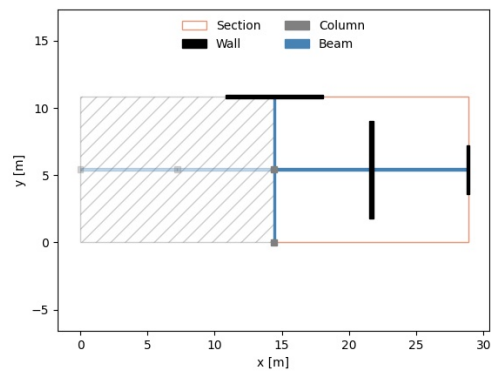
(a) Staircase-Dense - Upper section



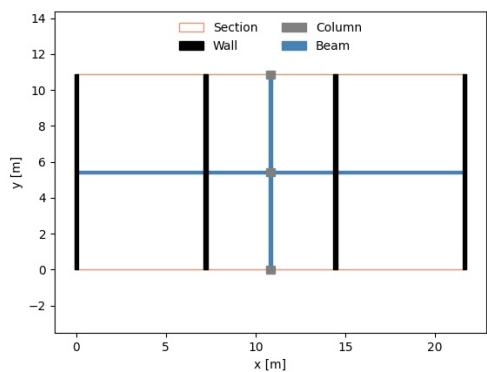
(b) Staircase-Triple - Lower section



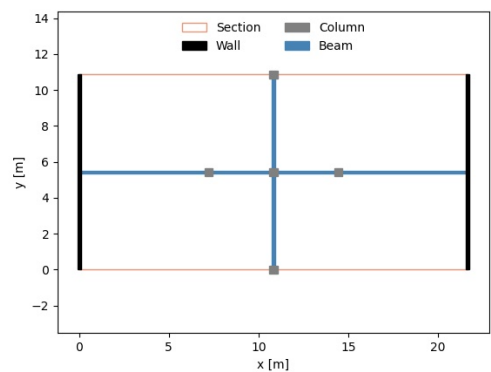
(c) Staircase-Triple - Middle section



(d) Staircase-Triple - Upper section



(e) Steenbergen-Symmetric - Lower section



(f) Steenbergen-Symmetric - Upper section

Figure H.2: MatrixModel top-views of test-cases (2)

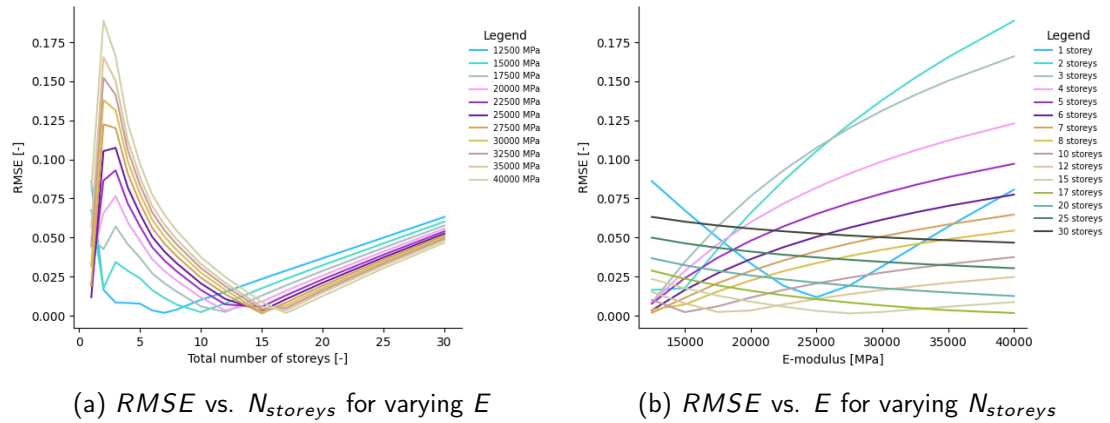


Figure H.3: RMSE results Simple-Dense

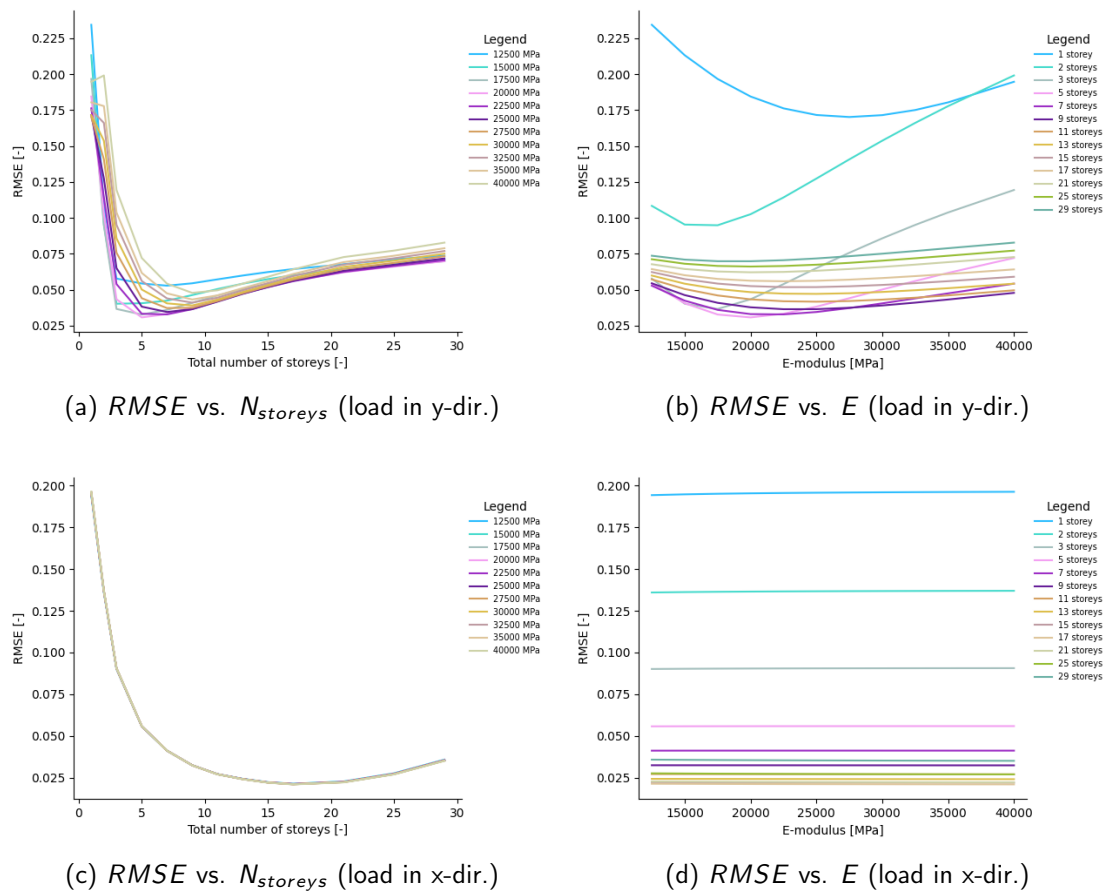


Figure H.4: RMSE results 2D-Dense (primary walls only)

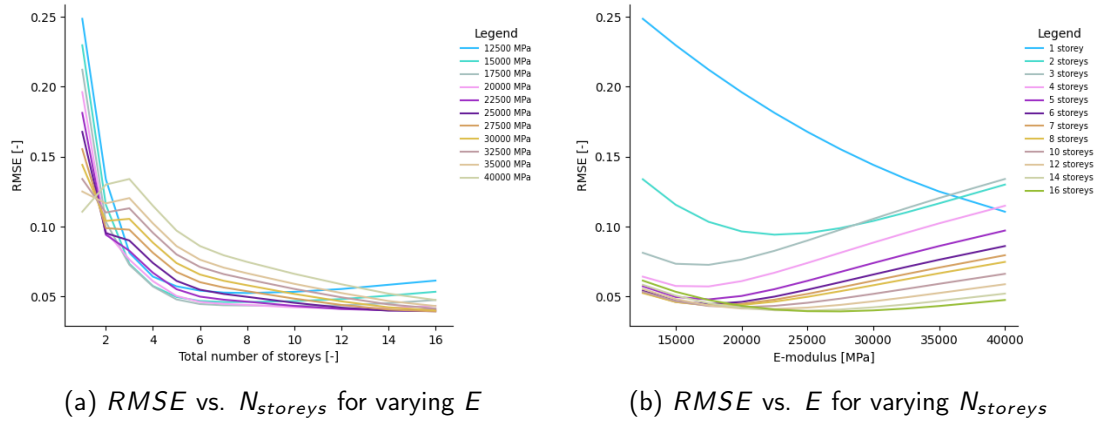


Figure H.5: RMSE results Simple-Scattered

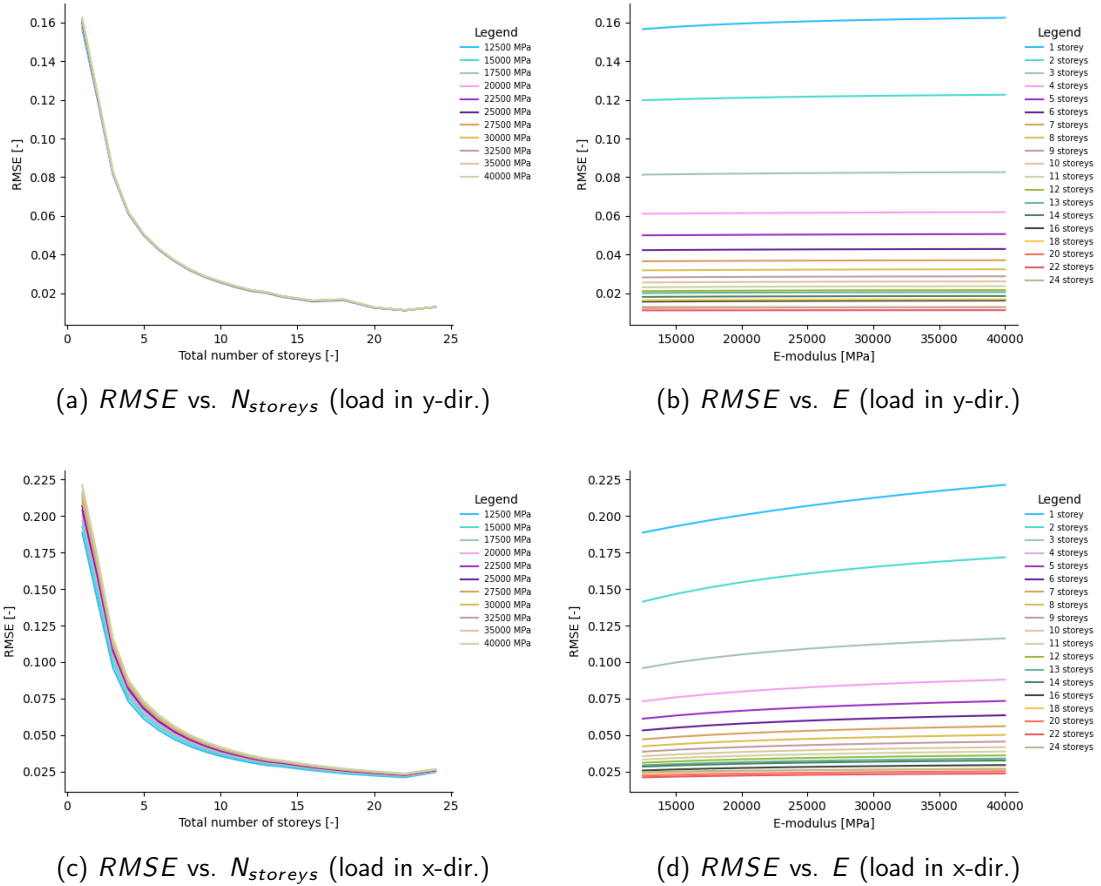
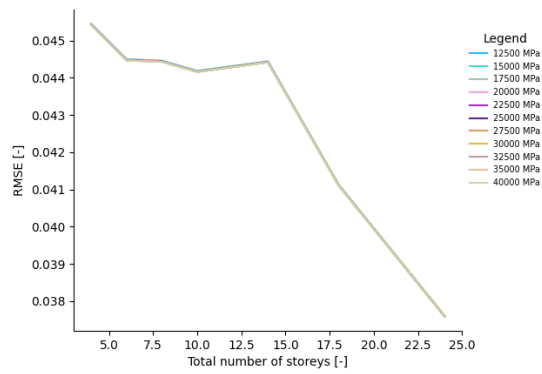
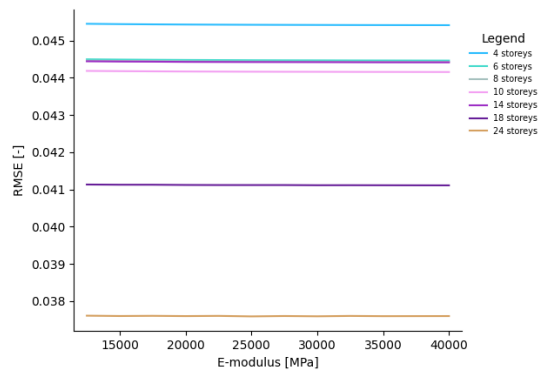


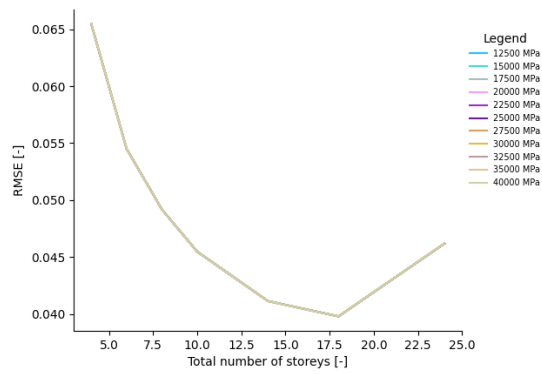
Figure H.6: RMSE results 2D-Scattered (primary walls only)



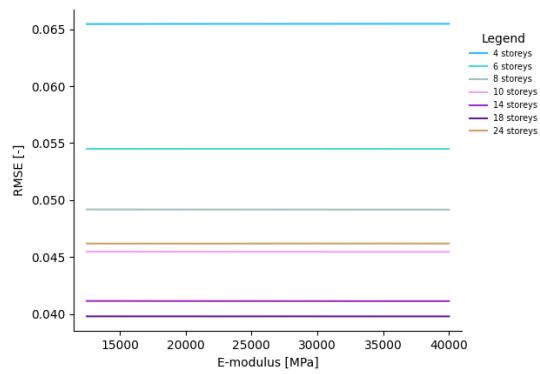
(a) RMSE vs. $N_{storeys}$ (load in y-dir.)



(b) RMSE vs. E (load in y-dir.)

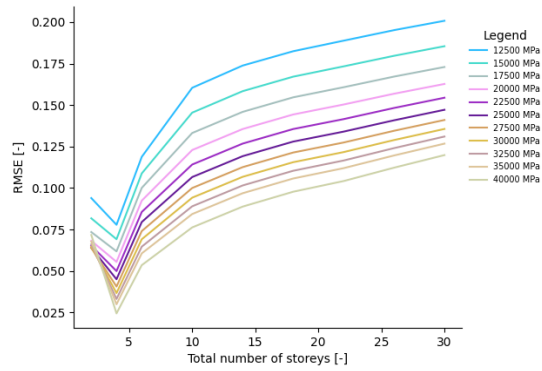


(c) RMSE vs. $N_{storeys}$ (load in x-dir.)

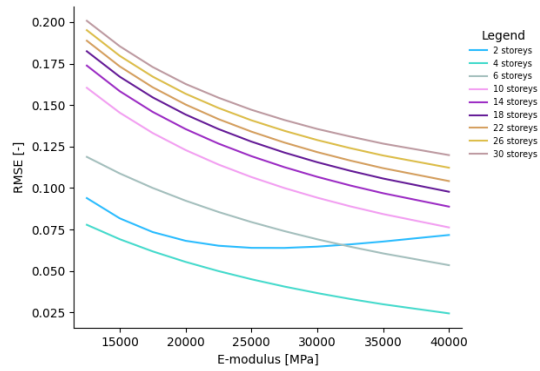


(d) RMSE vs. E (load in x-dir.)

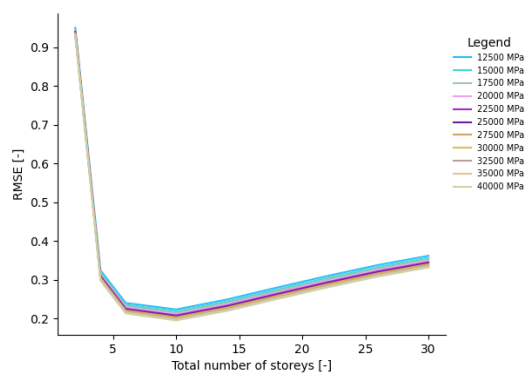
Figure H.7: RMSE results Core (primary walls only)



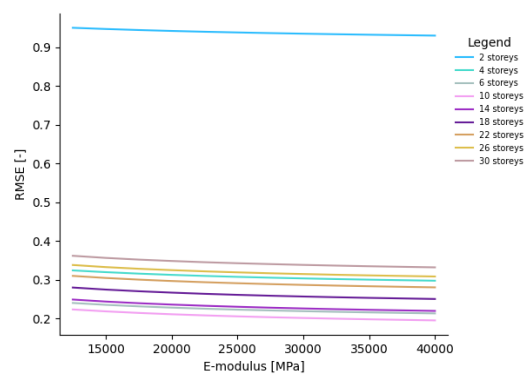
(a) *RMSE vs. $N_{storeys}$ (load in y-dir.)*



(b) *RMSE vs. E (load in y-dir.)*

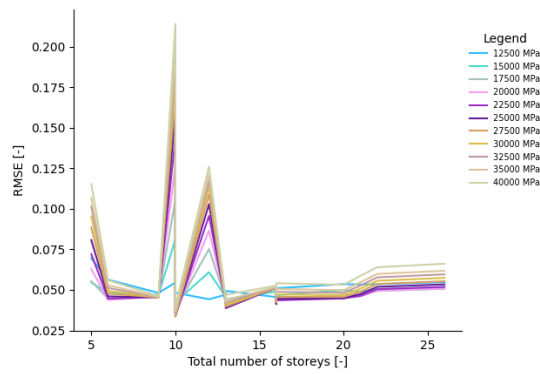


(c) *RMSE vs. $N_{storeys}$ (load in x-dir.)*

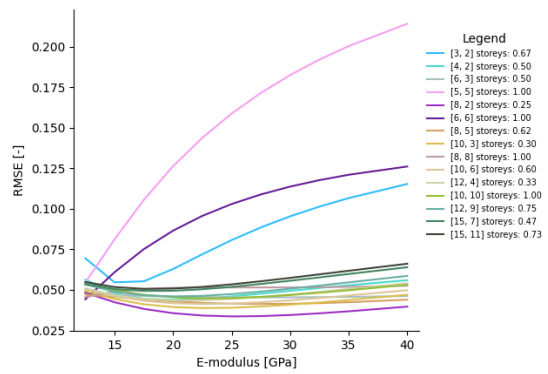


(d) *RMSE vs. E (load in x-dir.)*

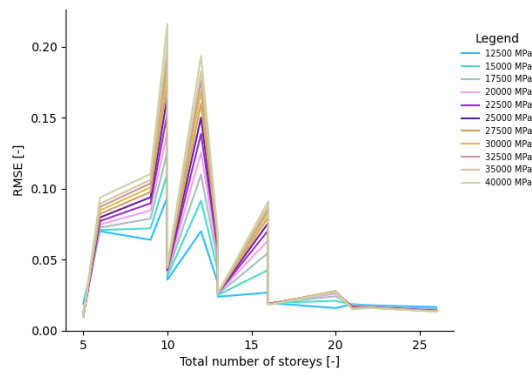
Figure H.8: RMSE results Hybrid (primary walls only)



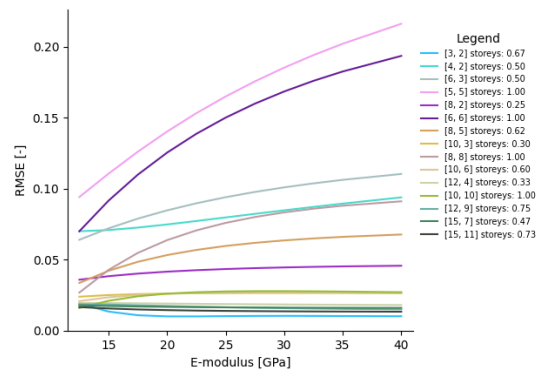
(a) *RMSE vs. $N_{storeys}$ (load in y-dir.)*



(b) *RMSE vs. E (load in y-dir.)*

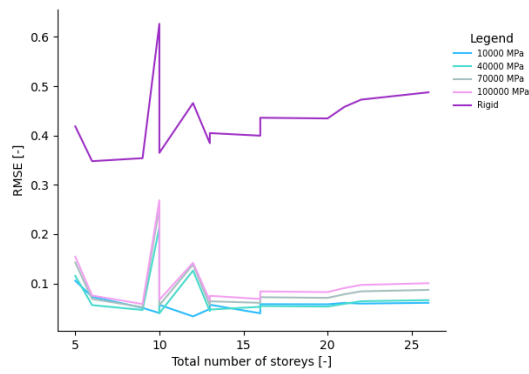


(c) *RMSE vs. $N_{storeys}$ (load in x-dir.)*

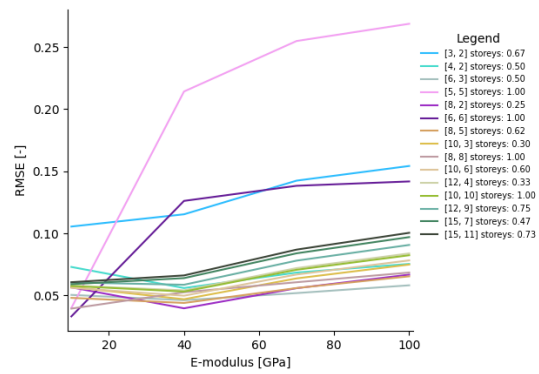


(d) *RMSE vs. E (load in x-dir.)*

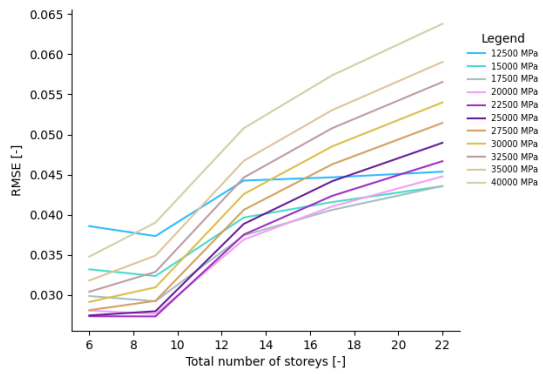
Figure H.9: RMSE results Staircase-Dense (primary walls only)



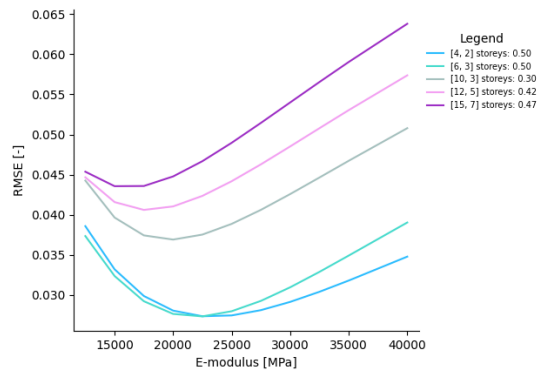
(a) $RMSE$ vs. $N_{storeys}$ (expanded stiffnesses)



(b) $RMSE$ vs. E (expanded stiffnesses)

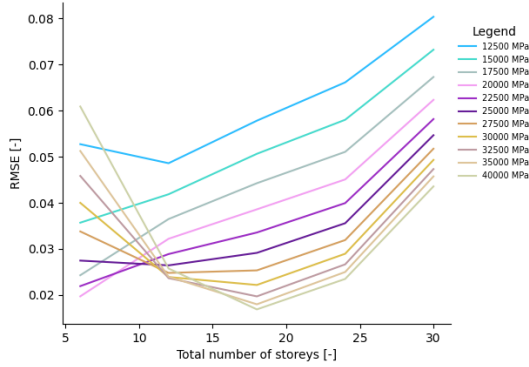


(c) $RMSE$ vs. $N_{storeys}$ ($t_{top-floor} = 1m$)

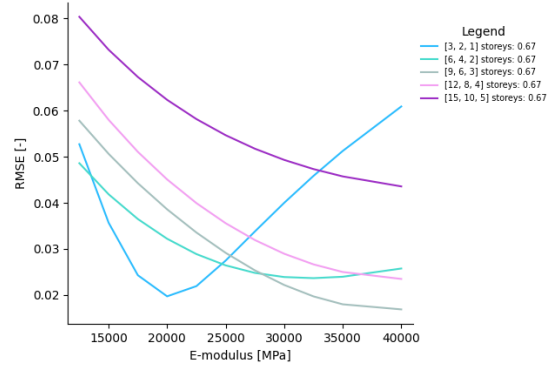


(d) $RMSE$ vs. E ($t_{top-floor} = 1m$)

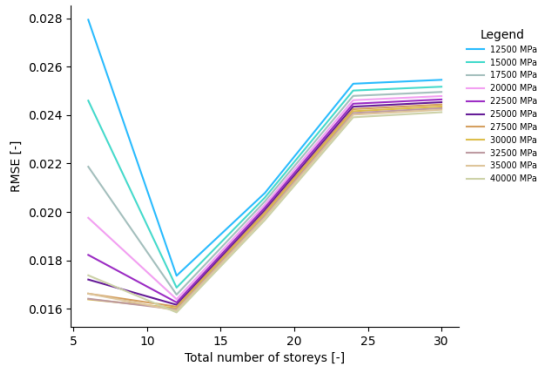
Figure H.10: Additional RMSE results Staircase-Dense (primary walls only; load in y-dir.)



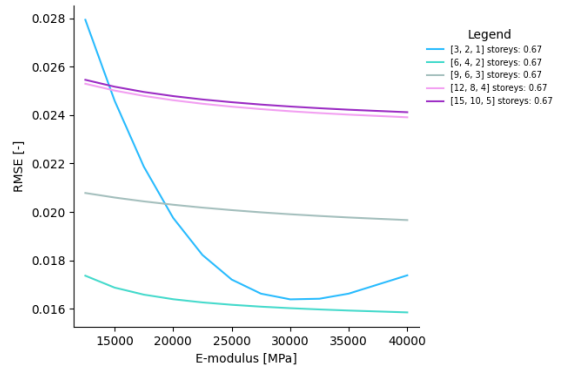
(a) *RMSE vs. $N_{storeys}$ (load in y-dir.)*



(b) *RMSE vs. E (load in y-dir.)*

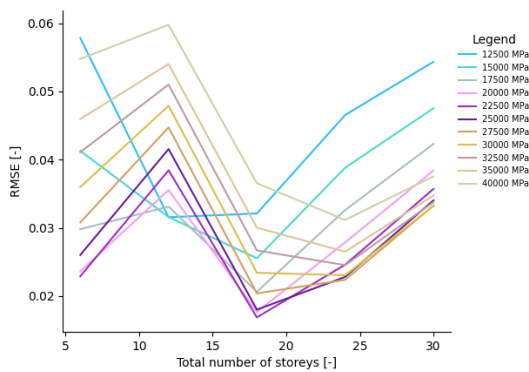


(c) *RMSE vs. $N_{storeys}$ (load in x-dir.)*

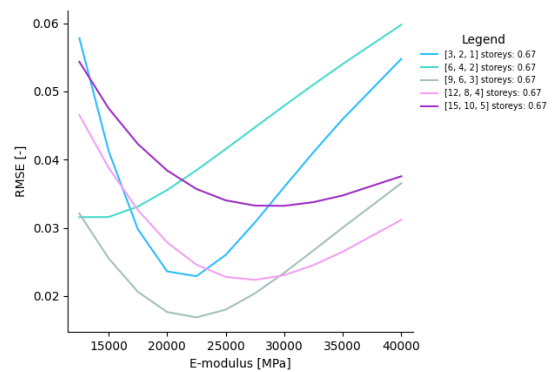


(d) *RMSE vs. E (load in x-dir.)*

Figure H.11: RMSE results Staircase-Triple (primary walls only)



(a) *RMSE vs. $N_{storeys}$ (load in y-dir.)*



(b) *RMSE vs. E (load in y-dir.)*

Figure H.12: RMSE results Staircase-Triple - 1m thick transition floor (primary walls only)

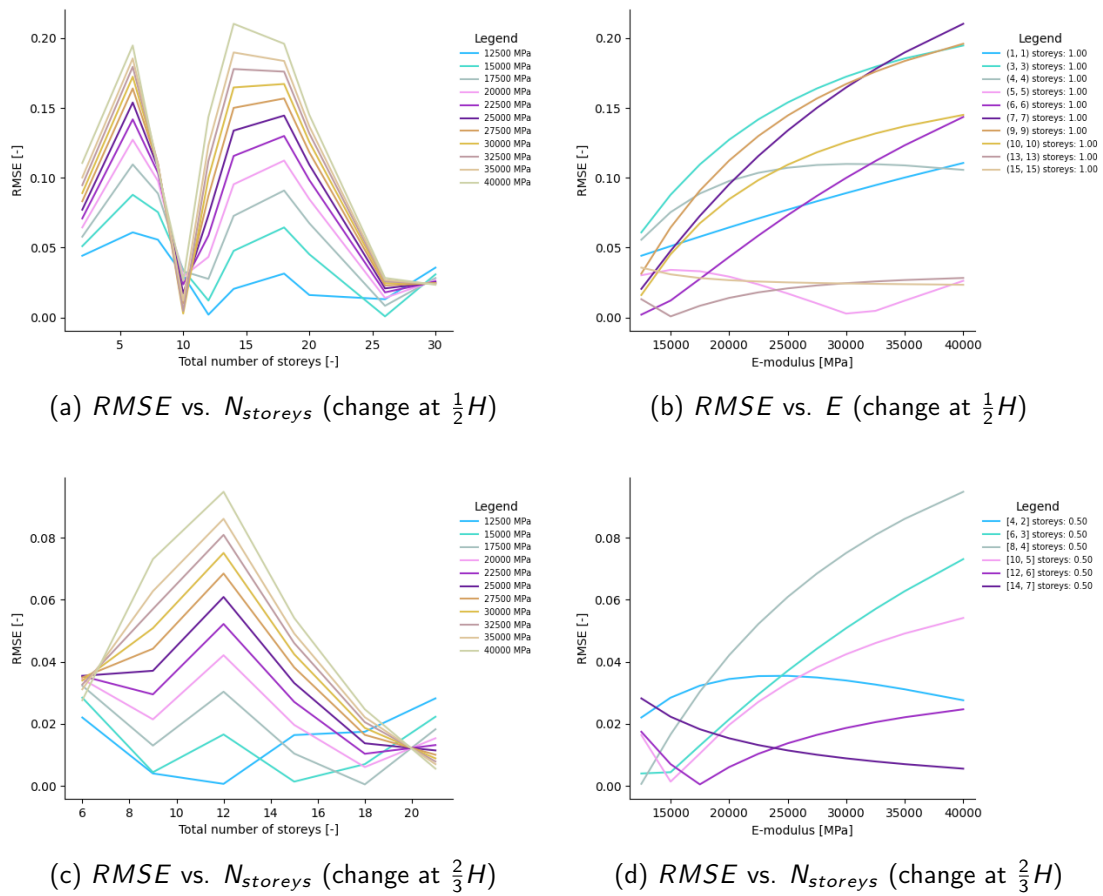


Figure H.13: RMSE results Steenberg-Symmetric

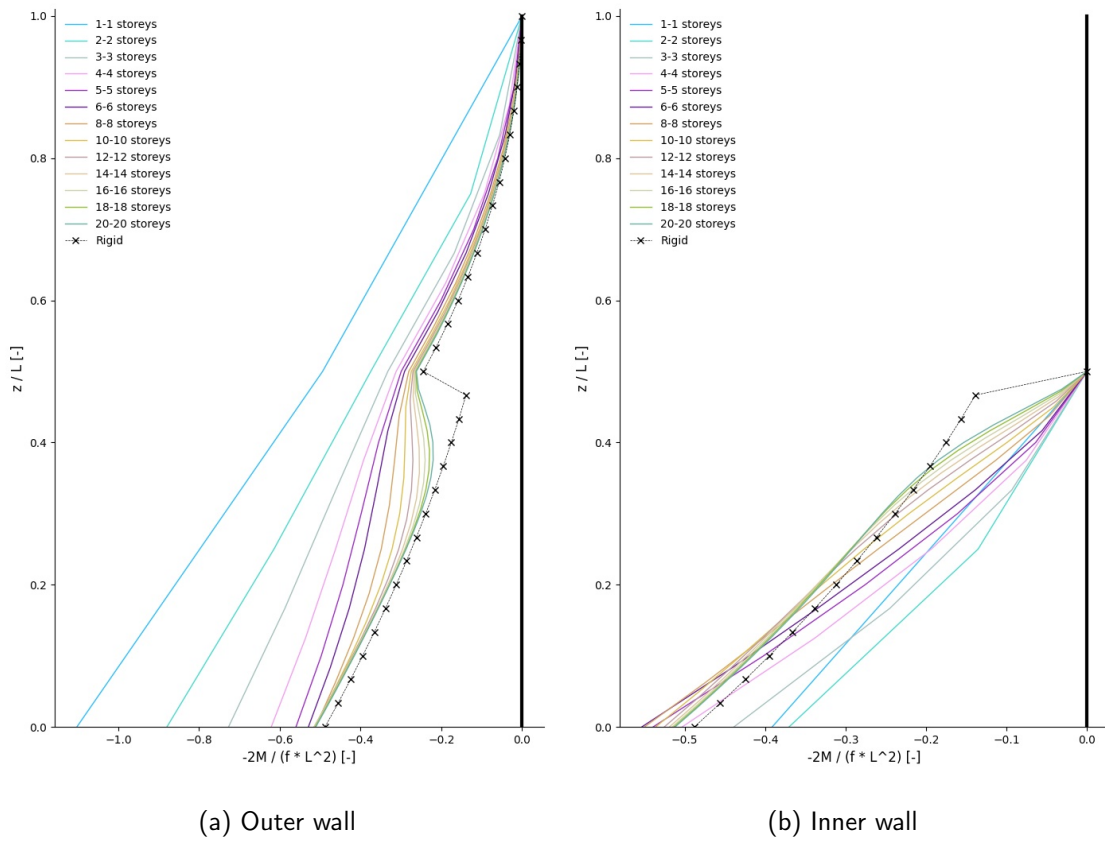


Figure H.14: Steenberg-Symmetric - Interpolated distribution M_x over relative height according to the CUPD Matrix Model ($E_{floor} = 20GPa$)

J | Floor Stiffness - Figures

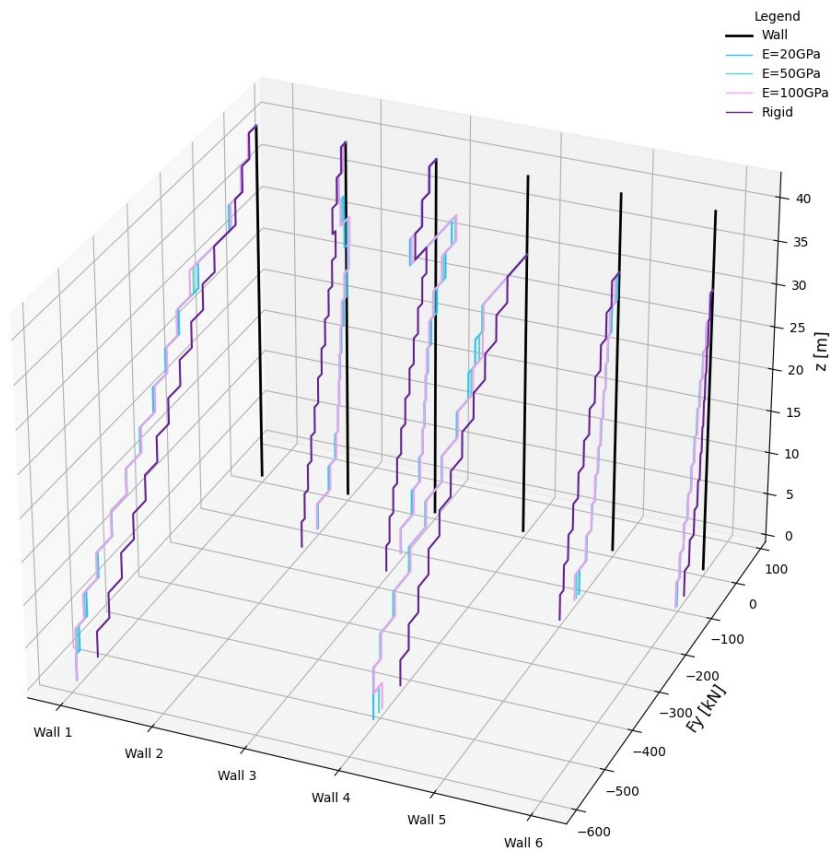


Figure J.1: Staircase-Dense: 11-3 - F_y distributions for varying E (primary walls only)

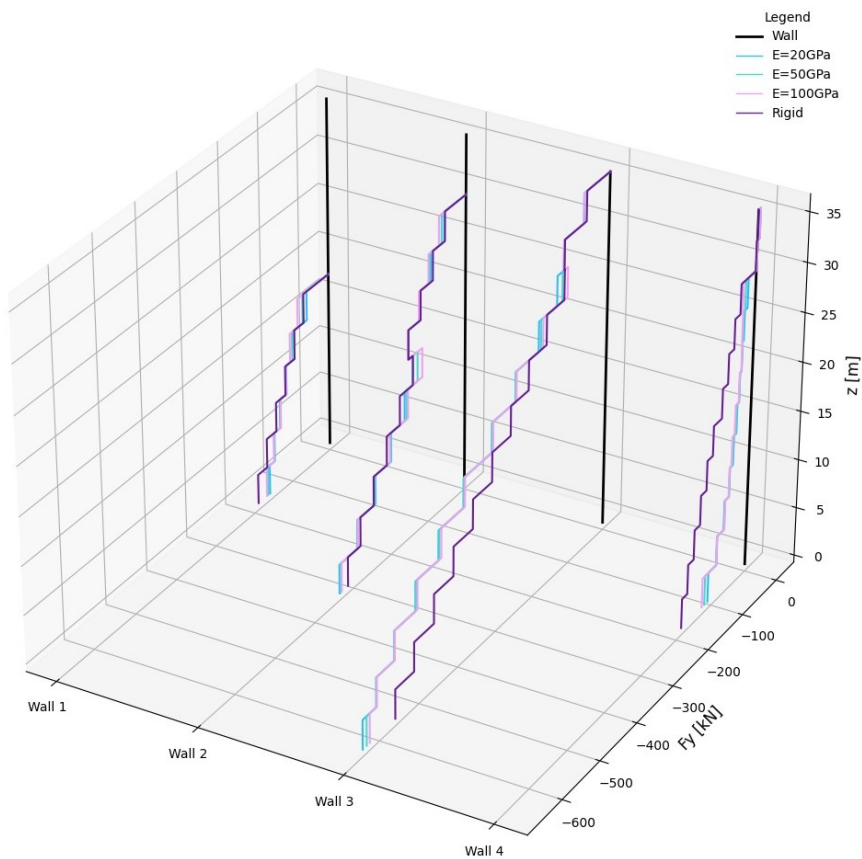
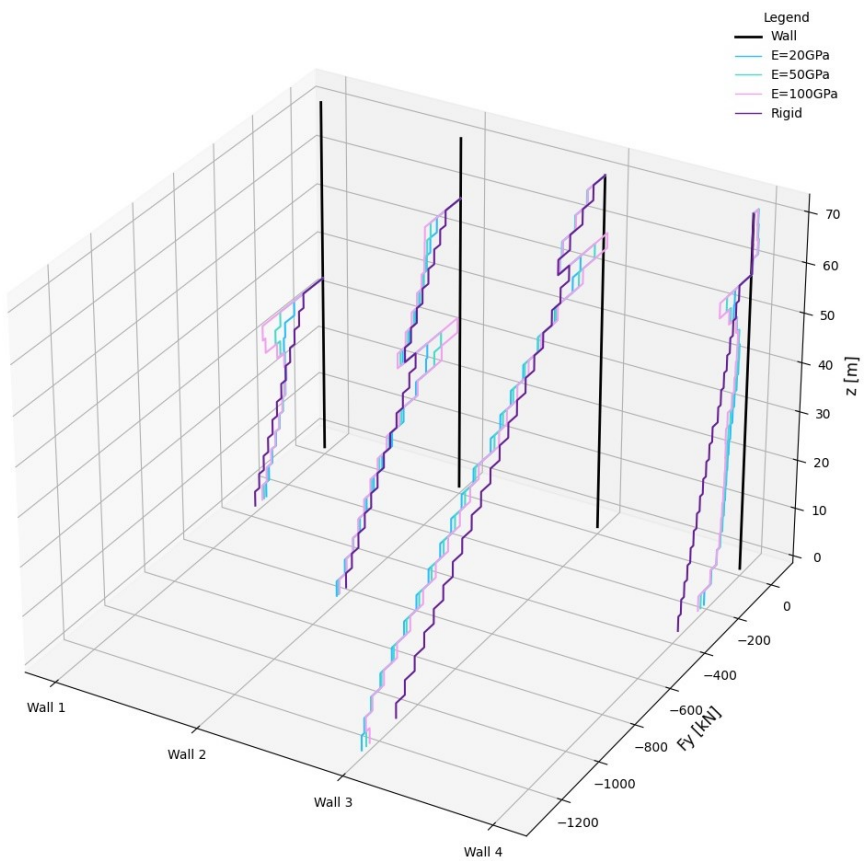
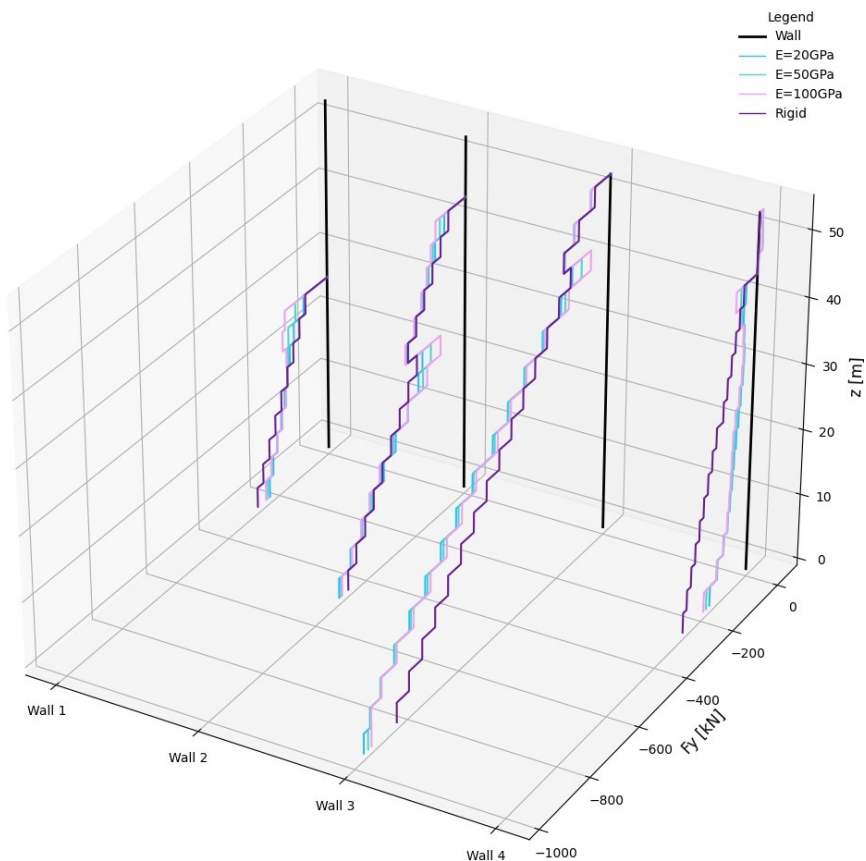
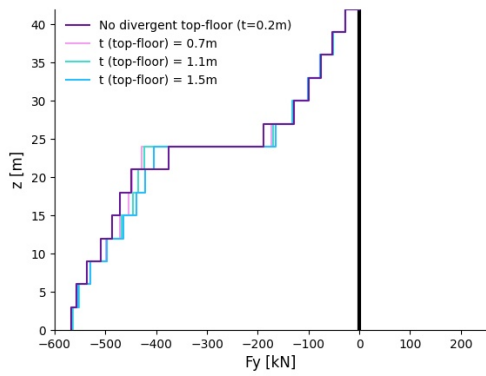


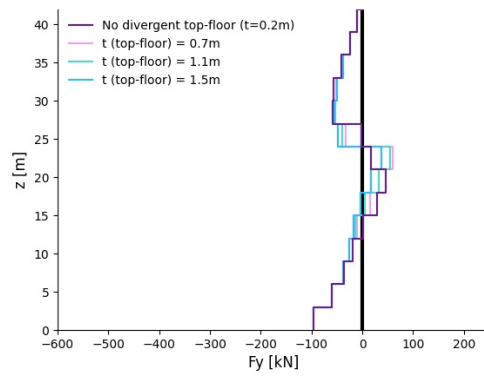
Figure J.2: Staircase-Triple: 6-4-2 - F_y distributions for varying E (primary walls only)



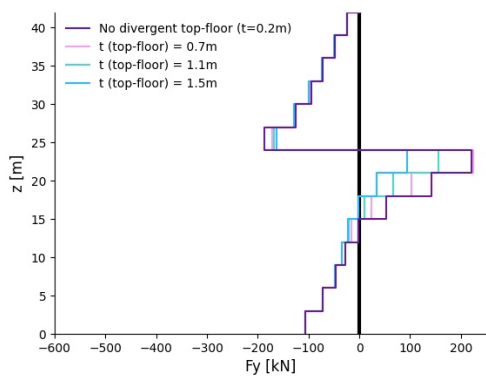
K | Floor Thickness - Figures



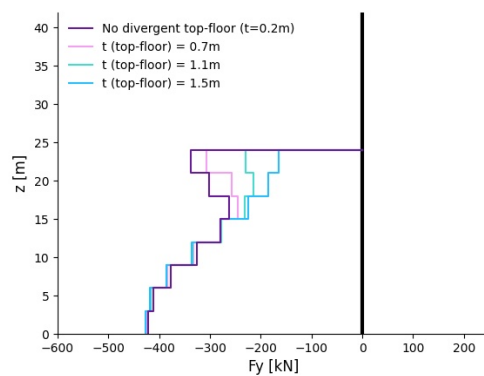
(a) Wall 1 (load in y-dir.)



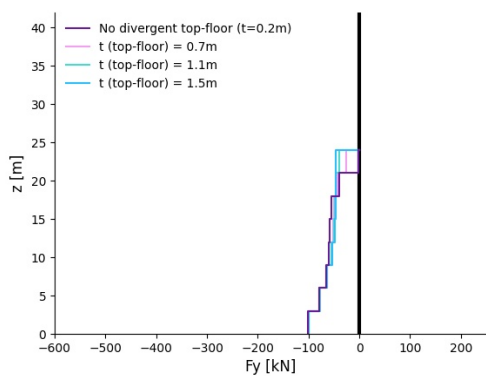
(b) Wall 2 (load in y-dir.)



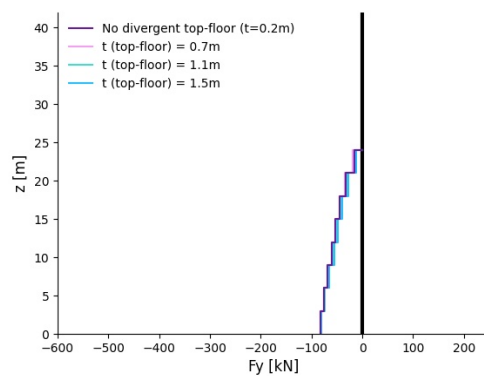
(c) Wall 3 (load in y-dir.)



(d) Wall 4 (load in y-dir.)



(e) Wall 5 (load in y-dir.)



(f) Wall 6 (load in y-dir.)

Figure K.1: Staircase-Dense 8-6 - F_y distributions for varying $t_{top-floor}$ (primary walls only)

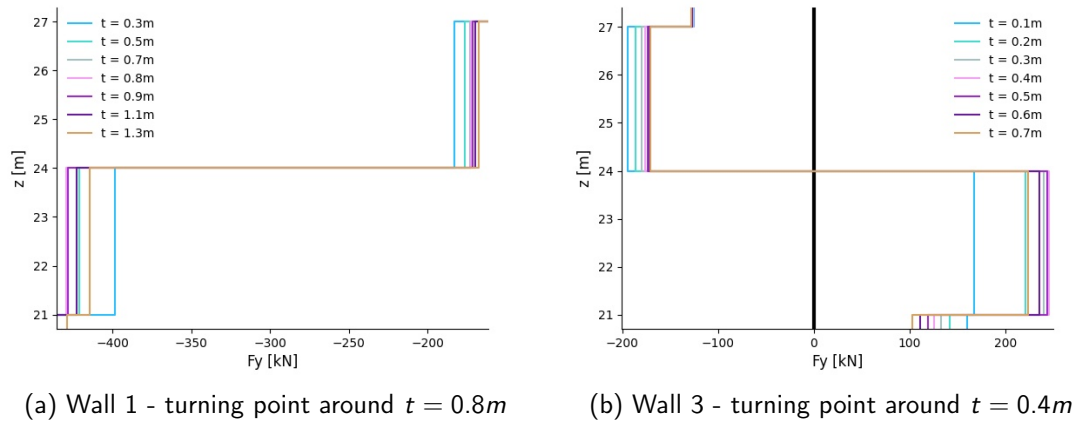


Figure K.2: Staircase-Dense 8-6 - F_y around non-proportionality for varying $t_{top-floor}$

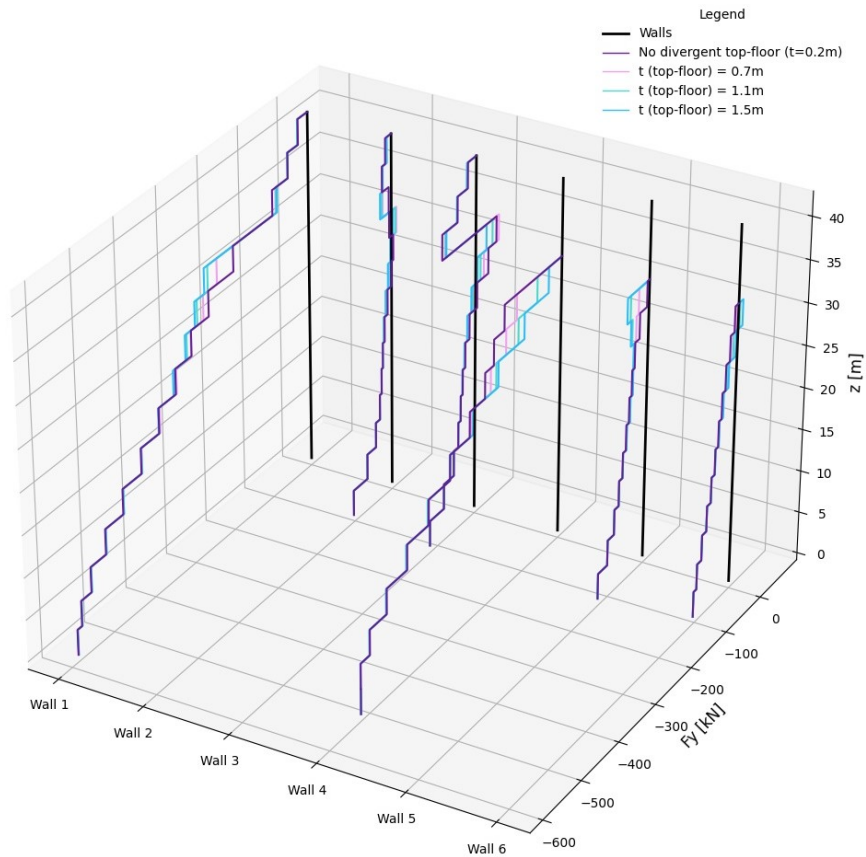


Figure K.3: Staircase-Dense: 11-3 - F_y distributions for varying $t_{top-floor}$ (primary walls only)

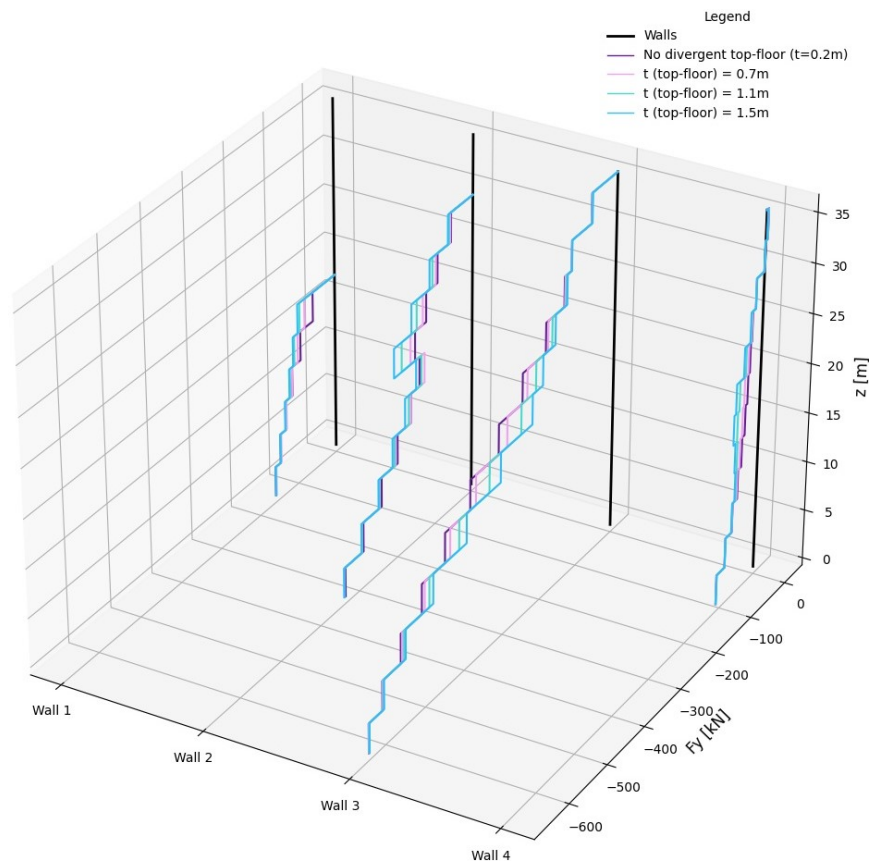


Figure K.4: Staircase-Triple: 6-4-2 - F_y distributions for varying $t_{top-floor}$ (primary walls only)